TECHNISCHE
UNIVERSITÄT
WIEN
Vienna | Austria

Dissertation

Model-based Control Strategies applied to Distribution Grids in Local Energy Communities

carried out for the purpose of obtaining the degree of Doctor of Technical Science (Dr.techn.) submitted at Faculty of Mechanical and Industrial Engineering, Vienna University of Technology

by

Bharath-Varsh Rao

Matr.Nr.: 1652953
Leopoldine-Padaurek-Straße
Floridsdorf, Vienna, Austria

under the supervision of

Ao.Univ.Prof. Dr.techn. Martin Kozek
Institute of Mechanics and Mechatronics
Vienna University of Technology

reviewed by

Univ.Prof. Dr.techn. Stefan Jakubek
Institute of Mechanics and Mechatronics
Vienna University of Technology
1060 Vienna, Austria

Univ.Prof. Dr.Ing. Wolfgang Gawlik
Jade University of Applied Sciences and
Vienna University of Technology
26389 Wilhelmshaven, Germany

I confirm, that going to press of this dissertation needs the confirmation of the examination committee.

Affidavit

I declare in lieu of oath, that I wrote this thesis and performed the associated research myself, using only literature cited in this volume. If text passages from sources are used literally, they are marked as such.
I confirm that this work is original and has not been submitted elsewhere for any examination, nor is it currently under consideration for a thesis elsewhere.

28. Oktober 2021, Vienna

Bharath-Varsh Rao

Acknowledgment

Abstract

This Ph.D. dissertation provides a collection of tools and methods performed since 2017 at the Austrian Institute of Technology, in association with the Institute of Mechanics and Mechatronics, Vienna University of Technology. The research was conducted within the Blockchain Grid (FFG No. 868656) project funded by the Austrian Research Promotion Agency. The publications resulted from the cooperation between the Austrian Institute of Technology, Siemens AG Österreich, Energienetze Steiermark, and Vienna University of Technology.

This Ph.D. presents research on control and optimization of the distribution grid and integrated energy assets in a local energy community. It also offers a solution to reconcile the physical settlement issue that a local energy market faces in a distribution grid by providing a method to limit the flexibilities to ensure overall grid security preemptively.

For several years, the amount of intermittent distributed energy resources (DER's) like photo-voltaic systems, wind generators, and new loads like electric vehicles, electric and thermal storage, and heat pumps has increased in distribution grids. Power system tools like load and optimal power flow, designed for transmission grids, are applied to distribution grids with limited or no modification. Since DER's and loads directly depend on weather factors like ambient temperature, irradiation, and other external disturbances, they, in turn, affect the performance of these tools. Therefore, novel optimal grid control methods are to be developed which are compatible with distribution grids. This dissertation presents a novel three-phase unbalanced holomorphic embedding load flow method in conjunction with a non-convex optimization solver. Additionally, a novel three-phase unbalanced model-based energy management system is presented to manage the flexibilities that a smart home can offer. A control scheme is introduced to derive relations between the grid level optimal power flow and individual flexibility controller consisting of energy management systems. All the methods are demonstrated at a pilot in Heimschuh, Steiermark, Austria.

Contents

Chapter 1

Overview

Local Energy Communities (LEC) are being widely introduced in Europe, as outlined in the Renewable Energy and the Electricity Market Directives, part of the Clean Energy Package from the European Commission [1]. This provides a framework for member nations to develop their own legislation on LECs. In Austria, the directives are transposed into the Renewable Energies Expansion Act (German: Erneuerbaren Ausbau Gesetz) and an amendment of the Electricity Industry and Organisation Act (German: Elektrizitaetswirtschafts und Organisationsgesetz) [2]. The most crucial goal of a LEC is the local production, consumption, trading of energy, and democratizing the energy system by empowering the citizens. LECs can incentivize the community members to install new or increase renewable energy production, conducive to the challenging climate goals set by the European Green Deal.

This Ph.D. details a series of methods and tools to enable LECs' optimal and safe operation and the underlying energy system. It compiles novel methods developed to control distribution grids, and local flexibilities, allowing a peer-to-peer local energy market.

Chapter 1 presents the motivation, problem statement, concepts developed, and related basic research for control of the distribution grid and various flexibilities on the grid and community member side. Chapter 2 presents the contributions and publications related to this Ph.D. dissertation.

1.1 Motivation and Problem Statement

In recent years, distributed energy resources (DERs) like photo-voltaic systems, micro-wind, and a new generation of integrated energy loads like electric, thermal storage, electric vehicles, heat pumps, and hydrogen electrolyzers, are being increasingly con-

nected to distribution grids. It is essential to operate and securely control the distribution grid to ensure the continuity of supply. LECs are expected to exasperate the issue by further motivating the increase of such devices, and Distribution System Operators (DSO) are obliged to facilitate the integration.

LECs will enable the creation of Local Energy Markets (LEMs) to trade and accounting energy within the community. A central limitation of a LEM is the lack of a physical settlement process. It is to ensure that the bids in a LEM, when executed, will not cause any grid violations. At a national or European level energy market, physical settlement is done with the help of a Transmission System Operator. However, due to the large number of customers and devices involved, it becomes impractical for DSO to perform the same in the distribution grids.

1.1.1 State-of-the-art review

In paper [3], OPF algorithms were classified into two categories; Class A algorithms use ordinary load flow methods to generate intermediate solutions, use Jacobian matrix, and other sensitivity relations to generate optimal solution iteratively. This method is susceptible to failure since it entirely depends on the accuracy of the load flow. If load flow converges, the solution already satisfies all the constraints. The optimization problem is solved using the sensitivity relation from arriving at an optimal one. Class B algorithms depend on exact optimal conditions, and load flow equations are used as equality constraints. Detailed formulation of OPF is needed, which includes the entire search space making it non-convex and is challenging to compute the global optimum. One of the main challenges is constraint handling. The two classes have various advantages and disadvantages. The performance of Class A depends on the load flow method used. Newton-Raphson and Gause-Siedel methods are well known in the community. The above-mentioned methods have certain limitations as detained in [4], leading to a non-converged state and failure of OPF. Since Class B uses the entire search space and is non-convex in nature, it is not easy to find a global optimum. Additionally, convex relaxation is needed or a heuristic optimization method.

A novel Class C method is presented in this work which combines Class A and Class B. Using a reliable load flow described in Section 2.1 method wrapped around a heuristic optimization method. The load flow generates accurate operable high voltage and phase angle solution at every iteration and is used as equality constraints. Since the models used for low voltage distribution networks are derived from transmission grids, this section presents a novel three-phase unbalanced optimal power flow. A detailed discussion can be found in Section 2.1.

Smart home energy management systems (HEMS) have been widely described in the literature [5–9]. Model predictive control (MPC), with its large popularity in the chemical industry, is increasingly being used in smart buildings and homes to handle the uncertainties associated with the building models, new intermittent generation, and loads. Various MPC-based HEMS are available in the literature. In [10], an MPC technique to optimize the air-conditioning and other energy-intensive appliances are presented. The objective is to minimize the energy peaks throughout the day. Authors in [11] have presented a HEMS with a variety of generations and loads with the goal to increase self-consumption, maximal utilization of PV system, and decrease operational costs. Work done in [12] presents an MPC method to control electric vehicles, hot-water tanks, and domestic heating to reduce energy consumption. Forecasting methods are used to predict the disturbances like uncontrollable loads and solar irradiation. Results lead to a minimization of energy costs and peak power.

However, most of the research relies only on single-phased electrical models. This can be observed in [9, 13], where building RES generation and loads are optimized. Additionally, most of the methods only control active power, and reactive power is eliminated. However, voltage is directly coupled with reactive power, and therefore, reactive power control is interesting. In this Ph.D., a novel three-phase unbalanced home energy management system is developed to achieve per-phase control of various flexibilities. Additionally, both active and reactive power control is presented (see Section 1.3.2).

In power system, stratified control is mainly used in microgrids as presented in [14–16]. However, these methods need detailed information about the flexibilities that they are controlling to generate the set-points. This is not typically available in a local energy community with a number of customers, and data privacy does not allow it. Moreover, in the literature, stratified control methods are designed to operate a specific type of device or flexibility as presented in [17–19], where electric vehicles are managed. Methods to include smart buildings are presented in [20, 21]. In this Ph.D., a generalized stratified control method, which generates set-points at the points of common couplings of individual flexibilities, is presented. This is device and flexibility independent, resulting in the inclusion of a wide variety of flexibilities into the community.

In the literature, there are numerous methods describing capacity management in distribution grids. They are either numerically iterative in nature or use mathematical optimization. The grid capacity, optimal hosting capacity, optimal placement problems are fundamental, based on optimal power flow (OPF) methods, as described in [3]. Various methods on hosting capacity are presented in [22–24].

Authors in [25], have presented a micro-grid energy and power management system that

is bi-level in nature. Two levels of control, namely, upper and lower, are implemented using evolutionary algorithms for power and energy management, respectively. Using this approach, the global optimum is challenging to achieve, and the flexibilities directly receive set-points. This is a significant limitation as detailed flexibility models are needed. In [26], an energy management system to control RES generation from solar, tidal, and wind is described. It is used for demand response programs, coupled with storage devices in a micro-grid. Linear multi-objective programming method is used. However, it does not provide a method for separating load types and provides a method for including a wide variety of flexibilities without the need for robust data. Authors in [27] detail a control problem with two approaches, the direct method and the Bellman principle of dynamic programming, with promising results. However, it does not involve any flow of energy. This method cannot be extended to a low voltage distribution network made up of power lines where energy flows must be taken into account. The term hosting capacity is commonly referred to as RES in distribution grids and can be used generally to include both generation and loads. In this Ph.D., the available capacity is dynamically managed among the flexibilities by generating active power limiting operational profiles at the points of couplings. If the flexibilities operate within these limits, no grid violations are observed at any part of the grid.

1.1.2 Problem definition

The underlying energy system of a LEC in Austria consists of a low voltage distribution grid along with multiple grids and community members' energy assets like community batteries, smart homes, and buildings. As discussed earlier, the goal of a LEC is to maximize the local production, consumption, and trading of energy. To do so, the distribution grid needs to be operated in an optimal fashion to accommodate all the grid and customer assets without any curtailment. Additionally, optimal power flow methods, which were developed for transmission grids, cannot be readily applied to distribution grids. They need to be modified to handle the diversity of flexibility types, objectives, functions, and constraints, which can be linear, mixed-integer, non-linear, non-convex. It should also be able to include the intermittency of DERs and the new generation of loads.

Pertaining to the assets connected at the community member side, the smart homes and buildings cannot typically accommodate per-phase control of the flexibilities and do not include both active and reactive power control. There is also a lack of a stratified control mechanism that can deal with a large number of flexibility types.

LEC will host LEMs in the distribution grid. LEMs currently do not address the grid

issues during the market mechanism. It is essential to ensure grid security irrespective of the volume and delivery of power traded on the LEM. There is a lack of a physical settlement mechanism in the LEMs.

1.2 Goals

The main goal of this Ph.D. is to design, simulate and demonstrate a generalized control structure for a low voltage distribution grid to optimally manage the power flows by utilizing the grid and consumer level flexibilities. The objective of such a control structure is to ensure grid stability by managing the intermittency of DERs and the new loads. It should also accommodate a variety of objectives and constraints that a LEC can impose, being technical or economical. Additionally, it should be able to include a variety of flexibility types with diverse control requirements.

Most distribution grids are three-phase unbalanced due to the uneven loading on each of the three phases. However, most energy management systems do not consider this detail and are single-phased. Therefore, a more realistic three-phase energy management system is needed for per-phase power control. To coordinate the smart buildings and other grid-level flexibilities like community electric storage, a control mechanism is required to manage the interactions between the grid and various flexibility controllers. With the introduction of LEMs in a distribution grid, a method to provide the physical market settlement is needed to ensure that the bids do not cause grid violation. This is to maximize the available grid capacity and accommodate all the community members into the LEM.

1.3 Methodology

In this Ph.D., four main pieces of research work are presented. Firstly, a novel "Class C" OPF algorithm with a novel three-phase unbalanced Holomorphic Embedding Load Flow method and genetic algorithm. Secondly, a novel three-phase unbalanced model-based Energy Management System. Thirdly, a stratified control structure to manage various flexibilities in a distribution grid. Lastly, an Optimal Capacity Management tool to enable a LEM by providing a physical settlement mechanism. Only a brief introduction to various models and methods is presented in this dissertation. Detailed information with results are recorded in various publications (see Chapter 2).

1.3.1 Three-phase Unbalanced Optimal Power Flow

Power flow equations associated with low voltage distribution networks are non-linear and non-convex. In this work, in the context of Class C algorithms, a three-phase unbalanced holomorphic embedding load flow method with a genetic algorithm is used to generate optimal set-points. Network models are adopted from [28].

OPF problem can be formulated as follows,

$$
\begin{aligned}
\underset{x}{\text{minimize}} \quad & F(x,u) \\
\text{subject to} \quad & H(x,u) = 0, \\
& G(x,u) \leq 0
\end{aligned} \tag{1.1}
$$

Where,

x and u are state and input variables.

$F(x,u)$ refers to the OPF objective function. Traditionally, typical objectives are network loss minimization, optimal dispatch, plant cost minimization.

Three-phase voltage unbalances objective minimization function is chosen and is of the form described in Equation. 1.2.

$$
\text{minimize } J = \sum_{k \in \Omega} \sum_{p \in P} (real(V_{k,balanced}^p) - real(V_k^p))^2 + (imag(V_{k,balanced}^p) - imag(V_k^p))^2 \tag{1.2}
$$

Where Ω refers to all the buses in the network and $P \in phases(a,b,c)$, voltages are represented in a rectangular coordinate system with both magnitude and phase angle being minimized related to the real and imaginary part of the complex value.

$G(x,u)$ and $H(x,u)$ are equality and inequality constraints, respectively. The three-phase unbalanced holomorphic embedding load flow method developed is used as equality constraints.

The three-phase unbalanced holomorphic embedding load flow developed in this work is based on the method developed in [29]. The load flow equations are modeled as follow,

$$
\begin{bmatrix}
A_1^a & A_1^b & A_1^c & A_2^a & A_2^b & A_2^c \\
A_{PQ_3}^a & A_{PQ_3}^b & A_{PQ_3}^c & A_{PQ_4}^a & A_{PQ_4}^b & A_{PQ_4}^c \\
A_{PV_3}^a & A_{PV_3}^b & A_{PV_3}^c & A_{PV_4}^a & A_{PV_4}^b & A_{PV_4}^c
\end{bmatrix}
\begin{bmatrix}
Re\{V^a[n]\} \\
Re\{V^b[n]\} \\
Re\{V^c[n]\} \\
Im\{V^a[n]\} \\
Im\{V^b[n]\} \\
Im\{V^c[n]\}
\end{bmatrix}
=
\begin{bmatrix}
r_{1,n-1} \\
r_{PQ_{2,n-1}} \\
r_{PV_{2,n-1}}
\end{bmatrix} \tag{1.3}
$$

Is of the form,

$$Ax = b \tag{1.4}$$

where the matrix A is clarified as,

$$
\begin{aligned}
A_{1_{ij}}^{P} &= G_{ij}^{P} + \delta i,jRe\{y_i^P\}, & i,j \in \Omega, P \in a,b,c \\
A_{2_{ij}}^{P} &= B_{ij}^{P} - \delta i,jIm\{y_i^P\}, & i,j \in \Omega, P \in a,b,c \\
A_{PQ3_{ij}}^{P} &= B_{ij}^{P} - \delta i,jIm\{y_i^P\}, & i,j \in \Omega_{PQ}, P \in a,b,c \\
A_{PV3_{ij}}^{P} &= 2\delta i,j, & i,j \in \Omega_{PV}, P \in a,b,c \\
A_{PQ4_{ij}}^{P} &= G_{ij}^{P} + \delta i,jIm\{y_i^P\}, & i,j \in \Omega_{PQ}, P \in a,b,c \\
A_{PV4_{ij}}^{P} &= 0, & i,j \in \Omega_{PV}, P \in a,b,c
\end{aligned}
\tag{1.5}
$$

where B and G are the susceptance and conductance matrices respectively. $\delta i,j = 1$ if $i = j$, else 0.
Elements on the right-hand side are defined as follows,

$$r_{1,n-1,i} = \delta_{n,1}(P_i - Re\{y_i\}) - Re\left\{ \sum_{m=1}^{n-1} V_i^*[m] \sum_{k\in\Omega} \sum_{p\in P} Y_{ik}^p V_k^p[n-m] \right\}, \qquad i \in \Omega \tag{1.6a}$$

$$r_{PQ2,n-1,i} = \delta_{n,1}(-Q_i - Im\{y_i\}) - Im\left\{ \sum_{m=1}^{n-1} V_i^*[m] \sum_{k\in\Omega} \sum_{p\in P} Y_{ik}^p V_k^p[n-m] \right\}, \qquad i \in \Omega_{PQ} \tag{1.6b}$$

$$r_{PV2,n-1,i} = -\sum_{m=1}^{n-1} \sum_{p\in P} V_i^*[m] V_i^p[n-m] + (1 + \alpha(M_i - 1)^2)[n], \qquad i \in \Omega_{PV} \tag{1.6c}$$

Where target voltage magnitude for PV bus is described using M_i.
Viskovatov Pade approximant algorithm is applied to learn the power series coefficients leading to voltages and phase angles results (see [30, 31]).

1.3.2 Three-phase Unbalanced model-based Energy Management

In this Ph.D., smart home flexibility is utilized to provide services to the grid. To aid that, a novel three-phase Unbalanced model-based Energy Management is presented in this section. Since DER's and loads are extremely sensitive to external parameters like

weather and solar irradiation, the controller chosen should be robust enough to handle all of these uncertainties.
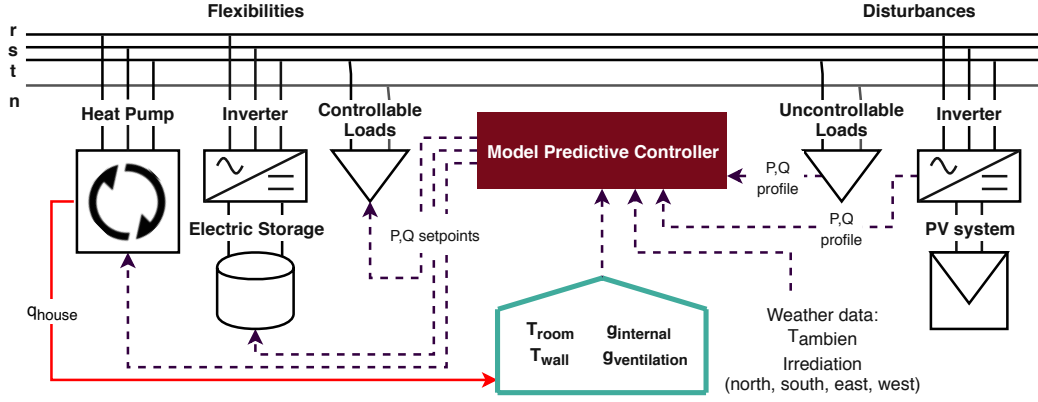

Figure 1.1: Schematic of three-phase HEMS with model predictive controller. It shows all the interconnections with respect to data exchange.

In this work, a novel three-phase Unbalanced Model Predictive Control is derived from performing control at smart homes with receding horizon control. Figure 1.1 describes the MPC and various data exchanges between devices in the smart home.

Smart home thermal models are derived from project iWPP-Flex [32]. They are linear single zone models developed based on data from real single-family homes in Austria. Four models are developed by generalizing the data representing major house types. Various appliance and flexibility models are described in detail in Section 2.2.

In this work, three conflicting objective functions are considered and are as follows,

1. **Maximize self consumption:** It is economical to maximize self-consumption in many countries in northern Europe and therefore, Equation (1.7) is considered. Since active power is only the dependent factor on electricity tariffs, reactive power is excluded.

$$J_{self\ consumption} = \sum_t \sum_{p \in P} (P_{grid}^p(t))^2 \tag{1.7}$$

Where $P_{grid}^p(t)$ is the per phase active power at the grid connection point.

2. **User comfort:** User comfort is very important in smart homes and therefore, Equation 1.8 is included. Temperature limits are defined by the user.

$$J_{user\ comfort} = \sum_t (T_{room}^{reference}(t) - T_{room}(t))^2 \tag{1.8}$$

3. **Grid Support:** The optimal set-points generated by the grid level controller are actively tracked by the smart home using the objective in Equation (1.9).

$$J_{grid\,support} = \sum_t \sum_p (P^\rho_{grid\,reference}(t) - P^\rho_{grid}(t))^2 + (Q^\rho_{grid\,reference}(t) - Q^\rho_{grid}(t))^2$$

(1.9)

Equation 1.10 describes the complete objective function. User-defined weights $\mathcal{S}$, $\mathcal{U}$, and $\mathcal{G}$ are introduced using which more importance can be given to the objectives.

$$\text{minimize } J = \mathcal{S}\,J_{self\,consumption} + \mathcal{U}\,J_{user\,comfort} + \mathcal{G}\,J_{grid\,support} \tag{1.10}$$

Weights can be changed online and are updated in the following sample time and are the most significant variables, having much influence on the performance of the controller. $P_{battery}$, $P_{heat\,pump}$ and $P_{controllable\,load}$ are controllable variables.

1.3.3 Stratified Control Structure

Stratified Control Structure derives control relationships between the low voltage distribution grid and various flexibilities local energy community.
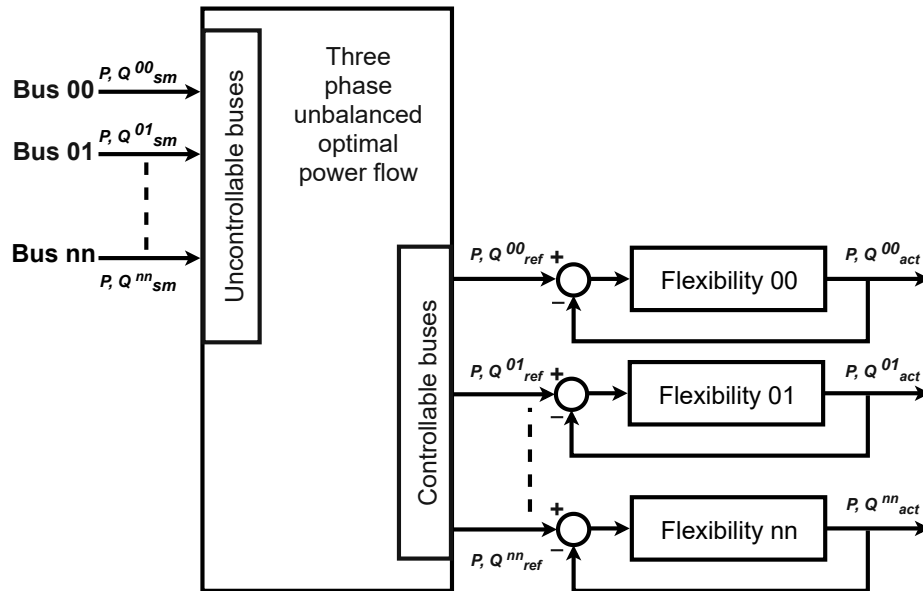

Figure 1.2: Schematic of the stratified control scheme with a grid level OPF controller and four smart homes with MPC controllers.

It consists of a grid controller and numerous flexibility controllers. The grid controller hosts a three-phase unbalanced power flow, generating optimal set-points for a certain number of controllable buses at critical nodes. Smart home controller hosts Model Predictive Control with various flexibilities, which are single or three-phased. The optimal set-points generated by the grid controller are actively tracked by smart homes connected to it, leading to a system-level optimization. Figure. 1.2 represents a stratified control scheme with a grid controller providing set-points to multiple flexibility controllers. The set-points from the grid level controller are generated at the points of common couplings without the need for sensitive building flexibility information to preserve privacy.

1.3.4 Optimal Capacity Management

Optimal Capacity Management (OCM) involves generating limiting active and reactive power operational profiles at the buses where flexibilities are connected. OCM is based on "Type C" Optimal Power Flow, consisting of a reliable flow solver, such as a Holomorphic Embedding Load Flow method, wrapped around a non-convex heuristic solver, such as a genetic algorithm. The flexibilities are required to operate within limits to ensure no violations are observed in any part of the distribution grid.
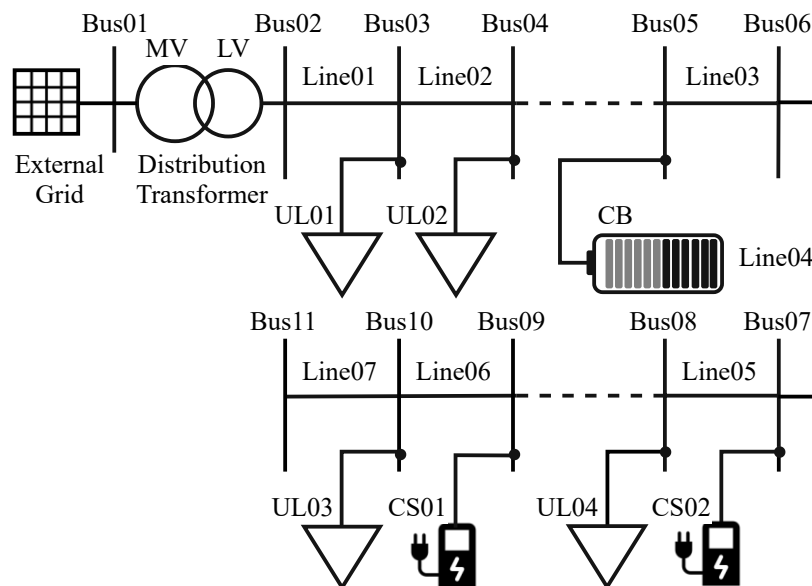

Figure 1.3: General schematic of a LEC in Austria, consisting of a community battery and two charging stations [33].
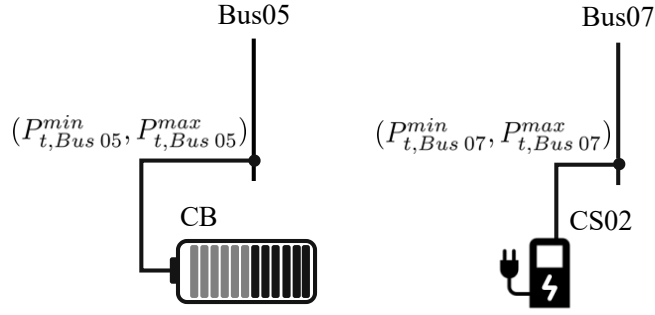
Figure 1.4: Active power limiting profiles generated at the points of common couplings of community battery and charging station 02 [33].

OCM is designed to include multiple objectives, like loss minimization, three-phase unbalance minimizations, maximizing hosting capacity, in addition to generating the operational limits. It can handle a variety of grid constraints like the voltage, loading of various elements and assets, active and reactive power flow limits, and thermal limits. The limiting profiles can be observed in Figure. 1.4. This is related to Figure.1.3, where, at Bus 05 and Bus 07, the community battery and charging station are connected.

The limiting profiles are generated using the following objective function,

$$F(x, u) = \sum_{t \in T} \sum_{c \in C} P_{c,t} \tag{1.11}$$

Where, (P_t^{min}, P_t^{max}) represents the limiting profiles and are generated as follows,

$$
\begin{aligned}
P_t^{min} &= \underset{u}{\text{minimize}} \\
F(x, u) \\
P_t^{max} &= -\underset{u}{\text{minimize}} \\
F(x, u)
\end{aligned}
\tag{1.12}
$$

Active powers at controllable devices are $P_{c,t}$, at the time step t. Set of flexibilities are represented as C and T is the time horizon. By minimizing and maximizing (- minimizing) Equation 1.11, to generate P^{min} and P^{max} values as represented in Equation 1.12.

With the help of these limiting profiles, the flexibilities are preemptively controlled to prevent grid violations in any part of the grid. This constitutes the physical settlement in a Local Energy Market.

1.3.5 Demonstration of methods in research projects

This Ph.D. is part of a research project, Blockchain Grid (FFGNo. 868656), funded by the Austrian Research Promotion Agency. Blockchain Grid project focuses on developing a peer-to-peer blockchain-based energy accounting system and a grid control mechanism for the maximal utilization of flexibilities in a low voltage distribution grid. OCM has been validated successfully in the Heimschuh smart grid pilot.

OCM is currently being applied in several Austrian and European level projects and is listed in Figure. 1.5. Various methods developed in this Ph.D. are being applied with limited changes.

Blockchain Grid
Instrument - FFG
Partners: 4
Countries: AT

CLUE
Instrument - ERA-Net
Partners: 24
Countries: AT, DE, SE, UK

LocalRES
Instrument – H2020 IA
Partners: 21
Countries: ES, AT, FR, BE, FI, IT, IE

REACT
Instrument – H2020 IA
Partners: 23
Countries: ES, IE, NL, DE, AT, FR, IT, SE, UK, EL
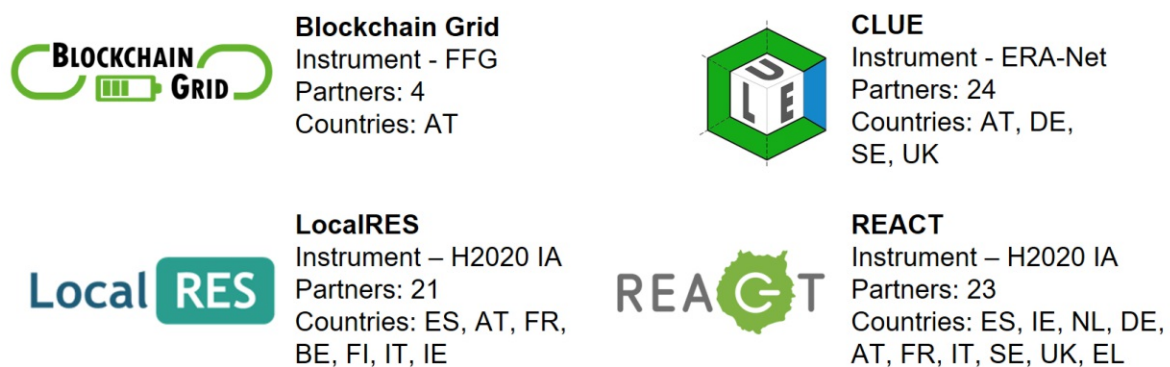
Figure 1.5: Methods applied to various Austrian and European Level Projects.

OCM is being deployed in the Austrian City of Gasen, where a LEC will be set up. This is done in the CLUE project. In the LocalRES project, a version of OCM will be deployed in the municipality of Ollersdorf in Burgenland in Austria. Similarly, OCM will be deployed in the islands of La Graciosa in the Canary Islands of Spain and Aran Islands in Ireland within the REACT project.

1.4 Summary of Scientific approaches

In **Publication A**, see section 2.1, a novel "Class C" optimal power flow is presented. Class C OPF algorithms involve the use of a reliable load flow along with a non-convex optimization solver. In this paper, a novel three-phase unbalanced Holomorphic Embedding Load Flow method is presented. To check the accuracy of the solution, it is compared against the Newton-Raphson method in DIgSILENT Power Factory. Voltage results from thousand random load flow simulations by varying active and reactive power at load buses from $\pm$ 100kW and $\pm$ 8 kVAr. Mann-Whitney U test is apples to the result and tabulated with other statistical information. It is observed that the means are statistically insignificant, leading to the acceptance of the null hypothesis. Using this load flow technique, a non-convex heuristics solver genetic algorithm presents an optimal power flow scheme. A use case consisting of a real network in Austria is considered for evaluation. A three-phase voltage unbalance minimization objective function is used. By running the proposed TOPF, optimal schedules were generated at controllable buses. Observations regarding the objective function value, voltage profiles, active and reactive power profiles are made regarding real, forecasted, and optimal schedules.

In **Publication B**, see section 2.2, a novel three-phase unbalanced home energy management system is presented. It includes typical distributed generation like photovoltaic systems, loads like electric storage, heat pumps, and various smart home models, constructed using realistic models representing typical homes in Austria. The models are three-phase linear in nature and model both active and reactive powers. Three conflicting objective functions with three objective user-defined weights are presented. The control scheme is described for three-phase with various chronological events. Simulation results for unbalanced active and reactive power control for three phases are provided. Multi-objective mixed-integer quadratic programming model predictive control is presented.

In **Publication C**, see section 2.3, a stratified control method is presented to derive control relationships between the distribution grid and various flexibilities in a local energy community. The communication is facilitated over a Blockchain. The flexibilities used are smart buildings and community-level electric storage. The grid level controller uses an OPF type C with a three-phase unbalanced optimal power flow, comprising a three-phase unbalanced holomorphic embedding load flow method and genetic programming. Optimal schedules are generated at certain controllable buses. The flexibilities connected at those buses, with their internal controller, try to tract the schedules generated by the grid controller. The flexibility controller consists of mixed-integer quadratic programming-based model predictive control. Each flexibility

controller is unique and depends on the available flexibility in the building premises or community electric storage. To test the control scheme, a real network and home controller to four smart houses are used. The objective function is three-phase voltage unbalance minimization at all the buses in the network.

In **Publication D**, see section 2.3, an Optimal Capacity Management method, using OPF Type C is presented. This method reconciles the physical settlement issue affected by a local energy market. It preemptively calculated the active power operational limits at a certain number of controllable buses where flexibilities are connected. To observe these limits, flexibility is required to ensure system-level optimization even before the bids in a local energy market are executed. OCM comprises a holomorphic embedding load flow method and genetic programming to generate the operational limits. The method is demonstrated and validated in a real pilot in Austria.

1.5 Scientific Contributions of this Work

The methods developed in this Ph.D. can be applied universally. Class C type of OPF algorithms can be applied to various real distribution networks without limitations on the size of the network, number of components, and can handle most types of objectives and constraints (linear, mixed-integer, quadratic, non-linear, and non-convex). However, communication infrastructure to process control actions for the entire network can be a bottleneck. Model predictive control Methods developed can be applied to any smart home or building type with a diverse set of single and three-phase loads and renewable energy generators. Grid level controller as part of the stratified control scheme generates set-points at the points of common couplings of flexibilities. Therefore, the method does not depend on the type of flexibility connected, leading to the inclusion of a diverse set of flexibilities and controllable assets. Similarly, the operational limits generated by the optimal capacity manager are flexibility type independent. However, the method is limited to a particular feeder (feeder-specific OCM implementation).
The scientific contributions of this work and can be summarized:

- Development of a novel class of optimal power flow algorithms – Class C
    - Three-phase unbalanced Holomorphic Embedding Load Flow Method (THELM).
    - Benchmarking of THELM against three phase unbalanced Newton-Raphson method.
    - Three phase unbalanced optimal power flow scheme using THELM and Genetic Algorithm.
    - Three phase unbalance minimization objective applied to real networks.

- Development of three phase unbalanced home energy management system
    - Multi-objective optimization to maximize self consumption, comfort and grid support.
    - Three phase active and reactive power models for flexibilities.
    - Mixed-integer quadratic programming Model Predictive Control (MPC).
    - Control both active and reactive power.

- Stratified control structure for optimal scheduling of flexibilities in the low voltage distribution networks
    - Control relationships between the grid and various flexibilities in a local energy community.

– Stratified control applied to the real network in Austria with a number of buildings and a community level electric storage.

– Generating the set-points at the points of common couplings leading to a flexibility model or data-independent grid controller, preserving the consumer privacy.

- Application of Class C OPF in Optimal Capacity Management

  – Reconciling the physical settlement issues in a Local Energy Market by preemptively generating limiting operational profiles at the location of flexibilities to ensure grid stability.

  – Demonstration of the OCM in a pilot in Heimschuh, Styria, Austria, leading to technology readiness level 7.

Chapter 2

Publications

List of selected journal publications:

Publication A

Publication B

Publication C

Publication D

Rao, B.V.; Stefan, M.; Brunnhofer, T.; Schwalbe, R.; Karl, R.; Kupzog, F.; Taljan, G; Zeilinger, F.; Stern, P.; Kozek, M.

Optimal capacity management applied to a low voltage distribution grid in a local peer-to-peer energy community

2.1 Publication A

Rao, B.V.; Kupzog, F.; Kozek, M.
Three-Phase Unbalanced Optimal Power Flow Using Holomorphic Embedding Load Flow Method
Sustainability 2019, 11, 1774. https://doi.org/10.3390/su11061774

Own contribution

Concept development, problem analysis, methodology creation, formal analysis, implementation of algorithms, coding, data cleaning and management, simulation studies, structuring and writing of the manuscript was done by the candidate, under the supervision of second and third authors. Methodology and problem statement discussion, editing of the manuscript was done by second and third authors.

sustainability

MDPI

Article

Three-Phase Unbalanced Optimal Power Flow Using Holomorphic Embedding Load Flow Method

Bharath Varsh Rao [1,*] , Friederich Kupzog [1] and Martin Kozek [2]

[1] Electric Energy Systems—Center for Energy, AIT Austrian Institute of Technology, 1210 Vienna, Austria; friederich.kupzog@ait.ac.at

[2] Institute of Mechanics and Mechatronics—Faculty of Mechanical and Industrial Engineering, Vienna University of Technology, 1060 Vienna, Austria; martin.kozek@tuwien.ac.at

* Correspondence: bharath-varsh.rao@ait.ac.at; Tel.: +43-664-8825-6043

check for updates

Abstract: Distribution networks are typically unbalanced due to loads being unevenly distributed over the three phases and untransposed lines. Additionally, unbalance is further increased with high penetration of single-phased distributed generators. Load and optimal power flows, when applied to distribution networks, use models developed for transmission grids with limited modification. The performance of optimal power flow depends on external factors such as ambient temperature and irradiation, since they have strong influence on loads and distributed energy resources such as photo voltaic systems. To help mitigate the issues mentioned above, the authors present a novel class of optimal power flow algorithm which is applied to low-voltage distribution networks. It involves the use of a novel three-phase unbalanced holomorphic embedding load flow method in conjunction with a non-convex optimization method to obtain the optimal set-points based on a suitable objective function. This novel three-phase load flow method is benchmarked against the well-known power factory Newton-Raphson algorithm for various test networks. Mann-Whitney U test is performed for the voltage magnitude data generated by both methods and null hypothesis is accepted. A use case involving a real network in Austria and a method to generate optimal schedules for various controllable buses is provided.

1. Introduction

In recent years, with the integration of distributed generators, electric storage, electrical vehicles, and demand response units, the role of distribution systems is changing. Distributed energy units (DERs) are posing problems mainly in the low-voltage networks with their intermittency and uncontrollability. New innovative solutions are required to maintain grid security. Management of low-voltage distribution networks are challenging since they contain large array of devices which need to be controlled, and monitoring systems are limited. The above DERs along with loads should be run in a sustainable fashion since it is one of the biggest challenges. Various methods to control the DERs are presented in [1].

A so-called advanced distribution management system (ADMS) has come into existence, evolving from the transmission network's supervisory control and data acquisition systems (SCADA). This is possible with the increase in smart meters and monitoring devices in the network which provides data acquisition abilities [2]. ADMS provides functionalities such as load flow analysis, optimal power flow, monitoring and control capabilities similar to SCADA systems [3]. This must in theory, host advance functionalities such as adaptive protection leading to self-healing, real-time monitoring, dynamic

network reconfiguration and control [4–8]. This will provide intelligence to the grid with topology processor, state estimation, load and generation modeling [3]. The grid needs to be operated optimally and the power flows should be optimal to reduce losses, increase security, and maximize economic benefit. Energy balance should be maintained for secure operation of the network to maintain the frequency and voltage within its limits.

Optimal Power Flow (OPF) is one of the most fundamental functionalities of ADMS. In the literature, various OPF algorithms can be found. The authors in [9] describe an OPF algorithm to control active, reactive power, and transformer taps. The objective is to minimize system costs and losses. This method is based on Newton-Raphson load flow. Feasible power flow is solved, and the optimum is close to the load flow solution. Therefore, Jacobian information is used to calculate the optimum in a linear fashion. In [10], a non-linear programming technique is used to provide solution to OPF problem the objectives being economic dispatch and generation cost minimization. Same as before, load flow is performed to determine a feasible solution. Fletcher-Powell method is used to minimize the objective function. A general economic dispatch problem is implemented in [11]. This approach is similar to that in [9,10]. In [12], an OPF method for power system planning is provided. It used generalized reduced gradient technique to find the optimum. Hessian Matrix-based OPF method is illustrated in [13]. It combines non-linear programming, Newton-based methods and uses Hessian matrix load flow to minimize the quadratic objective. In [14], an OPF algorithm using Newton's method with Hessian in place of Jacobian matrix and Lagrangian multipliers is provided. It provides good convergence when compared to its predecessors. An OPF problem which includes steady-state security is presented in [15]. It is an extension of [9] which includes exact constraints on outage contingencies. In [16], a solution to the optimal dispatch problem using Jacobian matrix is implemented. It provides rapid convergence which can be used in online control. An OPF algorithm based on reduced gradient method is proposed in [17]. It is used to minimize generator loading and optimize voltage levels. Load flow equations are represented as equality constraints. The authors in [18] have described an OPF method using reduced Hessian matrix with systematic constraint handling. It provides accurate solution, good convergence, and description about acceleration factor is provided. In [19], modified recursive quadratic programming (MRQP)-based OPF is implemented. MRQP is based on [11]. An algorithm to solve large OPF problem is presented in [20]. It decomposes the original large problem into set of subproblems which are constrained linearly using augmented Lagrangian.

In 1991, a landmark paper [21] classified various OPF techniques into two categories. Class A describes a series of algorithms which uses ordinary load flow to get an intermediate solution and this solution is under normal circumstances is close to the optimal load flow solutions. Using Jacobian matrix and various other sensitivity relations, optimization is performed iteratively. At each iteration, new load flow is performed. The optimal solution of this class strongly depends on the accuracy of load flow solution. With a load flow solution, set of voltages, and phase angles, Jacobian matrix and set of incremental power flow equations are available or can be extended. If a load flow solution exists, it already satisfies all the constraints. The optimization problem is solved separately by incorporating the sensitivity relation from before to arrive at an optimal one. In [9] an implementation of Class A algorithm is provided. Another example of such implementation is provided in parts one and two in [22] and [23] respectively using linear programming.

Class B refers to the class of algorithms which depend on exact optimal conditions and therefore use load flow equations as equality constraints. The optimal solution is dependent on detailed formulation of the OPF problem with the entire search space. This does not need a load flow solution. However, these kinds of problems are non-convex in nature. Therefore, convex relaxation or non-convex solvers are needed to compute the optimum which poses its own difficulties. It deals with the optimality conditions from Lagrangian function and comprises of derivatives of constraints and objective functions. Since the Hessian matrix is sparse and remains constant, it further increases the simplicity of this method and ease at which the optimum is achieved. Constraint handling is

one of the biggest challenges of this class of algorithms. Using a heuristic method, constraints are handled as penalty terms which requires refactoring at every step and therefore, leads to degradation of the performance.

The above two classes of algorithms has various advantages and disadvantages. Performance of Class A directly depends in the performance of load flow techniques such as Newton-Raphson, Gauss-Seidel and widely used Fast Decoupled Method. It is shown in [24] that the above-mentioned methods have convergence and robustness issues. This may result in inaccurate load flow solutions. If the load flow does not result in a so-called high voltage or operable solution, Class A algorithms fails. In Class B algorithms, getting a global operable solution is challenging since it needs convex relaxation or heuristic techniques and the operable solution is difficult to achieve by respecting all the constraints.

The authors in this paper present a third class of algorithms, a Class C. This class combines Class A and Class B. It uses a reliable load flow described in Section 2 method wrapped around a heuristic to determine the optimal solution. The load flow provides accurate operable voltage and phase angle solution at every step and the heuristic uses this as equality constraints as described in Class B. Class C algorithms present various advantages. Operable voltage and phase angle solution is obtained at each iteration with the help of THELM. THELM always finds a solution, if it exists, irrespective of initial conditions whereas, Newton-Raphson load flow method leads to a non-convergent solution at very low or high loading conditions [24]. Since THELM is used in Class C method, the results are high voltage and operable. Global OPF solution can be obtained with a non-convex solver.

The following contributions and structure of the paper is as follows,

1. Load Flow Solution to three-phase unbalanced distribution network using Holomorphic Embedding Load Flow Method (HELM) is described in Section 2.
2. Benchmarking of HELM against established Newton-Raphson load flow solver from DIgSILENT PowerFactory [25] which is a well-known power system simulation and analysis software. This is discussed in Section 2.
3. OPF using Distributed Genetic Algorithm, a Class C algorithm is described in detail in Section 3
4. Simulation of OPF is performed to generate active and reactive power schedules at controllable nodes (see Section 5). This algorithm is applied to a real network in Austria.

2. Three-Phase Unbalanced Load Flow Method

A solution to the load flow problem is mostly obtained using numerical iterative methods such as Gauss-Seidel with its slow convergence and improved Newton-Raphson method, which provides better convergence [26,27]. Newton-Raphson method is computationally expensive since it must calculate Jacobean matrix at each iteration step in-spite of using sparse matrix techniques [28]. Various decoupled methods have been implemented which exploits the weak link between active power and voltage, in which Jacobian matrix needs to be calculated only once. One such method is Fast Decoupled Load Flow method which is widely used in the community [29]. The above-mentioned iterative techniques face similar problems with no guaranteed convergence since it depends on the initial conditions. This is due to the fact that load flow equations are non-convex in nature with multiple solutions. It is difficult to control the way these iterative methods converge to an operable solution [24]. In the literature, multiple implementations to improve the convergence of such traditional algorithm have been illustrated with limited success [30–36].

To use load flow methods in near or real-time applications, the physical models should fully deterministic and solved with reliability. HELM is one such candidate which can full fill these requirements [24].

Three-Phase Holomorphic Embedding Load Flow Method

Power flow equations, for example, the load bus equation described in Equation (1) is inherently non-analytical. Holomorphic principles can be applied to such equations by means of embedding a complex variable α such that the resulting problem is analytic in nature.

$$\sum_{k \in \Omega} Y_{ik} V_k = \frac{S_i^*}{V_i^*}, \;\; i \in \Omega_{PQ} \tag{1}$$

Voltage of the slack bus is assumed to be $V_0 = 1.0$ pu. and Bus 00 (see Appendix A) is always set to be slack bus.

Holomorphic embedding can be done in various methods. Equation (2) represents the simplest form. Bus voltages are the functions of the demand scalable complex variable α.

$$\sum_{k \in \Omega} Y_{ik} V_k(\alpha) = \frac{\alpha S_i^*}{V_i^*(\alpha^*)}, \;\; i \in \Omega_{PQ} \tag{2}$$

The research work in [24] suggests that the operable voltage solution can be obtained by analytic continuum of Equation (2) at $\alpha = 1$ using the unique solution which exists when $\alpha = 0$

$$\sum_{k \in \Omega} Y_{ik} V_k(\alpha) = \frac{\alpha S_i^*}{\overline{V}_i(\alpha^*)}, \;\; i \in \Omega_{PQ} \tag{3}$$

$$\sum_{k \in \Omega} Y_{ik}^* \overline{V}_k(\alpha) = \frac{\alpha S_i}{V_i(\alpha)}, \;\; i \in \Omega_{PQ} \tag{4}$$

Equations (3) and (4), represent a set of polynomial equations and by using the Grobner bases, V_i and $\overline{V}_i$ are holomorphic except for finite singularities.

$$\overline{V}_i(\alpha) = (V_i(\alpha^*))^*, \;\; i \in \Omega \tag{5}$$

According to [24], if Equation (5) holds good, then Equations (3) and (4) can be reduced to Equation (2). Equation (5) is referred to as reflecting condition.

Since voltages of from Equation (2) for $\alpha = 0$ as discussed above, it can be extended to power series described in Equation (6) and (7) at $\alpha = 0$.

$$V_i(\alpha) = \sum_{n=0}^{\infty} V_i[n] \alpha^n, \;\; i \in \Omega \tag{6}$$

$$\frac{1}{V_i(\alpha)} = W_i(\alpha) = \sum_{n=0}^{\infty} W_i[n] \alpha^n, \;\; i \in \Omega \tag{7}$$

Equation (9) is obtained by substituting 7 into 2 and power series coefficients can be calculated to a desired degree.

$$\sum_{k \in \Omega} Y_{ik}^* \sum_{n=0}^{\inf} V_k[n](\alpha^n) = \alpha S_i^* W_i^*[n] \alpha^n \tag{8}$$

The following steps are involved to calculate voltages.

1. For $\alpha = 0$, solve Equation (9) to obtain a linear equation where the left-hand side of the equation represents the slack bus at which $V_0[\alpha] = 1$.

$$\sum_{k \in \Omega} Y_{ik} V_k[0] = 0, \;\; i \in \Omega_{PQ} \tag{9}$$

2. The reduced Y bus matrix is assumed to be non-singular. Equation (10) can be obtained based on the non-singularity assumption.

$$W_i[0] = \frac{1}{V_i[0]} \tag{10}$$

3. Remaining power series coefficients can be obtained to the desired n^{th} degree by equating the coefficients from Equation (11)

$$\sum_{k\in\Omega} Y_{ik}V_k[0] = S_i^* W_i^*[n-1], \;\; i \in \Omega_{PQ} \;\; n \geq 1 \tag{11}$$

$W_i[n-1]$ are calculated using the lower order coefficients described in Equation (12).

$$W_i[n-1] = -\frac{\sum_{m=0}^{n-2} V_i[n-m-1]W_i[m]}{V_i[0]} \tag{12}$$

4. Pade approximations which are particular kind of rational approximations are used for analytical continuum to determine the voltages at $\alpha = 1$.

Based on the fundamentals of HELM discussed above, various research work dealing with enhancing or improving the method is available. One of the major deficiencies of the HELM described in [24] is that the PV/Generator bus is not defined. A PV bus model was presented in [37]. Ref. [38] presents an improved PV bus model and the major contribution of this paper is to provide alternative models capable of solving general networks. The authors have provided four methods with various parameters for PV bus. In the literature, three-phase formulation of HELM is lacking. In this paper, method four developed in [38] is extended to a novel three-phase unbalanced formulation which can be seen below. Equation (13) represents a general form of three-phase unbalanced HELM. Network models including various device models such as loads, generators, transformers are derived from the models developed in [39]. The seed solution, non-singularity of matrix A in Equation (14) and the reflective conditions of holomorphic functions are taken, as is, from [38]. Three-phase unbalanced form for a multi-bus system for PQ and PV bus types is presented below.

$$\begin{bmatrix} A_1^a & A_1^b & A_1^c & A_2^a & A_2^b & A_2^c \\ A_{PQ_3}^a & A_{PQ_3}^b & A_{PQ_3}^c & A_{PQ_4}^a & A_{PQ_4}^b & A_{PQ_4}^c \\ A_{PV_3}^a & A_{PV_3}^b & A_{PV_3}^c & A_{PV_4}^a & A_{PV_4}^b & A_{PV_4}^c \end{bmatrix} \begin{bmatrix} Re\{V^a[n]\} \\ Re\{V^b[n]\} \\ Re\{V^c[n]\} \\ Im\{V^a[n]\} \\ Im\{V^b[n]\} \\ Im\{V^c[n]\} \end{bmatrix} = \begin{bmatrix} r_{1,n-1} \\ r_{PQ_{2,n-1}} \\ r_{PV_{2,n-1}} \end{bmatrix} \tag{13}$$

Is of the form,

$$Ax = b \tag{14}$$

where the matrix A can be further clarified as,

$$
\begin{aligned}
A_{1_{ij}}^P &= G_{ij}^P + \delta i, jRe\{y_i^P\}, & i,j \in \Omega, P \in a,b,c \\
A_{2_{ij}}^P &= B_{ij}^P - \delta i, jIm\{y_i^P\}, & i,j \in \Omega, P \in a,b,c \\
A_{PQ_{3_{ij}}}^P &= B_{ij}^P - \delta i, jIm\{y_i^P\}, & i,j \in \Omega_{PQ}, P \in a,b,c \\
A_{PV_{3_{ij}}}^P &= 2\delta i, j, & i,j \in \Omega_{PV}, P \in a,b,c \\
A_{PQ_{4_{ij}}}^P &= G_{ij}^P + \delta i, jIm\{y_i^P\}, & i,j \in \Omega_{PQ}, P \in a,b,c \\
A_{PV_{4_{ij}}}^P &= 0, & i,j \in \Omega_{PV}, P \in a,b,c
\end{aligned}
\tag{15}
$$

where G and B are the conductance and susceptance, respectively. $\delta i, j = 1$ if $i = j$, else 0.

The right-hand side matrix elements are defined as follows,

$$r_{1,n-1,i} = \delta_{n,1}(P_i - Re\{y_i\}) - Re\left\{\sum_{m=1}^{n-1} V_i^*[m] \sum_{k\in\Omega} \sum_{p\in P} Y_{ik} V_k[n-m]\right\}, \qquad i \in \Omega \tag{16a}$$

$$r_{PQ2,n-1,i} = \delta_{n,1}(-Q_i - Im\{y_i\}) - Im\left\{\sum_{m=1}^{n-1} V_i^*[m] \sum_{k\in\Omega} \sum_{p\in P} Y_{ik} V_k[n-m]\right\}, \qquad i \in \Omega_{PQ} \tag{16b}$$

$$r_{PV2,n-1,i} = -\sum_{m=1}^{n-1} \sum_{p\in P} V_i^*[m] V_i[n-m] + (1 + \alpha(M_i - 1)^2)[n], \qquad i \in \Omega_{PV} \tag{16c}$$

where, M_i is the target voltage magnitude for PV bus.

The power series were calculated for using the above equations and Viskovatov Pade approximant algorithm is used to determine the voltages and phase angles similar to the ones in [24,37].

3. Optimal Power Flow Model

As described in Section 1, OPF algorithms can be classified under three classes. There have been a lot of research on OPF and this can be seen in the vast array of work available in the literature.

Type C algorithms requires non-convex solvers to perform optimization problems. Non-convex solvers have been previously used to solve OPF problems but, they are used in the context of Class B algorithms. The authors in [40] have provided a method to plan reactive power flows optimally using generic algorithm as it provides optimum which is a global one. The proposed method is applied to two 51 and 224 bus networks. An OPF problem is solved using generic algorithm in [41] as a unified power flow controller to regulate branch voltages with respect to both angle and magnitude. It minimizes real power losses and security limits of power flows are maintained. Reactive power planning using hybrid genetic algorithm is presented in [42]. It uses genetic algorithm at the highest level and linear programming to get the optimum sequentially. This can be considered as a modified version of Class A. It uses genetic algorithm instead of just load flow to determine the initial converged solution to the OPF problem.

In [43], a feeder reconfiguration technique is presented. It uses genetic algorithm in the context of OPF to reduce losses in a distribution system. Switches are opened to determine the initial population. The authors in [44], have presented a hybrid evolutionary algorithm with multi-objective OPF. It is used to minimize losses, voltage, and power flow deviations and generator costs. In [45], optimal placement and sizing of capacitor banks in distributed networks using genetic algorithm is presented. The objective is to simultaneously improve the power quality and sizing of fixed capacitor banks.

In this paper, the OPF problem is formulated as follows,

$$\begin{aligned}
\underset{x}{\text{minimize}} \quad & F(x,u) \\
\text{subject to} \quad & u \in U \\
& G(x,u) = 0, \\
& H(x,u) \leq 0
\end{aligned} \tag{17}$$

where,

x and u represent sets of state and input variables.

$F(x,u)$ is the objective function for the OPF problem. Typical objectives are total generator cost, loss minimization in network and in this paper, the objective function chosen is the three-phase unbalance minimization (see Section 4).

$G(x,u)$ and $H(x,u)$ represents the equality and inequality constraints of the OPF problem.

In the context of type C algorithms, accurate and reliable load flow is used as equality constraints. In this case, THELM is used.

Typical inequality constraints for a three-phase unbalanced distribution grids are enlisted below,

Limits on active power (kW) of a (generator) PV node:	$P_{Low_i} \leq P_{PV_i} \leq P_{High_i}$
Limits on voltage (V (pu.)) of a PV or PQ node:	$|V_{Low_i}| \leq |V_i| \leq |V_{High_i}|$
Limits on tap positions of a transformer:	$t_{Low_i} \leq t_i \leq t_{High_i}$
Limits on phase shift angles of a transformer:	$\theta_{Low_i} \leq \theta_i \leq \theta_{High_i}$
Limits on shunt capacitances or reactances:	$s_{Low_i} \leq s_i \leq s_{High_i}$
Limits on reactive power (kVAr) generation of a PV node:	$Q_{Low_i} \leq Q_{PV_i} \leq Q_{High_i}$
Upper limits on active power flow in transmission lines or transformers:	$P_{i,j} \leq P_{High_{i,j}}$
Upper limits on MVA flows in lines or transformers:	$P_{i,j}^2 + Q_{i,j}^2 \leq S_{High_{i,j}}^2$
Upper limits on current magnitudes in lines or transformers:	$|I_{i,j}| \leq |I_{High_{i,j}}|$
Limits on voltage angles between nodes:	$\Theta_{Low_i} \leq \Theta_i - \Theta_j \leq \Theta_{High_i}$

In this paper, the non-convex solver used is a genetic algorithm, to minimize the objective function. Genetic algorithm is chosen due to its wide use in OPF techniques, ease of parallelizability to handle large networks and its probabilistic transition rule. The authors have used the method developed in [46]. Genetic algorithms of the kind, mixed integer non-linear non-convex is used to include all the constraints mentioned above. To accommodate THELM in genetic algorithm, it is included in the fitness function and penalty functions are used to include constraints.

4. Three-Phase Unbalance Minimization

As mentioned in Section 1, it is essential to manage the distribution network optimally and in a balanced fashion. Various methods have been presented in the literature to minimize three-phase unbalance. In [47], a method to minimize three-phase unbalance is presented. Reactive power compensation is performed using flexible AC transmission system (FACTS) devices to minimize the three-phase unbalance. It is applied to a simple study case of four bus system. This method does not provide optimal scheduling of loads and does not include all the buses in the network. It is applicable only to local grid where the FACTS devices are located. The authors in [48] have provided a method to minimizing network unbalance using phase swapping. A genetic and greedy algorithm is used to optimally swap the phases to generate a convenient solution, leading to a minimum number of swaps to minimize network unbalance. In [49], plug-in hybrid electric vehicles are used to minimize local three-phase unbalance. It does not include a grid perspective and is done only on the point of common coupling.

In this paper, OPF from Section 3 is applied to a real network in Austria. Figure 1 represents a real low-voltage distribution network. In this use case, the objective function is to minimize three-phase voltage unbalance which can be seen in Equation (18). This objective can be realized in multiple ways and in this paper, reference balanced voltages are used.

$$\text{minimize } J = \sum_{k \in \Omega} \sum_{p \in P} (real(V_{k,balanced}^p) - real(V_k^p))^2 + (imag(V_{k,balanced}^p) - imag(V_k^p))^2 \quad (18)$$

where, $P \in phases(a, b, c)$ and B represented all the buses in the network. The voltages are represented in rectangular coordinate system with real part of voltage being the magnitude and imaginary part being the phase angle. Both real and imaginary value are considered because both phase and angle of voltages need to be balanced.
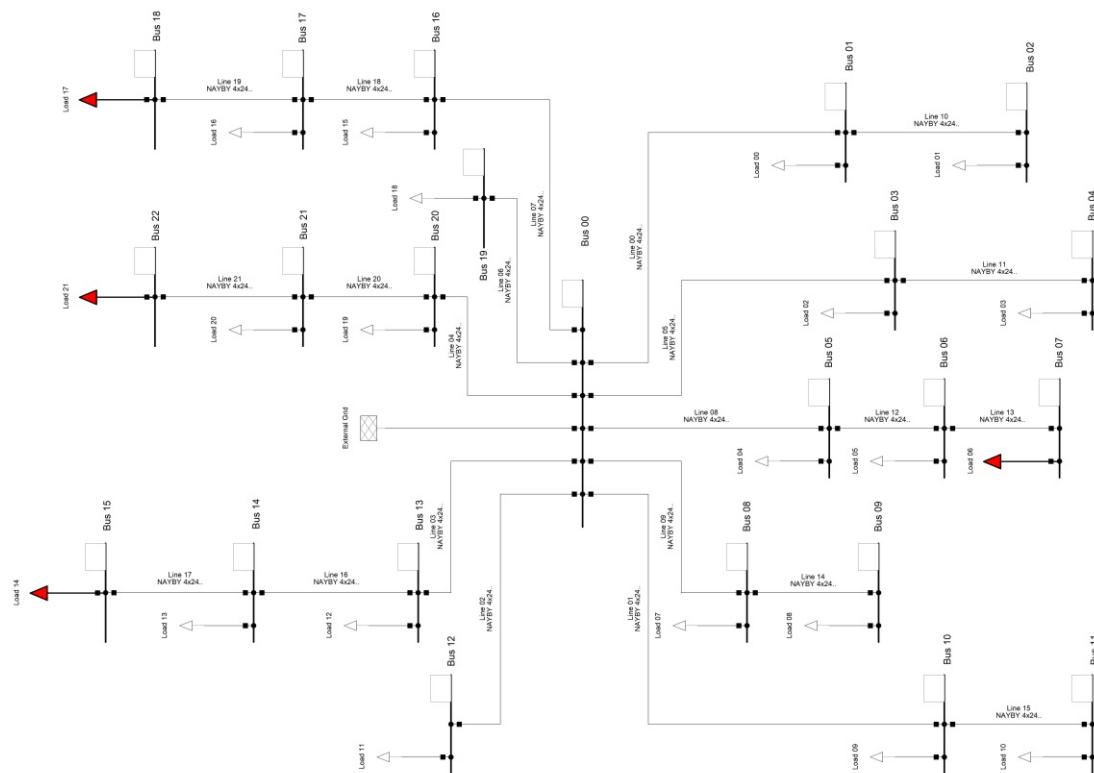
Figure 1. Topology of a real network in Austria with controllable loads at Bus 07, Bus 15, Bus 18, Bus 22. It represents a three-phase unbalance low-voltage distribution network with bus voltages rated at 0.4 kV.

The controllable variables are per phase active (P) and reactive powers (Q) at buses 07, 15, 18, and 22. The single-phase loads are replaced with three-phase loads (see Figure 2).
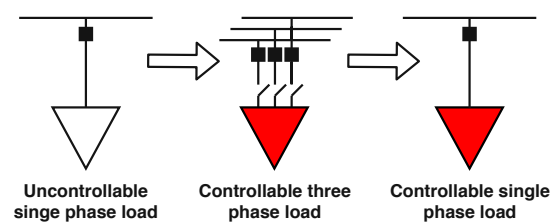
Figure 2. Single-phase loads are replaced by three-phase ones which can take both positive and negative values.

For simplicity of representation, these three-phase loads are represented as single-phase loads with red coloring. This can be observed in Figure 1. P and Q on individual loads can be modulated by the OPF algorithm and can take values which are both positive and negative essentially, acting as a prosumer node.

5. Simulation Results

This section provides simulation results to the concepts presented in the previous sections. In Section 5.1, THELM described in Section 2 is validated against DIgSILENT PowerFactory Newton-Raphson algorithm. In Section 5.2, simulation results for three-phase unbalanced optimal power is presented with the three-phase unbalance minimization objective presented in Section 4.

5.1. Validation of THELM

THELM is benchmarked against load flow solver in an established power system analysis tool, DIgSILENT PowerFactory. Various simple networks are drawn with increased level of complexity (see Appendix A).

Voltages from 1000 random load flows by varying active and reactive power at load buses from ± 10 kW and ± 0.8 kVAr (which accounts for power factor 0.9) are generated and tabulated below.

Mann-Whitney U test is used to compare the sample means of voltage magnitudes from the two methods, since the samples are non-parametric in nature. It checks whether to accept or reject the null hypothesis. Mann-Whitney U test is similar to student's T test but is suitable for non-parametric samples. A sample of 100 voltages from both THELM and Power Factory NR methods are used. Various statistical information and test results are tabulated in Table 1. Columns mean, standard deviation, min, 25%, 50%, 75%, max are calculated by taking the absolute difference between their respective voltages. All the data above is calculated by taking the average between various buses and phases. From the column statistic and p-value, it can be observed that their means are statistically insignificant, and the null hypothesis is accepted. The results from the test suggests that THELM produces results which are acceptable for load flow analysis with lower deviations from one another.

**Table 1.** Benchmarking THELM against Power Factory NR method.

	Mean	Std	Min	25%	50%	75%	Max	Statistic	p Value
Test 00	0.00489	0.00350	1.14×10^{-5}	0.00194	0.00430	0.00724	0.01591	2.38719	0.016977
Test 01	0.00572	0.00414	1.01×10^{-5}	0.00237	0.00496	0.00846	0.01938	3.23993	0.001195
Test 02	0.00209	0.00027	0.00167	0.00186	0.00205	0.00228	0.00287	5.47075	4.48×10^{-8}
Test 03	0.00015	0.00028	9.38×10^{-8}	4.57×10^{-5}	9.85×10^{-5}	0.00018	0.00529	-4.69619	2.65×10^{-6}
Test 04	0.00343	0.00246	1.08×10^{-5}	0.00144	0.00296	0.00508	0.01125	-5.6259	1.84×10^{-8}
Test 05	0.00178	0.00023	0.00142	0.00159	0.00175	0.00195	0.00241	-5.83359	5.42×10^{-9}
Test 06	0.05586	0.01114	0.02464	0.04779	0.05540	0.06339	0.09113	5.69187	1.25×10^{-8}

*5.2. Simulation Results for Three-Phase Unbalanced Optimal Power Flow*

Simulation is performed for the real grid detailed in Figure 1 using OPF algorithm described in Section 3. It is performed for one day from 2018-8-31 00:00:00 to 2018-9-01 00:00:00 with the sampling time of 15min (96 intervals). Load profiles are from smart-meter data, from real households and are acquired from all the buses in the network updating a database. Forecasted profiles are inputs to the OPF algorithm and optimal schedules are generated based on it. Load forecasting is performed for this time horizon using convolutional neural networks, using data until 2018-8-30 23:45:00. It is performed for one day (day ahead forecast) and more details able it is not provided since it is out of scope.

Load flow solution is non-causal in nature and to generate an optimal schedule for controllable buses, it must be run for all 96 intervals. OPF is performed using Class C algorithm presented in Section 3 for controllable buses described in Section 4. It can also be observed that the optimal schedules are generated for all the three phases and can take both positive and negative values. Real profile is recorded during day for uncontrollable loads at the buses.

Forecasted, optimal and real active and reactive power consumption profiles at one of the controllable buses (Bus 15) can be seen in Figures 3 and 4 respectively. At Bus 15, all the loads are single phased (connected to phase C).
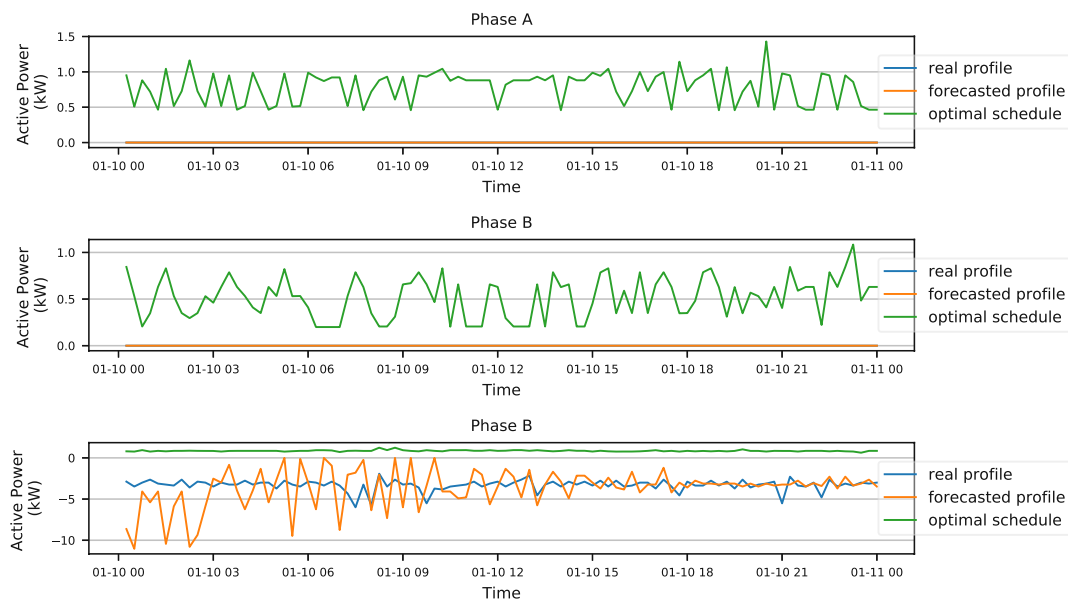
Figure 3. Active power of real, forecasted, and optimal profiles at Bus 15. It can be observed that the real and forecasted data is zero for phases A and B. This is for to the fact that the loads are single phased and connected only to phase C. During the OPF, they are replaced with three-phase controllable loads. On the x-axis, data time format is MM-dd HH. Data is from 2018-8-31 00:00:00 to 2018-9-01 00:00:00.
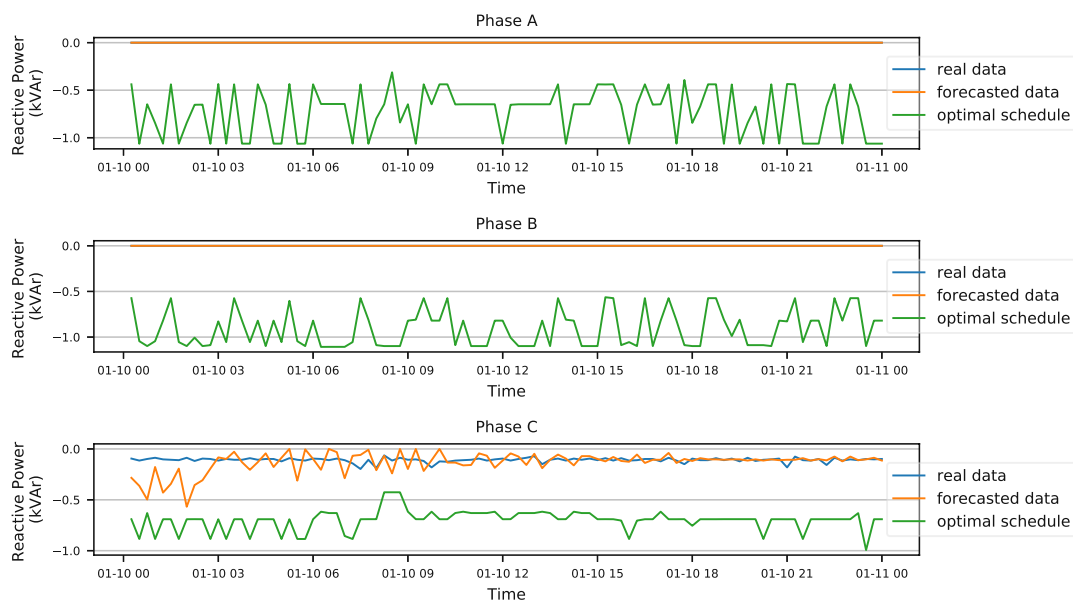
Figure 4. Reactive Power of real, forecasted, and optimal schedules at Bus 15. On the x-axis, data time format is MM-dd HH. Data is from 2018-8-31 00:00:00 to 2018-9-01 00:00:00.

Active and reactive power for all the phases can be observed in Figures 3 and 4.

Using the three schedules shown in Figures 3 and 4, load flows are performed using THELM described in Section 2. Loads flows are performed for all intervals and are represented using box-plots.

Figure 5 describes the averaged objective function values based on Equation (18). It can be observed that the three-phase unbalance has been reduced from 0.879 for real and forecasted profiles

to 0.529 for optimal profiles which accounts for 39% unbalance minimization based on the defined objective function (see Section 4).
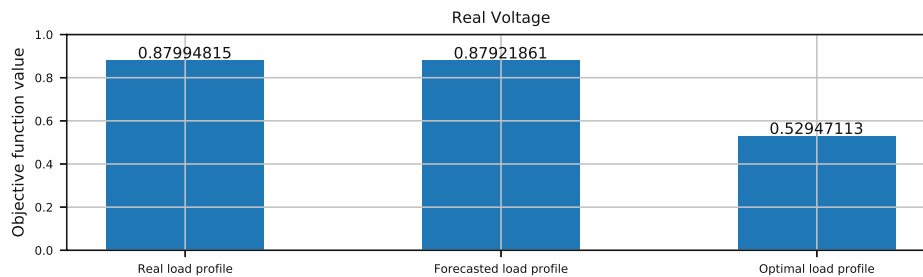

Figure 5. Average values of optimal power flow objective for real, forecasted, optimal voltage and phase angles based on Equation (18).

From Figure 6, it can be observed that the voltages are indeed balanced, and the average values are close to balanced voltages. Additionally, the nature of the objective function used has also caused the voltages to cluster around 1 pu. since the balanced real part of the balanced voltage is exactly 1 pu.
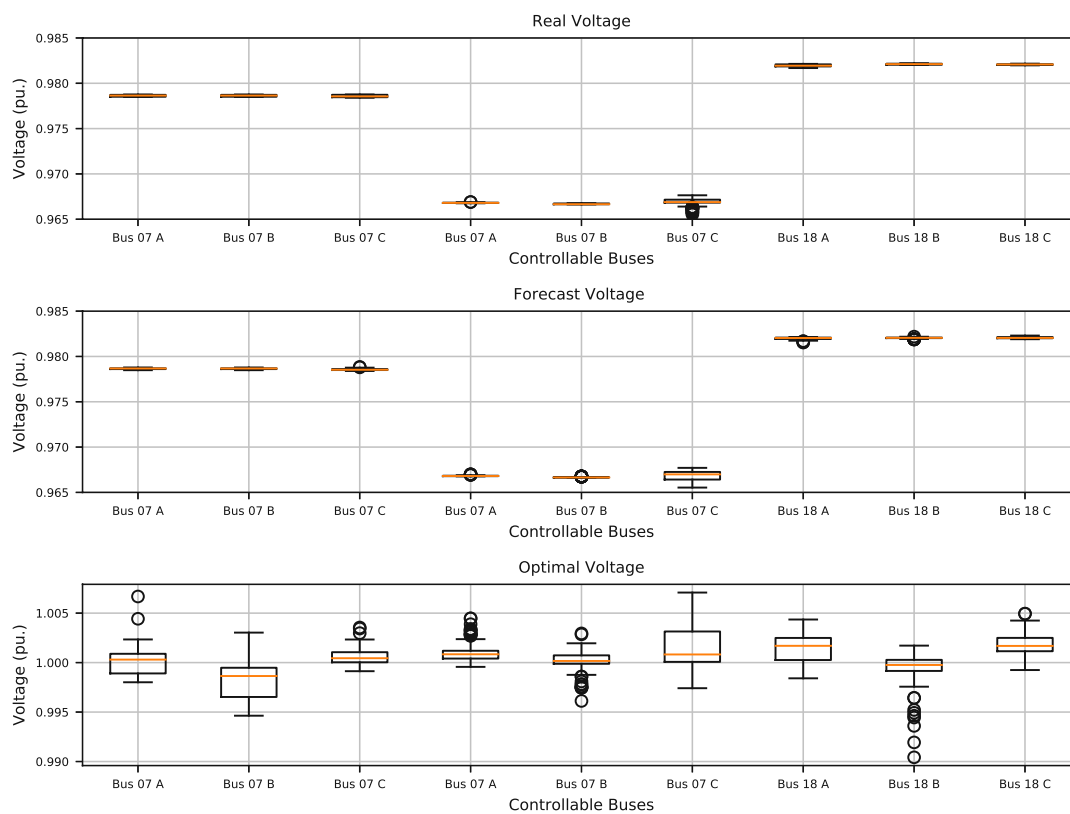

Figure 6. Voltage profiles generated from real, forecasted and optimal schedules from Figures 3 and 4.

6. Conclusions and Outlook

In this paper, a novel class of OPF algorithm is presented. It uses a novel three-phase unbalanced HELM presented in Section 2. Benchmarks are performed to test the performance of THELM and DIgSILENT Power Factory Newton-Raphson method described in Section 5.1. These benchmarks were performed on various test networks. Mann-Whitney U test was performed, and it was concluded that the results from both load flow methods were statistically indistinguishable and null hypothesis was accepted. Using THELM, optimal power flow method was developed using genetic algorithm in Section 3, describing the type C class of algorithms. The novel Class C algorithm provides various advantages over Class A and B OPF algorithms as discussed in Section 1. A use case with an objective function to minimize three-phase unbalance was applied to a real network in Austria in Section 5. The reason for choosing this objective is motivated by the requirements of the network operator and to handle the unbalance locally. It involves the generation of active and reactive power schedules for four controllable buses using smart-meter forecasts from other uncontrollable loads in the network (see Figure 1). Optimal schedules for these buses were generated and used to produce voltages using THELM and the results were described in Figure 6. It can be observed that the three-phase voltage unbalance has reduced up to 39% and the optimal average objective function values can be observed in Figure 5.

In future work, the scalability and replicability of the method needs to be analyzed. The method needs to be applied to various larger networks with large number of nodes. Simulation time and code optimization is not considered a priority for this study. To use this method in a real-time or near-real-time operation, the algorithm needs to be optimized. In this work, only three-phase unbalance minimization is used. OPF with various other objective functions need to be considered.

Appendix A. Test Networks

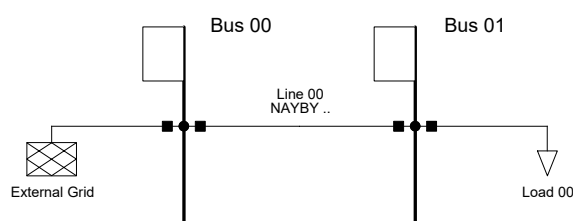Various test networks used for the analysis described in Section 5.1.
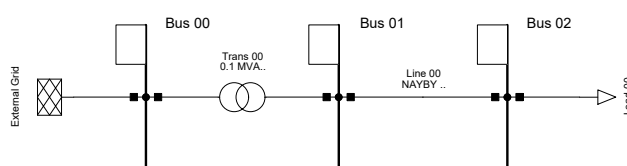

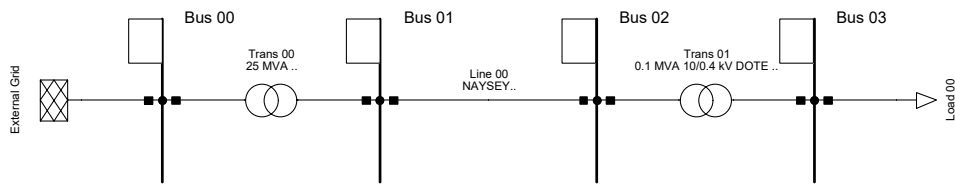
Figure A1. Test 00.
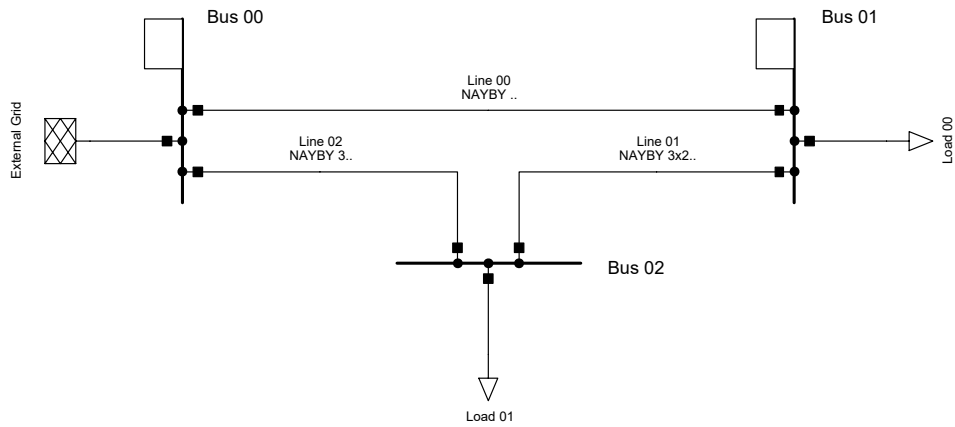

Figure A2. Test 01.

Figure A3. Test 02.
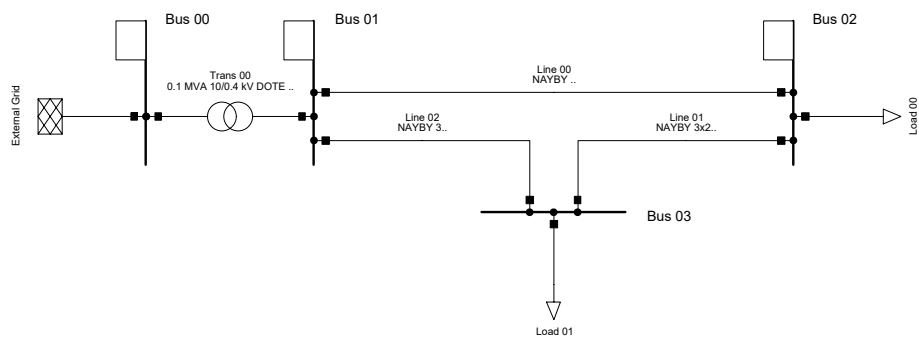

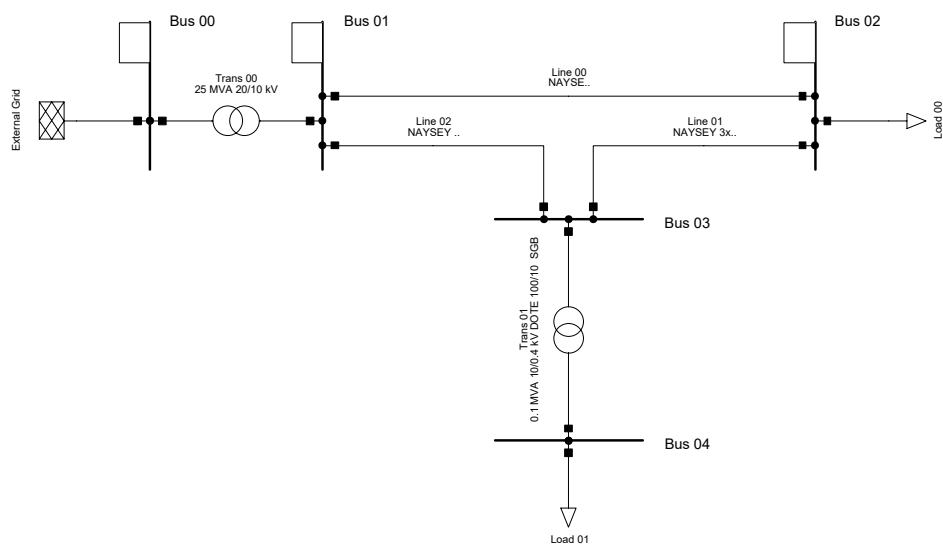**Figure A4.** Test 03.

Figure A5. Test 04.
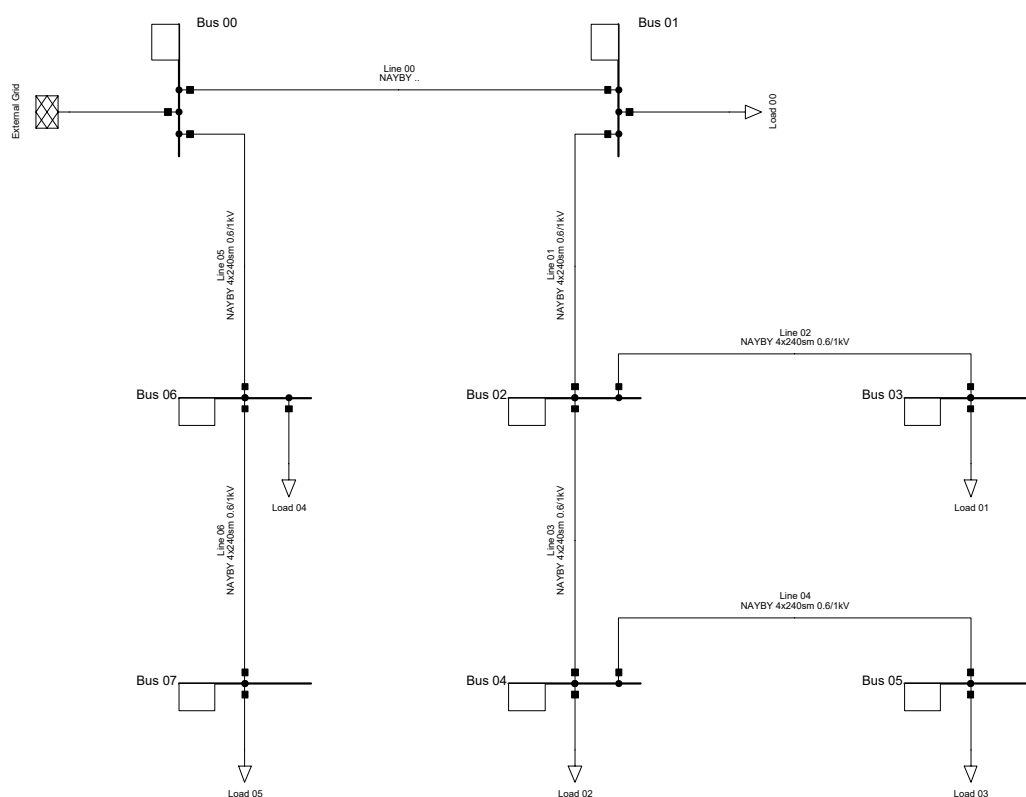

Figure A6. Test 05.

Figure A7. Test 06.

References

1. Serițan, G.; Porumb, R.; Cepișcă, C.; Grigorescu, S. Integration of Dispersed Power Generation. In *Electricity Distribution: Intelligent Solutions for Electricity Transmission and Distribution Networks*; Energy Systems; Karampelas, P., Ekonomou, L., Eds.; Springer: Berlin/Heidelberg, Germany, 2016; pp. 27–61. [CrossRef]
2. Campos, F.; Marques, L.; Silva, N.; Melo, F.; Seca, L.; Gouveia, C.; Madureira, A.; Pereira, J. ADMS4LV #8211; Advanced Distribution Management System for Active Management of LV Grids. *CIRED Open Access Proc. J.* **2017**, *2017*, 920–923. [CrossRef]
3. Fan, J.; Borlase, S. The Evolution of Distribution. *IEEE Power Energy Mag.* **2009**, *7*, 63–68. [CrossRef]
4. Horowitz, S.H.; Phadke, A.G. Boosting Immunity to Blackouts. *IEEE Power Energy Mag.* **2003**, *1*, 47–53. [CrossRef]
5. Novosel, D.; Begovic, M.M.; Madani, V. Shedding Light on Blackouts. *IEEE Power Energy Mag.* **2004**, *2*, 32–43. [CrossRef]
6. Taylor, C.W.; Erickson, D.C.; Martin, K.E.; Wilson, R.E.; Venkatasubramanian, V. WACS-Wide-Area Stability and Voltage Control System: R D and Online Demonstration. *Proc. IEEE* **2005**, *93*, 892–906. [CrossRef]
7. Ilic, M.D.; Allen, H.; Chapman, W.; King, C.A.; Lang, J.H.; Litvinov, E. Preventing Future Blackouts by Means of Enhanced Electric Power Systems Control: From Complexity to Order. *Proc. IEEE* **2005**, *93*, 1920–1941. [CrossRef]
8. Santo, M.D.; Vaccaro, A.; Villacci, D.; Zimeo, E. A Distributed Architecture for Online Power Systems Security Analysis. *IEEE Trans. Ind. Electron.* **2004**, *51*, 1238–1248. [CrossRef]
9. Dommel, H.W.; Tinney, W.F. Optimal Power Flow Solutions. *IEEE Trans. Power Appar. Syst.* **1968**, *PAS-87*, 1866–1876. [CrossRef]
10. Sasson, A.M. Combined Use of the Powell and Fletcher—Powell Nonlinear Programming Methods for Optimal Load Flows. *IEEE Trans. Power Appar. Syst.* **1969**, *PAS-88*, 1530–1537. [CrossRef]
11. El-abiad, A.H.; Jaimes, F.J. A Method for Optimum Scheduling of Power and Voltage Magnitude. *IEEE Trans. Power Appar. Syst.* **1969**, *PAS-88*, 413–422. [CrossRef]

12. Peschon, J.; Bree, D.W.; Hajdu, L.P. Optimal Power-Flow Solutions for Power System Planning. *Proc. IEEE* **1972**, *60*, 64–70. [CrossRef]
13. Sasson, A.M.; Viloria, F.; Aboytes, F. Optimal Load Flow Solution Using the Hessian Matrix. *IEEE Trans. Power Appar. Syst.* **1973**, *PAS-92*, 31–41. [CrossRef]
14. Rashed, A.M.H.; Kelly, D.H. Optimal Load Flow Solution Using Lagrangian Multipliers and the Hessian Matrix. *IEEE Trans. Power Appar. Syst.* **1974**, *PAS-93*, 1292–1297. [CrossRef]
15. Alsac, O.; Stott, B. Optimal Load Flow with Steady-State Security. *IEEE Trans. Power Appar. Syst.* **1974**, *PAS-93*, 745–751. [CrossRef]
16. Happ, H.H. Optimal Power Dispatch. *IEEE Trans. Power Appar. Syst.* **1974**, *PAS-93*, 820–830. [CrossRef]
17. Mukherjee, P.K.; Dhar, R.N. Optimal Load-Flow Solution by Reduced-Gradient Method. *Proc. Inst. Electr. Eng.* **1974**, *121*, 481–487. [CrossRef]
18. Bala, J.L.; Thanikachalam, A. An Improved Second Order Method for Optimal Load Flow. *IEEE Trans. Power Appar. Syst.* **1978**, *PAS-97*, 1239–1244. [CrossRef]
19. Lipowski, J.S.; Charalambous, C. Solution of Optimal Load Flow Problem by Modified Recursive Quadratic-Programming Method. *Transm. Distrib. IEE Proc. C Gener.* **1981**, *128*, 288–294. [CrossRef]
20. Burchett, R.C.; Happ, H.H.; Wirgau, K.A. Large Scale Optimal Power Flow. *IEEE Trans. Power Appar. Syst.* **1982**, *PAS-101*, 3722–3732. [CrossRef]
21. Glavitsch, H.; Bacher, R. Optimal Power Flow Algorithms. *Control Dyn. Syst.* **1991**, *41*, 135–205. [CrossRef]
22. Stott, B.; Hobson, E. Power System Security Control Calculations Using Linear Programming, Part I. *IEEE Trans. Power Appar. Syst.* **1978**, *PAS-97*, 1713–1720. [CrossRef]
23. Stott, B.; Hobson, E. Power System Security Control Calculations Using Linear Programming, Part II. *IEEE Trans. Power Appar. Syst.* **1978**, *PAS-97*, 1721–1731. [CrossRef]
24. Trias, A. The Holomorphic Embedding Load Flow Method. In Proceedings of the 2012 IEEE Power and Energy Society General Meeting, San Diego, CA, USA, 22–26 July 2012; pp. 1–8. [CrossRef]
25. Home—DIgSILENT. Available online: https://www.digsilent.de/en/ (accessed on 1 February 2019).
26. Ward, J.B.; Hale, H.W. Digital Computer Solution of Power-Flow Problems [Includes Discussion]. *Trans. Am. Inst. Electr. Eng. Part III Power Appar. Syst.* **1956**, *75*, 398–404. [CrossRef]
27. Tinney, W.F.; Hart, C.E. Power Flow Solution by Newton's Method. *IEEE Trans. Power Appar. Syst.* **1967**, *PAS-86*, 1449–1460. [CrossRef]
28. Tinney, W.F.; Walker, J.W. Direct Solutions of Sparse Network Equations by Optimally Ordered Triangular Factorization. *Proc. IEEE* **1967**, *55*, 1801–1809. [CrossRef]
29. van Amerongen, R.A.M. A General-Purpose Version of the Fast Decoupled Load Flow. *IEEE Trans. Power Syst.* **1989**, *4*, 760–770. [CrossRef]
30. Stott, B. Effective Starting Process for Newton-Raphson Load Flows. *Proc. Inst. Electr. Eng.* **1971**, *118*, 983–987. [CrossRef]
31. Tripathy, S.C.; Prasad, G.D.; Malik, O.P.; Hope, G.S. Load-Flow Solutions for Ill-Conditioned Power Systems by a Newton-Like Method. *IEEE Power Eng. Rev.* **1982**, *PER-2*, 25–26. [CrossRef]
32. Schaffer, M.D.; Tylavsky, D.J. A Nondiverging Polar-Form Newton-Based Power Flow. *IEEE Trans. Ind. Appl.* **1988**, *24*, 870–877. [CrossRef]
33. Tylavsky, D.J.; Crouch, P.E.; Jarriel, L.F.; Chen, H. Advances in Fast Power Flow Algorithms. *Control Dyn. Syst.* **1991**, *44*, 295–343. [CrossRef]
34. Crouch, P.E.; Tylavsky, D.J.; Chen, H.; Jarriel, L.; Adapa, R. Critically Coupled Algorithms for Solving the Power Flow Equation. *IEEE Trans. Power Syst.* **1992**, *7*, 451–457. [CrossRef]
35. Tylavsky, D.J.; Crouch, P.E.; Jarriel, L.F.; Singh, J.; Adapa, R. The Effects of Precision and Small Impedance Branches on Power Flow Robustness. *IEEE Trans. Power Syst.* **1994**, *9*, 6–14. [CrossRef]
36. Tylavsky, D.J.; Schaffer, M.D. A Nondiverging Power Flow Using a Least-Power-Type Theorem. *IEEE Trans. Ind. Appl.* **1987**, *IA-23*, 944–951. [CrossRef]
37. Subramanian, M.K.; Feng, Y.; Tylavsky, D. PV Bus Modeling in a Holomorphically Embedded Power-Flow Formulation. In Proceedings of the 2013 North American Power Symposium (NAPS), Manhattan, KS, USA, 22–24 September 2013. [CrossRef]
38. Wallace, I.; Roberts, D.; Grothey, A.; McKinnon, K.I.M. Alternative PV Bus Modelling with the Holomorphic Embedding Load Flow Method. *arXiv* **2016**, arXiv:1607.00163.

39. Bazrafshan, M.; Gatsis, N. Comprehensive Modeling of Three-Phase Distribution Systems via the Bus Admittance Matrix. *IEEE Trans. Power Syst.* **2018**, *33*, 2015–2029. [CrossRef]

40. Iba, K. Reactive Power Optimization by Genetic Algorithm. *IEEE Trans. Power Syst.* **1994**, *9*, 685–692. [CrossRef]

41. Lai, L.L.; Ma, J.T. Power Flow Control with UPFC Using Genetic Algorithms. In Proceedings of the International Conference on Intelligent System Application to Power Systems, Orlando, FL, USA, 28 January–2 February 1996; pp. 373–377. [CrossRef]

42. Urdaneta, A.J.; Gomez, J.F.; Sorrentino, E.; Flores, L.; Diaz, R. A Hybrid Genetic Algorithm for Optimal Reactive Power Planning Based upon Successive Linear Programming. *IEEE Trans. Power Syst.* **1999**, *14*, 1292–1298. [CrossRef]

43. Lin, W.M.; Cheng, F.S.; Tsay, M.T. Distribution Feeder Reconfiguration with Refined Genetic Algorithm. *Transm. Distrib. IEE Proc. Gener.* **2000**, *147*, 349–354. [CrossRef]

44. Das, D.B.; Patvardhan, C. Useful Multi-Objective Hybrid Evolutionary Approach to Optimal Power Flow. *Transm. Distrib. IEE Proc. Gener.* **2003**, *150*, 275–282. [CrossRef]

45. Masoum, M.A.S.; Ladjevardi, M.; Jafarian, A.; Fuchs, E.F. Optimal Placement, Replacement and Sizing of Capacitor Banks in Distorted Distribution Networks by Genetic Algorithms. *IEEE Trans. Power Deliv.* **2004**, *19*, 1794–1801. [CrossRef]

46. Back, T.; Fogel, D.B.; Michalewicz, Z. (Eds.) *Basic Algorithms and Operators*, 1st ed.; IOP Publishing Ltd.: Bristol, UK, 1999.

47. Korovkin, N.V.; Vu, Q.S.; Yazenin, R.A. A Method for Minimization of Unbalanced Mode in Three-Phase Power Systems. In Proceedings of the 2016 IEEE NW Russia Young Researchers in Electrical and Electronic Engineering Conference (EIConRusNW), St. Petersburg, Russia, 2–3 February 2016; pp. 611–614. [CrossRef]

48. Fernandes, C.M.M. Unbalance between Phases and Joule's Losses in Low Voltage Electric Power Distribution Networks. p. 9. Available online: https://fenix.tecnico.ulisboa.pt/downloadFile/395142112117/Resumo%20Alargado%20Carlos%20Fernandes.pdf (accessed on 15 February 2019).

49. Fernandez, J.; Bacha, S.; Riu, D.; Turker, H.; Paupert, M. Current Unbalance Reduction in Three-Phase Systems Using Single Phase PHEV Chargers. In Proceedings of the 2013 IEEE International Conference on Industrial Technology (ICIT), Cape Town, South Africa, 25–28 February 2013; pp. 1940–1945. [CrossRef]

2.2 Publication B

Rao, B.V.; Kupzog, F.; Kozek, M.
Phase Balancing Home Energy Management System Using Model Predictive Control
Energies 2018, 11, 3323. https://doi.org/10.3390/en11123323

Own contribution

Concept development, problem analysis, formal analysis, methodology, implementation of algorithms and coding, simulation studies, structuring and writing of the manuscript was done by the candidate, under the supervision of second and third authors. Methodology and problem statement discussion, editing and reviewing of the manuscript was done by second and third authors.

energies

MDPI

Article

Phase Balancing Home Energy Management System Using Model Predictive Control

Bharath Varsh Rao [1,*], Friederich Kupzog [1] and Martin Kozek [2]

[1]   Electric Energy Systems—Center for Energy, AIT Austrian Institute of Technology, 1210 Vienna, Austria; friederich.kupzog@ait.ac.at

[2]   Institute of Mechanics and Mechatronics—Faculty of Mechanical and Industrial Engineering, Vienna University of Technology, 1060 Vienna, Austria; martin.kozek@tuwien.ac.at

*   Correspondence: bharath-varsh.rao@ait.ac.at; Tel.: +43-664-88256043

check for
updates

Abstract: Most typical distribution networks are unbalanced due to unequal loading on each of the three phases and untransposed lines. In this paper, models and methods which can handle three-phase unbalanced scenarios are developed. The authors present a novel three-phase home energy management system to control both active and reactive power to provide per-phase optimization. Simplified single-phase algorithms are not sufficient to capture all the complexities a three-phase unbalance system poses. Distributed generators such as photo-voltaic systems, wind generators, and loads such as household electric and thermal demand connected to these networks directly depend on external factors such as weather, ambient temperature, and irradiation. They are also time dependent, containing daily, weekly, and seasonal cycles. Economic and phase-balanced operation of such generators and loads is very important to improve energy efficiency and maximize benefit while respecting consumer needs. Since homes and buildings are expected to consume a large share of electrical energy of a country, they are the ideal candidate to help solve these issues. The method developed will include typical distributed generation, loads, and various smart home models which were constructed using realistic models representing typical homes in Austria. A control scheme is provided which uses model predictive control with multi-objective mixed-integer quadratic programming to maximize self-consumption, user comfort and grid support.

Keywords: three-phase unbalance minimization; model predictive control; home energy management system

1. Introduction

The Energy Efficiency Directive of the European Commission provides great emphasis on the need to empower and integrate customers by considering them as key entity towards sustainable and energy efficient future [1]. Evolving systems such as smart meters are on a road map towards increased market integration. With the help of such devices, ICT aspects such as data mining, management, processing, and commutation are gaining lots of traction in smart grid [2].

In recent days, with rigorous funding and investment in renewable energy, large number of distributed energy resources such as photo-voltaic systems, wind generators, and new loads such as electric mobility and storage systems are gaining importance. They pose lots of challenges to the network such as voltage violations and line loading. Most of the typical distribution networks are unbalanced due to unequal loading on each of the three phases and untransposed lines [3]. Additionally, unbalance is further increased with the high penetration of single-phase distributed generators. Three-phase unbalance imposes various degrees of stresses on different components in distribution network. Losses on the lines and distribution transformers increase considerably with

the increase in phase unbalance [3]. Therefore, it is extremely important to consider three-phase models. They have strong dependencies on external factors such as weather, ambient temperature, and irradiation which follows daily, weekly, and seasonal cycles. Photo-voltaic systems inject large amounts of active power into the network, especially when the solar irradiation is high during midday. Voltage violations may occur due to partial stochastic power input. Therefore, it is important to include reactive power in models so that it can be used to performed voltage regulation.

Homes and buildings are projects to consume a large share of total energy production. Therefore, it makes sense to produce strategies to use them to help mitigate the issues discussed above. Most of the homes today are not capable of providing any kind of support to the grid. Certain upgrades need to be made so that they can perform demand response. Loads which can be controlled directly or indirectly to provide demand response is referred to as demand side management (DSM). DSM is also referred to as flexibility. DSM can be used to provide number of grid support functionalities such as shifting the peak load to off-peak hours or curtailing the load to reduce the peak demand [4]. Smart building customers are given the opportunity to schedule the devices on their own to maximize comfort level and based on this initial schedule, the optimizer maximizes economic return which will result in demand which is more leveled over time [5]. Additionally, the optimizer will either minimize payment or maximize comfort based on the consumer needs in which, the user comfort is represented as a group of linear constraints [6].

2. Related Work

To control various devices in smart homes and all the issues associated with it, the authors in paper have presented a control scheme using Model predictive control, which is an ideal candidate to handle dynamic systems with evolving disturbances described in the previous section.

Various implementations of model predictive controller (MPC) in buildings are available in the literature. The core principle or issue being addressed by bodies of research mentioned below is dynamic scheduling of various flexibilities in building. Most of the authors below have addressed this issue using various MPC algorithms, problem formulations and objectives.

After analyzing the large body of work in MPC for buildings, three major categories can be defined. MPC in buildings is mainly used for demand side and flexibility management, building temperature control and optimal usage of energy.

2.1. Demand Side and Flexibility Management

A multi-scale stochastic MPC is implemented to schedule heating, ventilation, air conditioning which is referred to as HVAC systems and controllable loads such as electric vehicles and washer/dryers is implemented in [7]. In [8], the authors have presented an MPC approach to tackle the load shifting problem in households equipped with controllable appliances and electric storage units. This approach used time of day tariff to minimize energy consumption. A decision-making framework for real time control of load serving entity of flexibilities used to provide ancillary services to the market is presented in [9]. This paper provides a generalized framework which includes wide array of flexibilities. An example with electric vehicle charging is provided in detail.

The authors in [10] have proposed a scheme which uses time varying real time pricing to schedule appliances in buildings in smart grid context. Thermal mass of the building is considered with a comfort indicator and a model associated with it is presented. Thermal mass storage is used to hedge against varying prices with a goal to minimize energy costs. Control approach for home energy management system (HEMS) under forecast uncertainty is presented in [11]. The smart home is controlled as a grid connected micro-grid with PV generation, battery systems, critical and controllable loads. Objective of MPC is to maximize the use of renewable energy generation and to minimize operation costs. It includes predictions of PV, load, and market prices. Various scenarios are considered with different forecasting accuracies.

The authors in [12] presented an MPC model for HVAC system in medium sized building with receding horizon control. It is used to provide demand side flexibilities. Objective is to operate the building economically while respecting the comfort of dwellers. MPC scheme provided is a robust one to participate in both reserve and spot markets. Sensitivity of the controller towards economic and technical constraints are evaluated. The National Electricity Market of Singapore (NEMS) is used as a study case for grid building integration studies.

In [13], a non-intrusive identification of components in smart home is provided with a sampling frequency of one hertz. These identified models are used to predict flexibilities. These flexibilities are shifted in time to minimize energy costs. An MPC technique for energy optimization in residential appliance is proposed in [14]. Home cooling and heating system control is proposed to analyze the effect of conventional thermostats. In [15], an MPC EMS system for residential micro grids is furnished. EMS optimally schedules smart appliances, heating systems, PV generators based on consumer preferences. Weather and demand forecasts are integrated in it. Mixed-integer linear programming (MILP) is the core of MPC which minimizes the system costs of this residential micro-grid. At each sample time, the optimization algorithm adjusts itself to account for updated weather dependent PV systems and heating units in a receding fashion. This method is coupled with accurate simulation of micro-grid including energy storage and flexible loads. Emulation of real-world grid conditions on standard network interface is presented. The authors in [16] have provided a method to maximize the use of renewable energy resources in islanded grids. PV systems are used to provide energy to home loads and pico hydro power plant. MPC is used to control the flow valve of hydro plant and to modulate the energy supply to fulfill the deficit during islanded conditions.

An economic MPC is illustrated in [17]. It includes PV combined heat and electrical storage system. Uncertainties from thermal behaviors of the building are quantified, formulated and MPC's capability to handle it is presented in this research work. An MPC scheme to control loads in residential buildings are presented in [18]. It also presents a novel load aggregation method using MPC for distribution networks. This method is tested with 342 bus network with 15,000 buildings. In [19], an MPC controller to perform demand side management is presented. It uses an ON/OFF PID controller and MPC to control air conditioning in rooms in houses. It also includes PV systems. Weekly expenses are calculated for each tariff is compared with control methods.

2.2. Temperature Control

The authors in [20], have presented a method to control temperature in building in a cost-effective manner. It uses linear programming heuristic to minimize the objective function of electricity cost to run air conditioning system. In [21], authors have presented models for Heat Recovery Ventilators connected to single zone building, its potential and nonlinear MPC is implemented to optimize energy consumption. Three distinct time zones are used namely, slow timescale for temperature of structural elements, fast timescale for air temperature and intermediate dynamics for recovery systems. A stochastic optimization technique is provided in [22]. This paper introduces several load classes such as heating, ventilation, air conditioning which is commonly referred to as HVAC systems. A first order thermal dynamic model is used with a mixed-integer MPC to generate load schedules. Real data is coupled with numerical solutions. The authors in [23] have proposed an MPC algorithm to control temperature in single zone building coupled with renewable energy generators such as solar and wind. MPC objective is to control temperature within certain permissible limits and optimal amount of power consumption.

In [24], a temperature control scheme with the consideration of occupants with three comfort indicators namely, strict, mild, loose levels are provided. It also includes window blind position control, illumination, and ambient temperature. Weather data such as solar irradiation, illumination, and ambient temperature is forecasted and used in MPC algorithm. Goal of MPC is to minimize energy consumption and maintain the desired level of comfort for occupants. Paper [25] focuses on analysis of MPC application to domestic appliances to optimize them. Relationship between MPC

weight adjustment and minimization of energy consumption is evaluated. In this context, water heater, room temperature control by air conditioning system and refrigerators are explored.

In [26], a centralized direct control of on/off thermostats is furnished. Device operation temperature, on/off status, more importantly, temperature ramps are calculated and communicated to the central controller. It is observed that, same or better performance can be achieved by communication of temperature ramps which are essential data points. It also reduces the communication needs significantly. Right information exchange is essential for better performance and data flow reduction is the concluding argument of this paper.

An MPC control scheme to provide the best tradeoff between temperature control and energy cost is described in [27]. It also provides a comparison between PID controller and MPC. The weights are modified to obtain the best solution to increase quality of various electrical and thermal models. The authors in [28], have presented an MPC for entire building with a comfort metric to ensure high priority to user comfort for each of the various zones in the building. Simulation results are provided for four months showing large percentage of reduction in electrical and thermal energy consumption.

2.3. Optimal Energy Usage

Paper [29] proposes an MPC control strategy in HEMS to optimize energy usage and optimal operational schedules for input variables. It also provides results which demonstrated revenue from selling power to the utility. In [30], authors have furnished an MPC approach to obtain savings in residential households. Impact of local power generation such as roof top PV systems is determined for off-peak, mid-peak and on-peak periods. Hybrid MPC formulation for buildings is provided in [31]. It describes the interactions between continuous and discrete systems. It involves a two-level computation structure. Individual systems are controlled with upper level discrete commands.

In [32], an approach to minimize energy in home and office building is presented with renewable energy resources such as PV systems. This is done using an MPC technique with mixed-integer programming to handle switching constraints. This method allows for sufficient performance with respect to energy regulation and efficiency. It is shown that with various seasons, an annual savings of about 1.72% can be achieved with this approach. An MPC approach is introduced in [33] which exploits its capacity to reduce energy consumption and improve efficiency to reduce energy bills. MPC was trained for two different weight sets which is compared to thermostat control with three typical household loads.

It is shown that it is necessary to augment control weights to maximize energy cost minimization potential. In [34], an energy scheduling approach for smart home appliances using stochastic MPC is presented. It comprises a combination of genetic algorithm and linear programming. It analyzes the competence of the algorithm proposed with the objective of energy reduction.

An MPC scheme with a sample time of one hour is presented in [35]. It includes hot water usage, electric vehicle, domestic heating and with an actuator with water tank to use it as heat storage. Total power and energy cost is minimized. MPC robustness is evaluated using forecasted load profiles of the household. It is shown that using energy storage, the overall energy consumption of the household can be minimized.

A comprehensive cost optimal design is presented for a building HVAC system which includes MPC to generate cost optimal solution is presented in [36] The controller provides an optimal hourly set point for cooling and heating devices. This method is applied to multi-zone building in Italy. In [37], a study to minimize the cost of electricity for coordinating houses connected a micro-grid. It uses multi-objective optimization for micro-grid control which includes a house and an independent local plant. The control algorithm minimizes losses by power exchanges between the plant and the house.

It can be clearly seen that, three-phase implementation of HEMS is lacking. The papers mentioned above only use simple single-phase flexibility models and appliances are single phased. Additionally, reactive power control is not addressed by any of the research work mentioned above. Since three-phase models are not used, phase unbalance minimization cannot be performed. In this paper, the authors

present a three-phase unbalanced HEMS in which, three objective functions, maximize user comfort, self-consumption and grid support is implemented. It also includes control scheme to manage both active and reactive powers and can handle number of electrical appliances with various configurations.

The contributions in this paper are enlisted below,

1. Various three-phase linear flexibility models are presented in Section 3.
2. Flexibilities are modeled in both active and reactive power.
3. Three objective functions are provided in Section 5 along with three objective weights which are user defined.
4. Control scheme is described in Section 6 for three-phase HEMS with various chronological events.
5. Simulation results for three-phase unbalanced HEMS with active and reactive power control is provided in Section 7.

3. System Models

HEMS is a platform which enables monitoring and control of various energy appliances in the household. It allows the deployment of various control strategies to achieve an objective. Smart home in this paper refers to a home which is fitted with a HEMS. Using this system, various objectives can be achieved. For example, keeping the room temperature within certain comfortable limits.

3.1. Overview

Smart home models can be segregated into two categories. Namely, thermal and electrical models coupled by a heat pump. The main reason to use a thermal model is to characterize indoor temperature due to the thermal inertia of the house, since consumer comfort is paramount. The controller is formulated to give complete control to the user, a user-centric approach. The models are linear in nature so that, simple control strategies can be produced. Figure 1 represents a three-phase HEMS. It contains both single and three-phase components and therefore, it is unbalanced. In this scenario, the heat pump is three phased, inverters for battery and PV are three phased, controllable, and uncontrollable loads are single phased. The control scheme provided in this paper can include variety of configurations such as single-phase—neutral, phase—phase, three-phase star configuration, three-phase star configuration with neutral, and three-phase delta configuration. This can be done using the constraint imposed on the grid connection point described in Section 4.4.
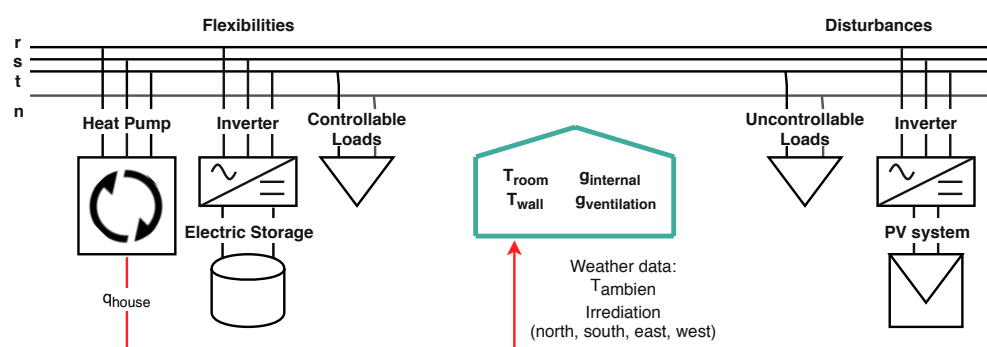
Figure 1. Schematic of three-phase HEMS representing various three-phase interconnections. It can be observed that, heat pump is the only component which connects thermal and electrical models.

3.2. Smart Home Thermal Model

Various linear single zone models representing single family homes with heat pumps and thermal parameters of the building are considered. They are based on nonlinear models which were constructed using data, representing physical behavior of real buildings in Vienna and Salzburg regions in Austria. Due to consumer privacy, more details about these homes cannot be provided. By generalizing these

models, four study cases are derived, and their essential distinguishing features are shown in Table 1. Nonlinear models were created in Dymola [38], which is a modeling and simulation tool, as part of the project iWPP-Flex [39]. They were linearized using the functions within Dymola and were mathematically verified.

Table 1. Building study cases which represent typical households in Austria. During the modeling stage of these houses, they only contained single-phase loads. To perform effective demand response, they had to be upgraded to include various other flexibilities such as single/three-phase heat pumps, controllable loads, electric storage, and PV system with three-phase inverters. Some of the important specifications such as heat demand, control method, and rated capacities which influences the control scheme are provided in this table.

House Hype	Passive House	Low-Energy House	Existing House	Renovated House
Heating demand	15 kWh/(m²a)	45 kWh/(m²a)	100 kWh/(m²a)	75 kWh/(m²a)
Heater	Under floor	Under floor	Radiator	Radiator
Heat exchange medium	Air-water	brine-water	brine-water	air-water
Power control	Variable	On/off	On/off	Variable
Rated capacity (Electrical/thermal)	1 kW/ 3 kW	1.2 kW/5 kW	4 kW/12kW	2.7 kW/7 kW

In the context of smart HEMS, the models of smart homes are recommended to be kept sufficiently simple to maintain generality, so that many building types can be accommodated. Therefore, first order models are implemented. Additionally, the focus of this work is not to use realistic building models but rather the control strategy and to minimize the objective function.

As a result, continuous state space models were generated and are assumed to be ordinary discrete linear time-invariant and is then discretized with a sampling time step of 15 min which can be observed in Equation (1).

$$x_{room}(t+1) = A_{room} \quad x_{room}(t) + B_{room} \quad u_{room}(t) \tag{1}$$

The state variables x_{room} of the building model are the room and wall temperature. The later represents the temperature of wall, floor, and ceiling of the house. A_{room} and B_{room} are the system matrices.

$$x_{room} = \begin{bmatrix} T_{wall} \\ T_{room} \end{bmatrix} \tag{2}$$

Limits on room and wall temperatures are given in Equations (3) and (4)

$$T_{wall}^{min} \leq T_{wall}(t) \leq T_{wall}^{max} \tag{3}$$

$$T_{room}^{min} \leq T_{room}(t) \leq T_{room}^{max} \tag{4}$$

The input quantities for the building are heat flow supplied by the heat pump, ambient temperature, solar irradiation from all directions, internal gains, and ventilation.

$$u_{room} = \begin{bmatrix} q_{room} \\ T_{ambient\ temperature} \\ i_{north} \\ i_{east} \\ i_{south} \\ i_{west} \\ g_{internal\ gain} \\ g_{ventilation} \end{bmatrix} \tag{5}$$

Limits on heat flows into the building are provided in Equation (6)

$$0 \leq q_{room}(t) \leq q_{room}^{max} \tag{6}$$

3.3. Heat Pump in Residential Building

Heat pump is used to provide the heat flow into the home which is the only controllable variable in the home model described in Section 3.2. Heat pump is the only coupling element between electrical and thermal systems as mentioned above.

Equation (7) describes the relationship between heat pump power and heat flows. The model represented below is that of a single-phase heat pump since it is in a modest home. This can be easily extended to three-phase by dividing the right-hand side of Equation (7) by 3 for per-phase balanced active power. Coefficient of performance (cop) is assumed to be constant with respect to time.

$$P_{heat\ pump}(t) = \frac{q_{room}(t)}{cop_{heat\ pump}} \tag{7}$$

Where, $P_{heat\ pump}$ is the active power and $cop_{heat\ pump}$ is the coefficient of performance. Low-energy and existing house contains on-off heat pump. To model this, a binary variable $B_{heat\ pump}$ with 0 for off and 1 for on is used.

$$P_{heat\ pump}(t) = B_{heat\ pump}\ P_{heat\ pump}^{rated} \tag{8}$$

The pump in heat pump consists of an induction motor. This motor is assumed to be lossless and with constant power factor ($pf_{heat\ pump}$) as described in Equation (9), using which reactive power ($Q_{heat\ pump}$) is calculated.

$$Q_{heat\ pump}(t) = tan(cos^{-1}(pf_{heat\ pump}))P_{heat\ pump}(t) \tag{9}$$

Since only heating period is considered, $P_{heat\ pump}$ and $Q_{heat\ pump} \geq 0$. Constraints on heat pump active power limits.

$$0 \leq P_{heat\ pump}(t) \leq P_{heat\ pump}^{max} \tag{10}$$

Constraints on heat pump reactive power limits,

$$0 \leq Q_{heat\ pump}(t) \leq Q_{heat\ pump}^{max} \tag{11}$$

where, $P_{heat\ pump}^{max}$ and $Q_{heat\ pump}^{max}$ are the maximum rated power active and reactive powers of head pump, respectively.

4. Electrical System Constraints

In recent years, lots of smart electrical appliances are becoming popular. It is possible to control the behavior of these appliances. In this paper, the authors have decided to use the following electrical appliances.

4.1. Electric Storage Constraints

For the maximal use of intermittent renewable energy generators and self-consumption, electric batteries are becoming very important in the recent days. Therefore, it is necessary to model and include them in the HEMS systems. In this paper, only linear battery models are used. Equation (12) represents the energy balance of electric storage system, a battery.

$$soc(t+1)\ C_{battery} = soc(t)\ C_{battery} + \Delta t\ \eta_{battery}\ P_{battery}(t) \tag{12}$$

It can be seen in Equation (12) that, $P_{battery}$ takes values both positive and negative. This is a form of linearization because, the battery charging and discharging efficiencies are different and therefore, nonlinear. This nonlinearity can be tackled by solving it as is, using a nonlinear solver or by splitting the $P_{battery}$ into $P_{charging}$ and $P_{discharge}$. The latter is coupled with a binary variable to make it either charge or discharge, leading to MILP. The authors have chosen to use the linear form and the reasons for it are provided in Section 4.2.

Constraints on soc limits are given below,

$$soc^{min} \leq soc(t) \leq soc^{max} \tag{13}$$

Constraints on battery charging and discharging power limits are as follows.

$$P_{battery}^{min} \leq P_{battery}(t) \leq P_{battery}^{max} \tag{14}$$

4.2. Three-Phase Inverter Constraints

The battery described in the previous section is connected to a three-phase inverter. The inverter can control active and reactive power flows on each of the phases. The relationship between battery and inverter is described using simple power balance Equation (15).

$$(P_{battery}(t))^2 = (P_{inverter}(t))^2 + (Q_{inverter}(t))^2 \tag{15}$$

Equation (15) is nonlinear. If on the precious section, a binary variable is defined and $P_{battery}$ is split into $P_{charging}$ and $P_{discharge}$, Equation (15) becomes nonlinear and non-convex. One way to deal with the nonconvexity is to limit the $Q_{inverter}$ with a constant power factor as shown in Equation (16). However, this is still nonlinear.

$$Q_{inverter}^{\rho}(t) = tan(cos^{-1}(pf_{inverter}))P_{inverter}^{\rho}(t) \tag{16}$$

where, ρ is the phase and $\rho \in phases(r, s, t)$. To remedy the nonlinearity, the inverter is only controlled at unity power factor. In other words, the reactive power is zero. This is represented in Equation (17)

$$(P_{battery}(t))^2 = (P_{inverter}(t))^2 \tag{17}$$

Individual phase powers are represented as follows,

$$P_{inverter}(t) = \sum_{\rho} P_{inverter}^{\rho}(t) \tag{18}$$

4.3. Constraints on Controllable Loads

Simple controllable loads are used with constant power factor operation as described in Equation (21). Controllable loads have the following constraints. Equations (19) and (20) are the active and reactive power constraints and Equation (21) is the relationship between them.

$$0 \leq P_{controllable\,load}^{\rho}(t) \leq P_{controllable\,load}^{max} \tag{19}$$

$$0 \leq Q_{controllable\,load}^{\rho}(t) \leq Q_{controllable\,load}^{max} \tag{20}$$

It is assumed that the power factor is constant with time. Typical power factor for household loads is between 0.90 to 0.95.

$$Q_{controllable\,load}^{\rho}(t) = tan(cos^{-1}(pf_{controllable\,load}))P_{controllable\,load}^{\rho}(t) \tag{21}$$

4.4. Constraints on Grid Connection Point

The grid connection point (point of common coupling) is where the smart home is connected to the grid. When excess power is fed into the grid, it is referred to as infeed and when power is drawn, it is referred to as consumption. Since P_{grid} takes both positive and negative values due to battery linearization, both infeed and consumption is represented by P_{grid}. It also represents the energy balance of all the electrical components in the smart home.

Equations (22) and (23) are constraints on limits of active and reactive power at the grid connection point.

$$P^{\rho}_{grid}(t) = P^{\rho}_{inverter}(t) + P^{\rho}_{heat\ pump}(t) + P^{\rho}_{controllable\ load}(t) + P^{\rho}_{uncontrollable\ load} \tag{22}$$

$$Q^{\rho}_{grid}(t) = Q^{\rho}_{heat\ pump}(t) + Q^{\rho}_{controllable\ load}(t) + Q^{\rho}_{uncontrollable\ load} \tag{23}$$

4.5. Various Disturbances Applied to HEMS

Various electrical and thermal disturbances are applied to HEMS during simulation which can be seen in Figure 2.
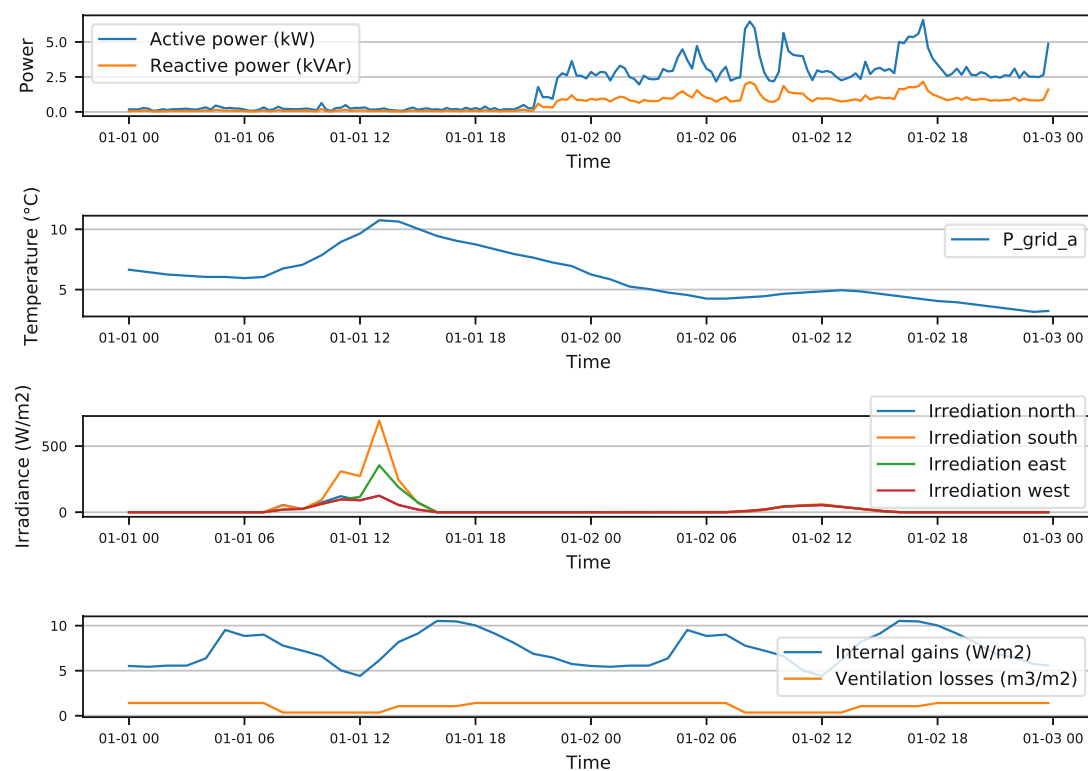
Figure 2. Profiles of disturbances applied to smart HEMS. On the x-axis, data time format is MM-dd HH. Data is from 01-01-2018 00:00:00 to 01-02-2018 00:00:00.

Disturbances are forecasted using a convolutional neural network which is not described in this paper. Uncontrollable loads data is from a smart meter from a real household in Austria. Various thermal disturbances such as ambient temperature and irradiation data is sourced from weather stations in Austria, ventilation, and internal gains from the project iWPP-Flex.

5. Objective Functions

In this paper, three different objectives are considered. These are explained in detail below.

5.1. Improve Self-Consumption

In many countries, with higher share of renewables, it is more economical to self-consume and therefore, the following objective function in Equation (24) is minimized. Since electricity tariffs only depend on active power, reactive power is excluded from the objective.

$$J_{self\,consumption} = \sum_t \sum_p (P_{grid}^\rho(t))^2 \tag{24}$$

On the other hand, in Austria, it is more economical to feed as mush power into the grid as possible since power sale tariff is higher than consumption tariffs. It can be done easily by maximizing equation. It is customary to involve a variable price signal along with P_{grid} which is the electricity tariff provided by the energy retailer. However, this is neglected for the sake of clarity.

5.2. Improve User Comfort

Since user comfort is paramount, this objective is introduced. It minimizes the difference between a reference temperature and actual room temperature in smart home. The limits of these temperature are defined by the user.

$$J_{user\,comfort} = \sum_t (T_{room}^{reference}(t) - T_{room}(t))^2 \tag{25}$$

5.3. Improve Grid Support

As mentioned in Section 1, smart homes can provide support to the grid by optimally controlling its renewable generation and consumption. Therefore, objective in Equation (26) is provided. It minimizes the difference between reference and actual active, reactive powers at grid connection point. This reference is generated from a large grid level optimal power flow controller based on a grid level objective function.

$$J_{grid\,support} = \sum_t \sum_p (P_{grid\,reference}^\rho(t) - P_{grid}^\rho(t))^2 + (Q_{grid\,reference}^\rho(t) - Q_{grid}^\rho(t))^2 \tag{26}$$

This paper does not include details or methods to generate this reference profile and instead uses it as is. If the smart home can follow this reference profile, grid level optimization is achieved. The objective on the grid can be loss minimization, line loading minimization, operational efficiency, unit dispatch and so on. In this paper, the reference profiles where generated with an objective to minimize the three-phase unbalance on the grid level. For this to work, multiple buildings connected at various locations in the network must follow its own reference profile provided by the grid controller, simultaneously.

5.4. Complete Objective Function

Complete objective function is provided in Equation (27). Weights $\mathcal{S}$, $\mathcal{U}$ and $\mathcal{G}$ are introduced with self-consumption, user comfort and grid support, respectively. By varying these weights, more importance can be given to the objectives.

$$\text{minimize } J = \mathcal{S}\,J_{self\,consumption} + \mathcal{U}\,J_{user\,comfort} + \mathcal{G}\,J_{grid\,support} \tag{27}$$

These weights can be varied on-line and the controller updates it in the next simulation step. There are the most prominent parameters which the user can determine and can have significant

influence over the controller and ultimately the optimum. Controllable variables are $P_{battery}$, $P_{heat\ pump}$ and $P_{controllable\ load}$.
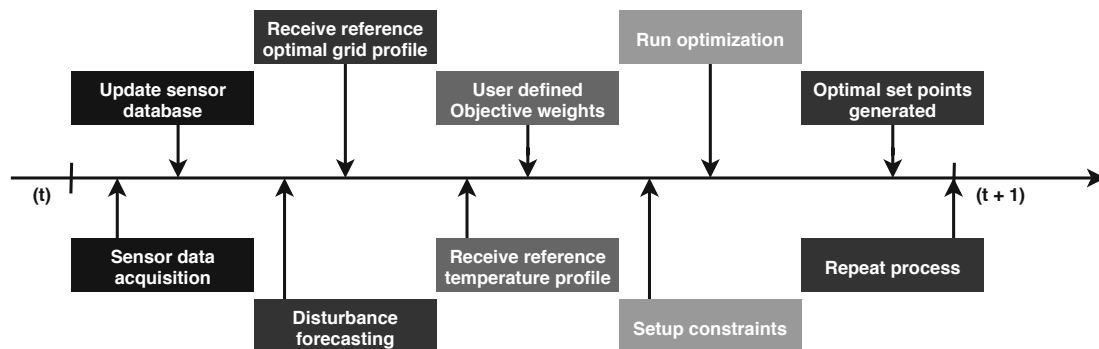
6. Control Scheme

Due to the high intermittency of renewable energy generators, loading in households along with dependencies on external factors such as weather and solar irradiation, it is extremely important to choose a controller which makes effective use of available predictions.

Therefore, the authors have chosen to use MPC. MPC control used is receding horizon control. Figure 3 describes an MPC and data exchange between various devices in smart home. MPC is responsible to generate optimal set-points to minimize the objective function.
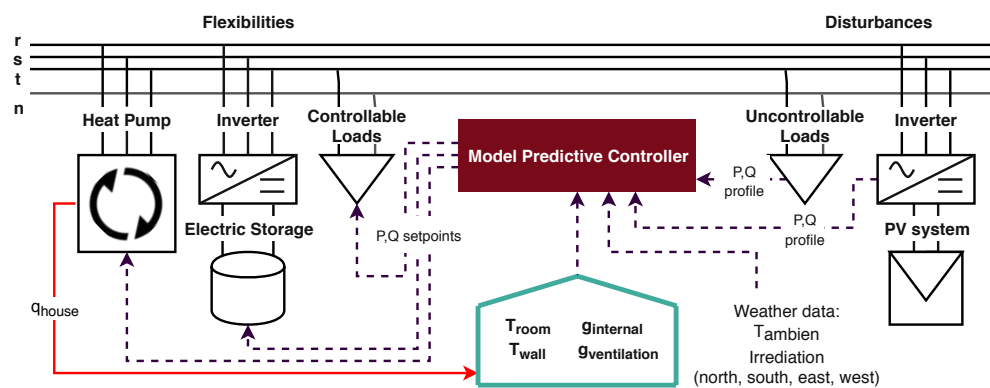
Figure 3. Schematic of three-phase HEMS with model predictive controller. It shows all the interconnections with respect to data exchange.

MPC control scheme is illustrated in Figure 4. It describes various functions which need to be executed within a sample duration.

Figure 4. Model predictive control scheme for three-phase HEMS. It describes various functions which are executed for a sample period.

The chronological control functions and events described in Figure 4 are described in detail below.

1. At time *t*, measure thermal disturbances such as irradiation, ambient temperature, ventilation losses and internal gains. Additionally, smart meters measures uncontrollable load and photo-voltaic generation.
2. These sensor data points are acquired by the data acquisition system and sensor database is updated. Figure 5 illustrates the sensor data acquisition system using in this work.

3.   Disturbances are forecasted for a given prediction horizon using an appropriate forecasting algorithm. In this paper, using convolutional neural networks.
4.   Active and reactive power optimal set-points are received from the grid level controller.
5.   Internal temperature reference signals are received.
6.   User defined objective weights are received.
7.   Objective functions are set up using Equations (24)–(27).
8.   Constraints from Equations (1)–(23) are setup.
9.   Optimal set-points are generated.
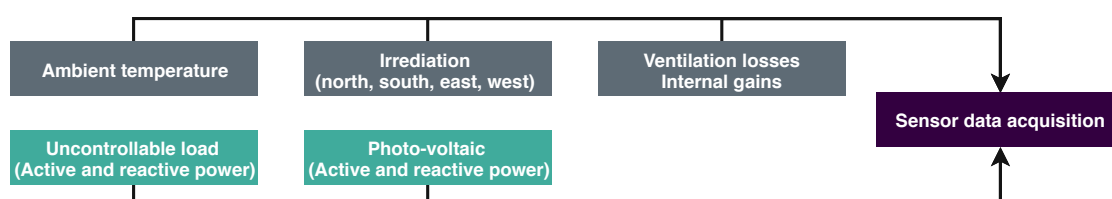10.   The process is repeated for next sample period, $(t+1)$.

Figure 5. Schematic of a sensor data acquisition system use in three-phase HEMS.

The optimization problem is solved by a suitable quadratic programming for passive, renovated house and mixed-integer quadratic programming for low-energy and existing houses as discussed in Section 3.3.

7. Simulation Results

In this section, simulation setup and results are provided. As mentioned earlier, the objective weights, $\mathcal{S}, \mathcal{U}$ and $\mathcal{G}$ are defined by the user, it is difficult to analyze the controller performance due to large number of combinations of these three variables.

To overcome this, only extreme cases of these weights are considered. This can be observed in Figure 6. The method of choosing weights in such fashion was inspired from [40] in which, mixed-integer quadratic programming is introduced with multi-objective optimization. The simulation is performed for the duration of 48 hours with prediction and control horizon of 24 hours.
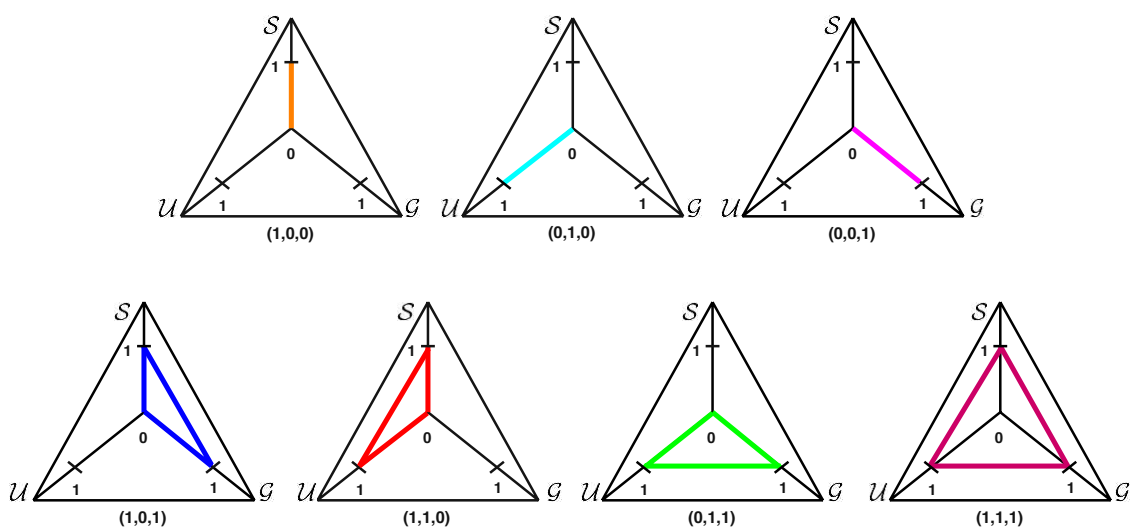

Figure 6. Objective weights, $\mathcal{S}, \mathcal{U}$ and $\mathcal{G}$ for various extreme cases.

Simulation parameters are provided in Table 2.

Table 2. Simulation parameters.

Variable	Value
Simulation parameters	
prediction horizon	24 h
control horizon	24 h
simulation duration	48 h
Building model	
T_{wall}^{min}	10 C
T_{wall}^{max}	40 C
T_{room}^{min}	18 C
T_{room}^{max}	25 C
$T_{initial}$	18 C
$T_{room}^{reference}$	20 C
Controllable load model	
$P_{controllable\ load}^{max}$	2 kW
$pf_{controllable\ load}$	0.95
Electric Storage model	
soc^{min}	0.3
soc^{max}	0.9
$C_{battery}$	20 kWh
$\eta_{battery}$	0.95
$P_{battery}^{min}$	–10 kW
$P_{battery}^{max}$	10 kW
Heat pump model	
cop	3
$pf_{heat\ pump}$	0.90
Passive house: $P_{heat\ pump}^{max}$	1 kW
Low-energy house: $P_{heat\ pump}^{max}$	1.2 kW
Existing house: $P_{heat\ pump}^{max}$	4 kW
Renovated house: $P_{heat\ pump}^{max}$	2.7 kW

7.1. Analysis of Results

Due to the large number of combinations of objective weights and controllable variables, results are analyzed based on the three objective functions. Four scenarios of objective weights are chosen for analysis. $(\mathcal{S}, \mathcal{U}, \mathcal{G}) = (0,0,1)$, $(0,1,0)$, $(1,0,0)$ and $(1,1,1)$. Additionally, to represent powers, only phase *r* is used. The results are plotted using boxplots. More information about it can be seen in Figure 7.
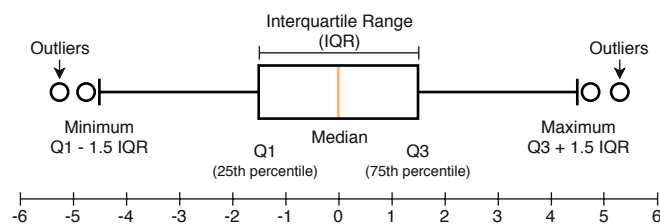
Figure 7. Boxplot is a standardized method to display data.

7.1.1. Improve Self-Consumption

Figure 8 describes the results for the objective function to minimize self-consumption (see, Equation (24)). It illustrates P_{grid} for various home types and for given simulation horizon.

It can be observed that for objective weights $(\mathcal{S}, \mathcal{U}, \mathcal{G}) = (1, 0, 0)$, the controller is trying to get P_{grid} close to zero which can be perceived from the medians which are at zero for all the house types. Same can be observed with objective weights $(\mathcal{S}, \mathcal{U}, \mathcal{G}) = (1, 1, 1)$. Since all three weights are equal, the results are not as effective as the one from before and $\mathcal{S}$ is not dominating other weights.
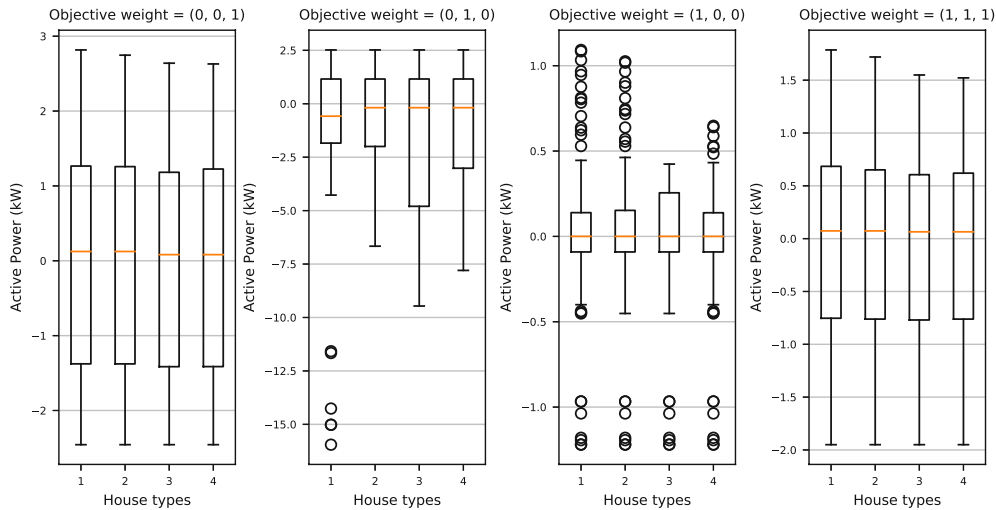

Figure 8. Schematic of Three-Phase HEMS.

7.1.2. Improve User Comfort

Objective terms $abs(T_{room}^{reference} - T_{room})$ is illustrated in Figure 9. Since the objective weight $\mathcal{U}$ is predominant, $(\mathcal{S}, \mathcal{U}, \mathcal{G}) = (0, 1, 0)$, the absolute difference between $T_{room}^{reference}$ and T_{room} is the least. It can be observed that the temperature median is very close to zero. From this, it can be inferred that the objective function to improve user comfort is maximized. However, since the building models are first order, the controller is quiet easily able to achieve similar results with $(\mathcal{S}, \mathcal{U}, \mathcal{G}) = (1, 1, 1)$.
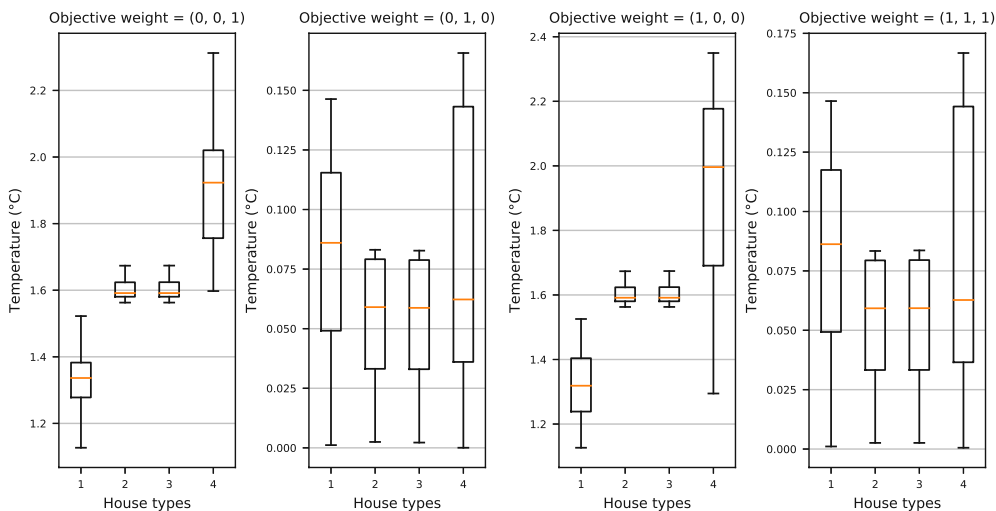

Figure 9. Schematic of Three-Phase HEMS.

7.1.3. Improve Grid Support

Figure 10 illustrates $abs(P_{grid\,reference}(t) - P_{grid})$. With the predominant weight in $(\mathcal{S}, \mathcal{U}, \mathcal{G}) = (0, 0, 1)$ is $\mathcal{G}$. Therefore, similar to previous objectives, it can be observed that the controller is able to minimize the absolute difference between the target profile and the profile at the grid connection

point. This is also illustrated in Figures 11 and 12 where, both active and reactive power profiles are presented for phase *r*.
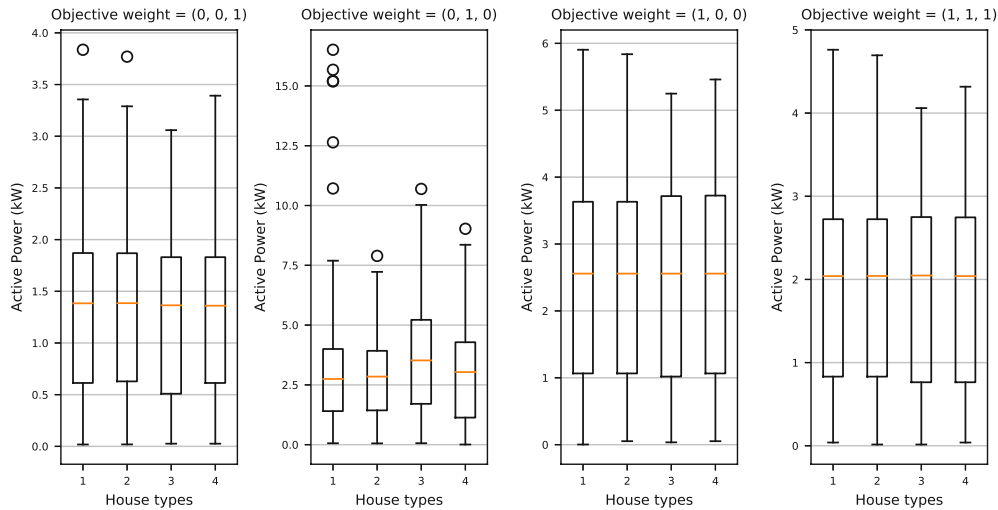

**Figure 10.** Schematic of Three-Phase HEMS.

Figures 11 and 12 describes all the parameters for passive house with objective weight scenario $(\mathcal{S}, \mathcal{U}, \mathcal{G}) = (0, 0, 1)$ for both active and reactive power. In Figure 11, since the objective weight scenario is to minimize $abs(P_{grid\,reference}(t) - P_{grid}) + abs(Q_{grid\,reference}(t) - Q_{grid})$, it can be observed that the P_{grid} is trying to closely follow the $P_{grid\,reference}$.

Figure 11. Per-phase active power controllable and disturbance variables for passive house and weight scenario $(\mathcal{S}, \mathcal{U}, \mathcal{G}) = (0, 0, 1)$

It is evident from Equation (23) that, there are no direct reactive power controllable variables for all the phases. This makes it difficult for the controller to actively tract $Q_{grid\,reference}$ which can be observed in Figure 12. In phase r, due to the existing single-phase appliances, better reactive control tracking is possible unlike phase s and t.
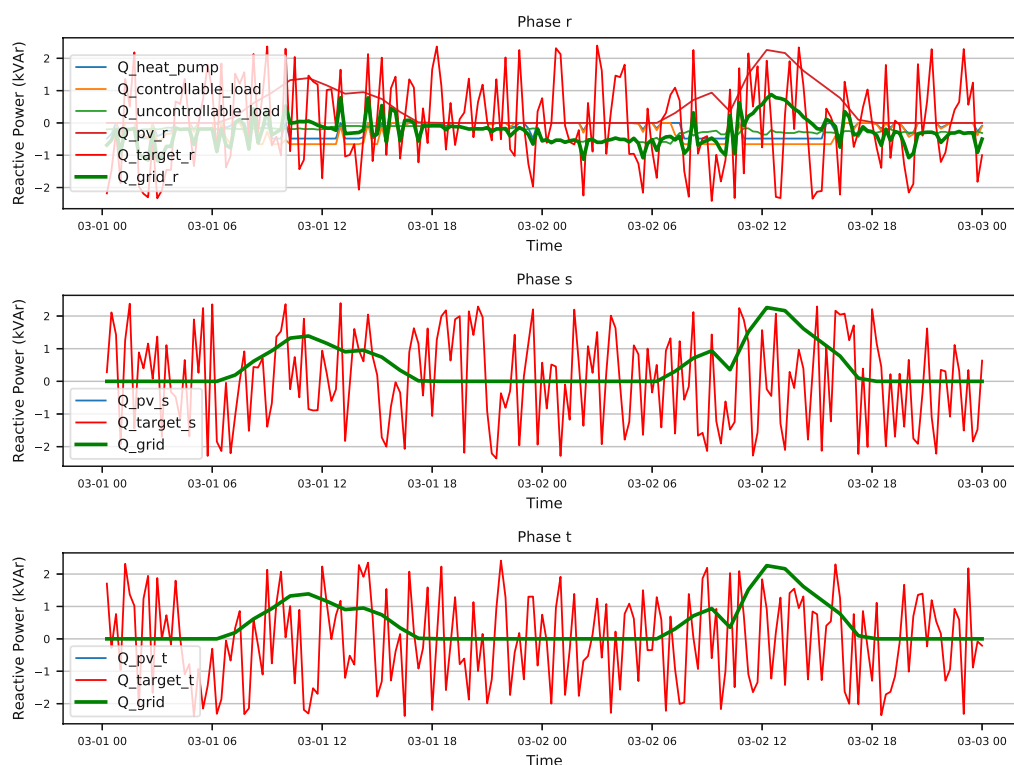
Figure 12. Per-phase reactive power controllable and disturbance variables for passive house and weight scenario $(\mathcal{S}, \mathcal{U}, \mathcal{G}) = (0, 0, 1)$

8. Conclusions and Outlook

In this paper, a novel three-phase balancing HEMS was presented along with control strategies for both active and reactive power. Four linear building models representing typical households in Austria were described. Various linear three-phase flexibility models were presented in detail. Three unique conflicting objective functions with three weights which are user defined is described. Model predictive control scheme was applied to this smart home for various extreme objective weight scenarios. Active and reactive power set-points were generated for all electrical controllable variables. Due to the vast number of combinations of objective weights, four extreme cases were chosen for analysis, $(\mathcal{S}, \mathcal{U}, \mathcal{G}) = (0, 0, 1)$, $(0, 1, 0)$, $(1, 0, 0)$ and $(1, 1, 1)$. Analysis was done based on three objective functions. It was shown that the results reflect the chosen objective weights for each of the three objective functions. In Figures 11 and 12, grid support maximization objective was illustrated for objective weights $(\mathcal{S}, \mathcal{U}, \mathcal{G}) = (0, 0, 1)$. In these figures, it was shown that P_{grid} and Q_{grid} are indeed able to track their reference profiles and implications being, the objectives on the grid level controller (three-phase unbalance minimization) are being met, leading to a grid level optimization.

The models presented in the paper were linear and first order in nature. In reality it makes sense to use higher order nonlinear models to closely match the real behavior of the smart home. Therefore, the model needs to be extended to nonlinear ones. Even though the scheme includes reactive power, it is not given high importance in this paper to keep it linear. Due to high share of renewable generators, it is interesting to be able to control reactive power in this context. The inverter connected to the

battery in this paper only works at unity power factor. However, by including reactive power control, better reactive power tracking can be performed. Additionally, with the power balance equation at the inverter is non-convex in nature. Therefore, the MPC needs to be extended to be able to solve such problems using a non-convex solver.

Author Contributions: Conceptualization, B.V.R. and F.K.; Formal analysis, M.K.; Investigation, B.V.R., F.K. and M.K.; Methodology, B.V.R. and M.K.; Resources, B.V.R. and F.K.; Validation, B.V.R. and M.K.; Visualization, B.V.R. and F.K.

Conflicts of Interest: The authors declare no conflict of interest.

References

1. General, D. Energy Efficiency Directive. Available online: https://ec.europa.eu/energy/en/studies (accessed on 20 August 2018).
2. Barbato, A.; Capone, A.; Barbato, A.; Capone, A. Optimization Models and Methods for Demand-Side Management of Residential Users: A Survey. *Energies* **2014**, *7*, 5787–5824. [CrossRef]
3. Sun, Y.; Li, P.; Li, S.; Zhang, L.; Sun, Y.; Li, P.; Li, S.; Zhang, L. Contribution Determination for Multiple Unbalanced Sources at the Point of Common Coupling. *Energies* **2017**, *10*, 171. [CrossRef]
4. Miceli, R. Energy Management and Smart Grids. *Energies* **2013**, *6*, 2262–2290. [CrossRef]
5. Pedrasa, M.A.A.; Spooner, T.D.; MacGill, I.F. Coordinated Scheduling of Residential Distributed Energy Resources to Optimize Smart Home Energy Services. *IEEE Trans. Smart Grid* **2010**, *1*, 134–143. [CrossRef]
6. Du, P.; Lu, N. Appliance Commitment for Household Load Scheduling. *IEEE Trans. Smart Grid* **2011**, *2*, 411–419. [CrossRef]
7. Jia, L.; Yu, Z.; Murphy-Hoye, M.C.; Pratt, A.; Piccioli, E.G.; Tong, L. Multi-Scale Stochastic Optimization for Home Energy Management. In Proceedings of the 2011 4th IEEE International Workshop on Computational Advances in Multi-Sensor Adaptive Processing (CAMSAP), San Juan, Puerto Rico, 13–16 December 2011; pp. 113–116.
8. Giorgio, A.D.; Pimpinella, L.; Liberati, F. A Model Predictive Control Approach to the Load Shifting Problem in a Household Equipped with an Energy Storage Unit. In Proceedings of the 2012 20th Mediterranean Conference on Control Automation (MED), Barcelona, Spain, 3–6 July 2012; pp. 1491–1498.
9. Alizadeh, M.; Scaglione, A.; Kesidis, G. Scalable Model Predictive Control of Demand for Ancillary Services. In Proceedings of the 2013 IEEE International Conference on Smart Grid Communications (SmartGridComm), Vancouver, BC, Canada, 21–24 October 2013; pp. 684–689.
10. Chen, C.; Wang, J.; Heo, Y.; Kishore, S. MPC-Based Appliance Scheduling for Residential Building Energy Management Controller. *IEEE Trans. Smart Grid* **2013**, *4*, 1401–1410. [CrossRef]
11. Chen, Z.; Zhang, Y.; Zhang, T. An Intelligent Control Approach to Home Energy Management under Forecast Uncertainties. In Proceedings of the 2015 IEEE 5th International Conference on Power Engineering, Energy and Electrical Drives (POWERENG), Riga, Latvia, 11–13 May 2013; pp. 657–662.
12. Hanif, S.; Melo, D.F.R.; Maasoumy, M.; Massier, T.; Hamacher, T.; Reindl, T. Model Predictive Control Scheme for Investigating Demand Side Flexibility in Singapore. In Proceedings of the 2015 50th International Universities Power Engineering Conference (UPEC), Stoke on Trent, UK, 1–4 September 2015; pp. 1–6.
13. Dufour, L.; Genoud, D.; Jara, A.; Treboux, J.; Ladevie, B.; Bezian, J.J. A Non-Intrusive Model to Predict the Exible Energy in a Residential Building. In Proceedings of the 2015 IEEE Wireless Communications and Networking Conference Workshops (WCNCW), New Orleans, LA, USA, 9–12 March 2015; pp. 69–74.
14. Oliveira, D.; Rodrigues, E.M.G.; Mendes, T.D.P.; Catalão, J.P.S.; Pouresmaeil, E. Model Predictive Control Technique for Energy Optimization in Residential Appliances. In Proceedings of the 2015 IEEE International Conference on Smart Energy Grid Engineering (SEGE), Oshawa, ON, Canada, 17–19 August 2015; pp. 1–6.
15. Parisio, A.; Wiezorek, C.; Kyntäjä, T.; Elo, J.; Johansson, K.H. An MPC-Based Energy Management System for Multiple Residential Microgrids. In Proceedings of the 2015 IEEE International Conference on Automation Science and Engineering (CASE), Gothenburg, Sweden, 24–28 August 2015; pp. 7–14.
16. Rofiq, A.; Widyotriatmo, A.; Ekawati, E. Model Predictive Control of Combined Renewable Energy Sources. In Proceedings of the 2015 International Conference on Technology, Informatics, Management, Engineering Environment (TIME-E), Samosir, Indonesia, 7–9 September 2015; pp. 127–132.

17. Hidalgo Rodríguez, D.I.; Myrzik, J.M. Economic Model Predictive Control for Optimal Operation of Home Microgrid with Photovoltaic-Combined Heat and Power Storage Systems. *IFAC-PapersOnLine* **2017**, *50*, 10027–10032. [CrossRef]

18. Mirakhorli, A.; Dong, B. Model Predictive Control for Building Loads Connected with a Residential Distribution Grid. *Appl. Energy* **2018**, *230*, 627–642. [CrossRef]

19. Godina, R.; Rodrigues, E.M.G.; Pouresmaeil, E.; Matias, J.C.O.; Catalão, J.P.S. Model Predictive Control Home Energy Management and Optimization Strategy with Demand Response. *Appl. Sci.* **2018**, *8*, 408. [CrossRef]

20. Arikiez, M.; Grasso, F.; Zito, M. Heuristics for the Cost-Effective Management of a Temperature Controlled Environment. In Proceedings of the 2015 IEEE Innovative Smart Grid Technologies—Asia (ISGT ASIA), Bangkok, Thailand, 3–6 November 2015; pp. 1–6.

21. Touretzky, C.R.; Baldea, M. Model Reduction and Nonlinear MPC for Energy Management in Buildings. In Proceedings of the 2013 American Control Conference, Washington, DC, USA, 17–19 June 2013; pp. 461–466.

22. Yu, Z.; Jia, L.; Murphy-Hoye, M.C.; Pratt, A.; Tong, L. Modeling and Stochastic Control for Home Energy Management. *IEEE Trans*. *Smart Grid* **2013**, *4*, 2244–2255. [CrossRef]

23. Momoh, J.A.; Zhang, F.; Gao, W. Optimizing Renewable Energy Control for Building Using Model Predictive Control. In Proceedings of the 2014 North American Power Symposium (NAPS), Pullman, WA, USA, 7–9 September 2014; pp. 1–6.

24. Agheb, S.; Tan, X.; Tsang, D.H.K. Model Predictive Control of Integrated Room Automation Considering Occupants Preference. In Proceedings of the 2015 IEEE International Conference on Smart Grid Communications (SmartGridComm), Miami, FL, USA, 2–5 November 2015; pp. 665–670.

25. Oliveira, D.; Rodrigues, E.M.G.; Godina, R.; Mendes, T.D.P.; Catalão, J.P.S.; Pouresmaeil, E. MPC Weights Tunning Role on the Energy Optimization in Residential Appliances. In Proceedings of the 2015 Australasian Universities Power Engineering Conference (AUPEC), Wollongong, NSW, Australia, 27–30 September 2015; pp. 1–6.

26. Vanouni, M.; Lu, N. Improving the Centralized Control of Thermostatically Controlled Appliances by Obtaining the Right Information. *IEEE Trans*. *Smart Grid* **2015**, *6*, 946–948. [CrossRef]

27. Godina, R.; Rodrigues, E.M.; Pouresmaeil, E.; Catalão, J.P. Optimal Residential Model Predictive Control Energy Management Performance with PV Microgeneration. *Comput*. *Oper*. *Res*. **2018** *96*, 143–156. [CrossRef]

28. Hilliard, T.; Swan, L.; Qin, Z. Experimental Implementation of Whole Building MPC with Zone Based Thermal Comfort Adjustments. *Build*. *Environ*. **2017**, *125*, 326–338. [CrossRef]

29. Alrumayh, O.; Bhattacharya, K. Model Predictive Control Based Home Energy Management System in Smart Grid. In Proceedings of the 2015 IEEE Electrical Power and Energy Conference (EPEC), London, ON, Canada, 26–28 October 2015; pp. 152–157.

30. Oliveira, D.; Rodrigues, E.M.G.; Godina, R.; Mendes, T.D.P.; Catalão, J.P.S.; Pouresmaeil, E. Enhancing Home Appliances Energy Optimization with Solar Power Integration. In Proceedings of the IEEE EUROCON 2015—International Conference on Computer as a Tool (EUROCON), Salamanca, Spain, 8–11 September 2015; pp. 1–6.

31. Kozák, .; Pytel, A.; Drahoš, P. Application of Hybrid Predictive Control for Intelligent Buildings. In Proceedings of the 2015 20th International Conference on Process Control, (PC), Strbske Pleso, Slovakia, 9–12 June 2015; pp. 203–208.

32. Zanoli, S.M.; Pepe, C.; Orlietti, L.; Barchiesi, D. A Model Predictive Control Strategy for Energy Saving and User Comfort Features in Building Automation. In Proceedings of the 2015 19th International Conference on System Theory, Control and Computing (ICSTCC), Cheile Gradistei, Romania, 14–16 October 2015; pp. 472–477.

33. Godina, R.; Rodrigues, E.M.G.; Pouresmaeil, E.; Matias, J.C.O.; Catalão, J.P.S. Model Predictive Control Technique for Energy Optimization in Residential Sector. In Proceedings of the 2016 IEEE 16th International Conference on Environment and Electrical Engineering (EEEIC), Florence, Italy, 7–10 June 2016; pp. 1–6.

34. Rahmani-andebili, M.; Shen, H. Energy Scheduling for a Smart Home Applying Stochastic Model Predictive Control. In Proceedings of the 2016 25th International Conference on Computer Communication and Networks (ICCCN), Waikoloa, HI, USA, 1–4 August 2016; pp. 1–6.

35. Sundström, C.; Jung, D.; Blom, A. Analysis of Optimal Energy Management in Smart Homes Using MPC. In Proceedings of the 2016 European Control Conference (ECC), Aalborg, Denmark, 29 June–1 July 2016; pp. 2066–2071.

36. Ascione, F.; Bianco, N.; De Stasio, C.; Mauro, G.M.; Vanoli, G.P. A New Comprehensive Approach for Cost-Optimal Building Design Integrated with the Multi-Objective Model Predictive Control of HVAC Systems. *Sustain. Cities Soc.* **2017**, *31*, 136–150. [CrossRef]

37. Arikiez, M.; Alotaibi, F.; Rehan, S.; Rohouma, W. Minimizing the Electricity Cost of Coordinating Houses on Microgrids. In Proceedings of the 2016 IEEE PES Innovative Smart Grid Technologies Conference Europe (ISGT-Europe), Ljubljana, Slovenia, 9–12 October 2016; pp. 1–6.

38. DYMOLA Systems Engineering. Available online: https://www.3ds.com/products-services/catia/products/dymola/ (accessed on 20 August 2018).

39. Esterl, T.; Leimgruber, L.; Ferhatbegovic, T.; Zottl, A.; Krottenthaler, M.; Weiss, B. Aggregating the flexibility of heat pumps and thermal storage systems in Austria. In Proceedings of the 2016 5th International Conference on Smart Cities and Green ICT Systems (SMARTGREENS), Rome, Italy, 23–25 April 2016; pp. 1–6.

40. Killian, M.; Zauner, M.; Kozek, M. Comprehensive Smart Home Energy Management System Using Mixed-Integer Quadratic-Programming. *Appl. Energy* **2018**, *222*, 662–672. [CrossRef]

2.3 Publication C

Rao, B.V.; Stefan, M.; Schwalbe, R.; Karl, R.; Kupzog, F.; Kozek, M.
Stratified Control Applied to a Three-Phase Unbalanced Low Voltage Distribution Grid in a Local Peer-to-Peer Energy Community

Own contribution

Conceptualization and methodology was developed by the candidate along with second, sixth and tenth author. Formal analysis, methodology, implementation of algorithms and coding was performed by the candidate. Modelling was performed by the candidate and the fourth author. Interfaces were developed by third, fourth, fifth, eighth and ninth author. Validation and investigation was performed by the candidate. Structuring and writing of the manuscript was done by the candidate under the supervision of sixth and tenth author.

energies

MDPI

Article

Stratified Control Applied to a Three-Phase Unbalanced Low Voltage Distribution Grid in a Local Peer-to-Peer Energy Community

Bharath Varsh Rao [1,*][iD], Mark Stefan [1][iD], Roman Schwalbe [1][iD], Roman Karl [1], Friederich Kupzog [1], and Martin Kozek [2][iD]

[1] Electric Energy Systems Center for Energy, AIT Austrian Institute of Technology, 1210 Vienna, Austria; mark.stefan@ait.ac.at (M.S.); roman.schwalbe@ait.ac.at (R.S.); roman.karl@ait.ac.at (R.K.); friederich.kupzog@ait.ac.at (F.K.)

[2] Institute of Mechanics and Mechatronics, Faculty of Mechanical and Industrial Engineering, Vienna University of Technology, 1060 Vienna, Austria; martin.kozek@tuwien.ac.at

* Correspondence: bharath-varsh.rao@ait.ac.at

Abstract: This paper presents control relationships between the low voltage distribution grid and flexibilities in a peer-to-peer local energy community using a stratified control strategy. With the increase in a diverse set of distributed energy resources and the next generation of loads such as electric storage, vehicles and heat pumps, it is paramount to maintain them optimally to guarantee grid security and supply continuity. Local energy communities are being introduced and gaining traction in recent years to drive the local production, distribution, consumption and trading of energy. The control scheme presented in this paper involves a stratified controller with grid and flexibility layers. The grid controller consists of a three-phase unbalanced optimal power flow using the holomorphic embedding load flow method wrapped around a genetic algorithm and various flexibility controllers, using three-phase unbalanced model predictive control. The control scheme generates active and reactive power set-points at points of common couplings where flexibilities are connected. The grid controller's optimal power flow can introduce additional grid support functionalities to further increase grid stability. Flexibility controllers are recommended to actively track the obtained set-points from the grid controller, to ensure system-level optimization. Blockchain enables this control scheme by providing appropriate data exchange between the layers. This scheme is applied to a real low voltage rural grid in Austria, and the result analysis is presented.

Keywords: local energy communities; Blockchain; stratified control; optimal power flows; holomorphic embedding load flow method; model predictive control; smart grids

1. Introduction

In recent years, local energy communities (LECs) are gaining interest in Europe and the world by introducing new regulations for its formation, operation and control. LECs' introduction is due to increased distributed renewable energy sources (DERs) and new loads such as electric vehicles, storage and heat pumps, hereafter referred to as next-gen loads, in low voltage distribution grids. This is to motivate the local generation, distribution, consumption and trading of energy. The research presented in this paper is conducted under the Blockchian Grid project funded by the Climate and Energy Fund and implemented in the RTI-initiative "Flagship region Energy" of the Austrian Research Promotion Agency. The most significant limitation of a local energy market associated within an LEC is the availability of a settlement process. Such processes are in place to ensure no violation occurs in the grid when the bids, accepted in the market, are executed. The need is due to the lack of controllability of DERs and next-gen-loads. In this context, a stratified control system, which manages both the grid and various DERs and flexibilities, could be one of the approaches.

In the literature, stratified control for flexibility management is extensively used. In [1], a stratified control scheme to control voltage and current is presented. It includes the optimal reconfiguration of various systems in micro-grid based on changing conditions. The first layer consists of the optimal sharing of load and the second level consists of dynamic optimization of droop gains. However, this approach is not designed for three phase systems as size of the problem will start to become large. Additionally, the second level consists of only droop gains where flexibilities, which offer on/off behavior cannot be included. The authors of [2] have proposed a hierarchical energy management system, to interconnect multiple micro-grids. At the higher level, micro-grid coordination operations are performed based on energy scheduling and generation of power reference values for other micro-grids.In the lower level, a chance-constrained MPC is applied for local operation management. The goal to maximize the local utilization of capacities and reduce the dependence on interconnected grids. A major limitation of this approach is that the higher level control does not include an optimal power flow based scheduling algorithm, leading to a sub-optimal solution. In [3], a hybrid stratified control to improve grid security is presented. In the lower level, the controllers are responsible for coordinating each of the individual control units. Whereas, in the higher level, continuous dynamic control of discrete controllers and with individual lower-level controllers is presented. The authors of [4] have presented a hierarchical iterative control algorithm to balance the grid optimally and, at the same time, meet consumer demand. The major limitation of the control strategies mentioned above is the need for detailed technical models of lower-level controllers. Detailed models are often not available or difficult to derive, making them unrealistic for implementation. Additionally, any change in the devices at the lower level needs to be recorded and appropriate adjustment in the algorithm needs to be made. However, in this paper, optimal schedules are generated at the PCC of flexibilities irrespective of what is connected to it. Moreover, the data exchange between each layer and within each layer needs to be sufficiently strong enough to handle a large number of variables being exchanged. Blockchain with a 15s block speed is used in this paper to write data into the chain, which is available in all other buses in the next sample.

The stratified controller consists of an OPF at the upper level. As discussed in [5], OPF algorithms can be classified into two types, A and B, respectively. Type A deals with algorithms that use load flow methods to generate a certain set of intermediate solutions for voltages and phase angles. Since the optimal solution is close to the load flow solution, using jacobian and other sensitivity relations, it can be sequentially determined. Various implementations of class A algorithms are presented in [6–8]. Class B deals with algorithms that use load flow equations as equality constraints, depending on the exact conditions and detailed formulation. It utilizes the entire search space. Since power grids are nonlinear and non-convex in nature, convex relaxation or non-convex solvers are to be used. It uses optimality conditions using Lagrangian functions with objective and constraint derivatives. In [9], a novel class C algorithm is presented in which a reliable load flow is coupled with a heuristic optimization method. This method helps to overcome the challenges presented by classes A and B, which are used in this paper.

Low voltage rural distribution grids are unbalanced due to untransposed lines and uneven loading on their three-phases [10]. The unbalance can be heightened with increase in single-phase DERs and next-gen loads [11,12]. They are dependent on weather parameters such as temperature and solar irradiation. Moreover, they are periodic, with hourly, daily, weekly and monthly cycles and are dependent on seasons. Three-phase unbalance, induces several issues in the grid. Most prominently, it increases losses in lines, grid devices and transformers. Transformers in the distribution grids are designed for balanced operation and would lead to uneven temperatures on the three phases, causing degradation [13]. Induction motors are significantly affected by voltage imbalance, causing accelerated aging due to high temperatures on winding with the highest loading and shorten the lifespan [14]. Torque fracturing can lead to permanent damage in motor winding with the increase in voltage unbalance [15]. Protection systems can be triggered

falsely due to the presence of negative and zero sequence currents in the lines [16]. Currently, models describing the low voltage distribution grids are based on the transmission system's supervisory control and data acquisition systems at the transmission level. This host functions like load (LF) and optimal power flow (OPF), using models that are single phased. They cannot be readily applied to distribution grids without modification to accommodate the new changes, as discussed above. To overcome this, the LF and OPF should include three-phase unbalance.

In the literature, various methods have been presented to minimize three-phase unbalance, which can be consolidated into three types. Namely, phase transposition, feeder reconfiguration, and power control. In [17], a method to minimize three-phase unbalance for both star and delta configurations is presented. This is performed by operating various devices connected to the IEEE 34 and 123 bus test systems. The grid is linearized to convert non-linearity non-convexity to mixed-integer linear programming. The authors of [18] have formulated a method to minimize three-phase unbalance by re-phasing and reconfiguration using optimization techniques and by optimally placing DER units. In [19], re-phasing and DER sizing are used to achieve three-phase unbalance minimization. A fuzzy multi-objective phase balancing optimization is used to do so. Various heuristic optimization techniques for three-phase unbalance minimization is presented in [16,20,21]. Various phase swapping algorithms are reviewed in [22]. In [23], power balance is used to minimize unbalance by optimally operating energy storage, and a similar method is presented in [24]. Various methods involving reactive power control for unbalance minimization are available in the literature. In [25], static variable compensators are used to balance the three phases. The authors of [26] describe a method to minimize zero and negative sequence current components in distribution grids. It involves the use of reactive power management using the online Karush–Kuhn–Tucker optimization method. This method is applied to IEEE 13-node test network. Most of the methods mentioned above are used in the planning phase. This does not include the dynamic behavior of unbalanced loads and generation. In this paper, the stratified controller is to minimize the three-phase voltage unbalance in real-time.

Flexibilities are controlled using model predictive control (MPC) and, in the literature, various implementations are available. In [27], a multi-time scale and stage optimization method is proposed to control flexibilities such as air conditioning, heating and ventilation systems, and plug-in hybrid electric vehicles are presented. It uses a constrained stochastic optimization algorithm using MPC to minimize costs, peak power and consumer comfort. Temperature data, thermal dynamics and real-time electricity pricing are included. The authors of [28] have presented an MPC approach to shifting loads among household devices and electric storage systems. Energy consumption is minimized by using time of day tariff and demand-side management (DSM) by optimally scheduling loads and charging and discharging times of the electric storage system. An appliance scheduling method in residential buildings using MPC is presented in [29]. It involves the use of thermal and non-thermal flexibilities by incorporating forecasts and database updates to minimize electricity costs. It includes a thermal dynamic of the building and is used as constraints to MPC. In [30], the MPC approach to controlling photo-voltaic combined heat and electric storage is presented. The operational cost of the combined heat and power unit is minimized. The authors of [31] have presented a method to control the air conditioning system in the room, along with the PV system. Demand response is provided using time of use tariff. Additionally, the controller is used to minimize energy consumption. In [32], the authors present a three-phase unbalanced model predictive control based smart building energy management system. It uses three-phase flexibility models with mixed-integer quadratic programming. In this paper, the smart building models and control strategies are derived from it.

To overcome the limitations presented in the literature, the authors present a novel stratified control scheme with grid and flexibility layers. The former consists of three-phase unbalanced optimal power flow using the holomorphic embedding load flow method

(HELM) and the latter, three-phase unbalanced model predictive control. Blockchain handles all exchanges of control variables (see Section 2). The flexibilities are connected at a certain number of buses which are considered controllable, and the grid level controller generates three-phase optimal active (P) and reactive power (Q) schedules at their points of common couplings (PCC). The grid level controller concentrates PQ consumption and in-feed values from smart meters, from all other uncontrollable loads in the LEC over the Blockchain for each sample time. Contrary to the methods presented in the literature, the grid level controller does not contain any information about the devices connected at the PCC, ensuring individual privacy. The stratified controller uses models that include three-phase controls for both PQ flows, resulting in per-phase power manipulation. These schedules are actively tracked by the flexibilities along with their objectives, leading to a system-level optimization. The grid level controller uses Optimal Power Flow (OPF), based on a three-phase unbalanced holomorphic embedding load flow method (HELM) and genetic algorithm with certain advantages over the existing methods (see Section 4). As discussed above, the DERs and next-gen loads are intermittent, dependent on external factors and, therefore, model predictive control (MPC) (see Section 5), with its proven robustness, is used to manage them optimally.

The contributions in this paper are listed below:

1. Stratified control structure for optimal scheduling of grid flexibility in an LEC using Blockchain (see Sections 3 and 6).
2. Online three-phase unbalance minimization control scheme in low voltage distribution networks (see Section 4.1.1) in an LEC.
3. Three-phase unbalance optimal power flow with receding horizon formulation for optimal flexibility placement (see Section 4.1.2) and voltage controllability (see Sections 4.1.3 and 6).
4. Schedules from the grid controller are generated at the PCC, ensuring privacy. No device information from the buildings is communicated to the grid controller.
5. Mixed integer quadratic three-phase unbalanced model predictive control hosted in flexibilities with various electrical connection configurations and thermal models (see Section 5.1).
6. Optimal scheduling of PQ set-points at critical buses, where smart buildings are connected and model predictive control results from flexibilities to the reference optimal schedules from the grid controller (see Section 7).
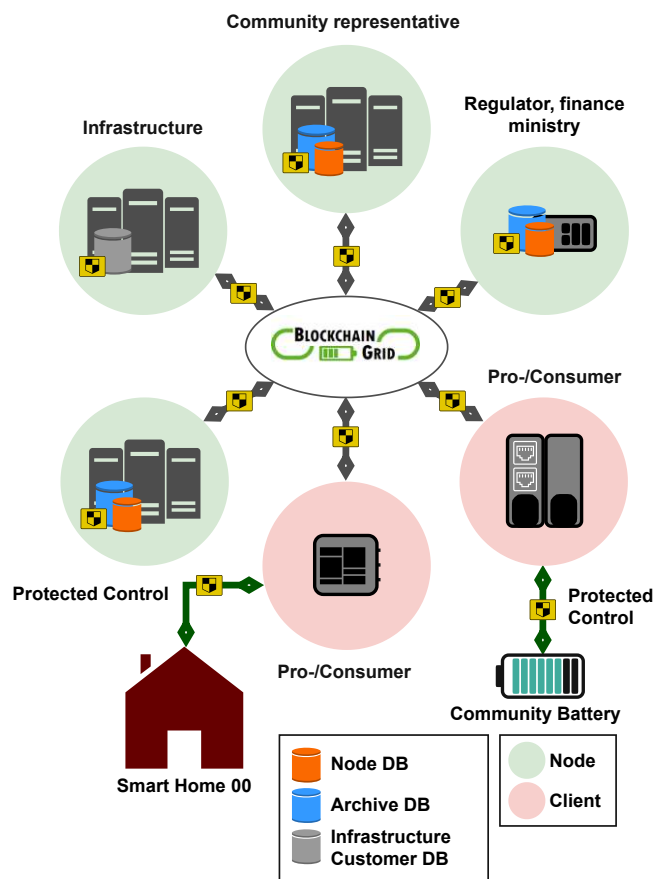
2. Blockchain System Architecture

The Ethereum client Open Ethereum is the basis for the Blockchain architecture adopted in this project. Various servers and communication components are seen in Figure 1. Any node in the network can write data into the Blockchain. In the project, this is constrained and limited by the LEC platform manager at the infrastructure server. Additionally, the grid controller is hosted on this server, which generates optimal set-points for various flexibility controllers in the LEC and facilitates the market processes. The consensus algorithm on how to agree on new blocks is Proof-of-Authority, in which only authorized participants, called sealers, are allowed to generate blocks containing transactions and add them to the Blockchain. Participants can also be dynamically added or removed by the platform operator.

There are two different types of nodes, full nodes, which also perform the sealing to add blocks, and nodes located at measurement devices, sensors and actuators. The latter ones do not perform any sealing and can be configured to run as light clients to lower the hardware requirements. Light clients do not keep the whole chain data, but can participate in the network by trusting other nodes.

Every 15 s a new block is added, which is much lower than the 1 min sample time. This way, it is guaranteed that transactions are processed in time for the next sample. Every sample, PQ values are fed into the Blockchain at all the buses in the grid. Information for the Blockchain, smart contracts, the role of participants and access rights are stored in the

infrastructure server. Real customer data (name, address, customer number) is associated with an Ethereum account address. This is managed and used by the Distribution System Operator (DSO) for billing-relevant purposes. The data exchange between the infrastructure server and the participants takes place via an encrypted connection. To be able to access the data, each participant receives an access identifier (username and password). This identifier is linked to the customer data by the infrastructure server.


Figure 1. Blockchain System Architecture implemented in the BlockchainGrid project at the LEC in Austria.

3. Stratified Control Scheme for Low Voltage Distribution Networks

In this section, the authors present a stratified control scheme for voltage management in a three-phase low voltage distribution grid, as part of an LEC. They are inherently unbalanced, as discussed in Section 1, and the unbalance is further increased by DERs and next-gen loads. It is paramount to minimize it for safe system operation. A methodology to generate optimal set-points at a certain number of controllable buses at critical nodes is presented. Flexibilities connected at these buses actively track these set-points using model predictive control. In this research, smart buildings with various flexibilities, such as electric storage and heat-pumps, are connected at these critical nodes (see Section 5).The upper level controller consists of an optimal power flow model using a three-phase unbalanced holomorphic embedding load flow method (HELM-OPF), characterized in Section 4 and mixed-integer quadratic programming model predictive control (MiQ-MPC) is described in Section 5. Figure 2 describes a general model schematic and Figure 3 describes the control structure.
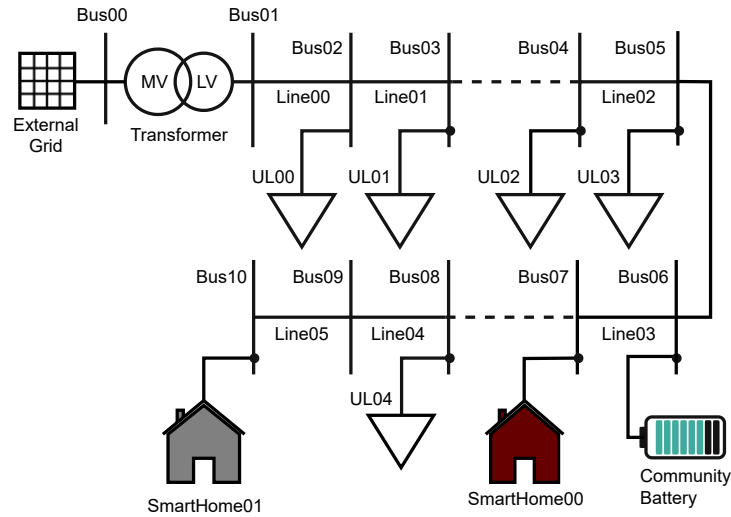
Figure 2. General schematic of a three-phase unbalanced distribution grid with a medium-voltage/low-voltage transformer, uncontrollable loads (UL), smart buildings and a community battery system.
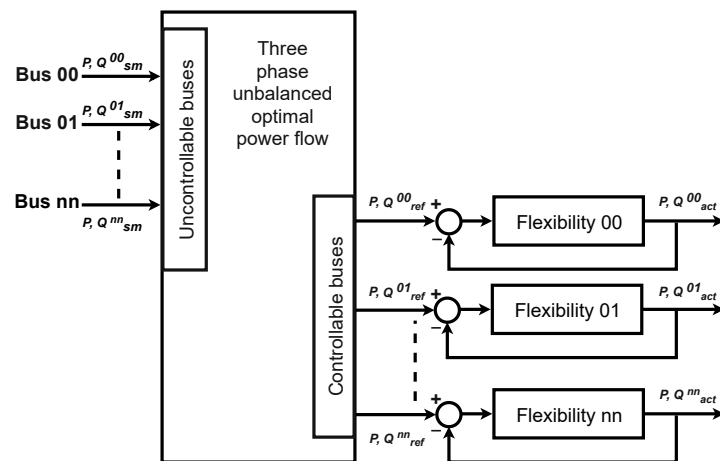
Figure 3. Structure of the stratified control scheme. Inputs to the grid controller are forecasted profiles of smart meter active and reactive (P_i^{sm}, Q_i^{sm}) profiles from loads located at various uncontrollable buses (Bus 00, Bus 01, ..., Bus nn). Outputs are optimal P_i^{ref} and Q_i^{ref} set-points that are calculated using HELM-OPF and fed into individual flexibility controllers. Using these reference profiles, the flexibility controller produces optimal set-points for its flexibility portfolio, which are P_i^{act} and Q_i^{act} using MiQ-MPC. Based on the available flexibility type and their sizing, the buildings may not be able to perfectly tract the reference profiles generated by the grid controller.

It is to be noted that the grid level controller does not directly provide set-points to the individual flexibilities as it does not have any device model information. It instead generated set-points at the buses where they are connected (at the PCC). This leads to the preservation of sensitive flexibility information and helps protect consumer privacy.

4. Grid Controller Formulation

Power grids are nonlinear and non-convex and it is strenuous to solve the OPF problem associated with it. Various methods have been presented to handle such non-linearity and non-convexity. In this paper, a solution to OPF using the non-convex optimization method is chosen. This is based on the method developed in [9]. It uses a three-phase unbalanced holomorphic embedding load flow method (HELM) with a genetic algorithm

to generate optimal set-points, a HELM-OPF method. The reason for using HELM is due to its robustness and ability to converge to a high voltage operable solution irrespective of its initial conditions (very high or low loading conditions) [9]. Using HELM, OPF is given access to the entire search space.

Three-phase unbalanced low voltage distribution network models are adopted from [33]. OPF is formulated as,

$$
\begin{aligned}
\underset{u}{\text{minimize}} \ J = & \quad F(x,u) \\
\text{subject to} & \quad H(x,u) = 0, \\
& \quad G(x,u) \leq 0,
\end{aligned}
\tag{1}
$$

where, x and u are state and input variable sets. Input variables are the active and reactive power injections at controllable buses; state variables are voltage and phase angles (see Figure 3).

$F(x,u)$ is the objective function for the HELM-OPF problem. Typical objectives are total generator cost and loss minimization in the network.

4.1. Objective Functions

In this paper, three objective functions are used. Objective Section 4.1.1 is used to minimize three-phase unbalance and is used online. Objective Section 4.1.2 is used to choose the best number of controllable buses where flexibilities are needed. Objective Section 4.1.3 is used to determine the voltage controllability.

4.1.1. Three-Phase Unbalance Minimization

The objective function is chosen to minimize three-phase voltage unbalance. There are various methods to realize the objective and, in this paper, balanced voltages are used as a reference, which is illustrated in Equation (2).

$$
\begin{aligned}
\text{minimize } J = \sum_{t \in T} \sum_{k \in Y} \sum_{p \in P} & (real(V_{k,balanced}^{p,t}) - real(V_k^{p,t}))^2 \\
& + (imag(V_{k,balanced}^{p,t}) - imag(V_k^{p,t}))^2,
\end{aligned}
\tag{2}
$$

where Y represents buses in the network (see Section 4.1.3 for various scenarios), T represents simulation time and $P \in phases(a, b, c)$. The rectangular coordinate system is used to represent voltages and to balance both magnitudes and phase angle; therefore, both real and imaginary parts of complex voltages are used. In Section 7, three different forms of the objective function are defined.

$G(x,u)$ and $H(x,u)$ are the equality and inequality constraints. Three-phase unbalanced HELM developed in [9] is used as equality constraints.

Inequality constraints with respect to distribution grids are as follows,

$$
P_{Low_i}^p \leq P_{PV_i}^p \leq P_{High_i}^p
\tag{3}
$$

$$
|V_{Low_i}^p| \leq |V_i^p| \leq |V_{High_i}^p|
\tag{4}
$$

$$
t_{Low_i} \leq t_i \leq t_{High_i}
\tag{5}
$$

$$
\theta_{Low_i} \leq \theta_i \leq \theta_{High_i}
\tag{6}
$$

$$
s_{Low_i} \leq s_i \leq s_{High_i}
\tag{7}
$$

$$
Q_{Low_i}^p \leq Q_{PV_i}^p \leq Q_{High_i}^p
\tag{8}
$$

$$
P_{i,j}^p \leq P_{High_{i,j}}^p
\tag{9}
$$

$$
P_{i,j}^{p2} + Q_{i,j}^{p2} \leq S_{High_{i,j}}^{p2}
\tag{10}
$$

$$
|I_{i,j}^p| \leq |I_{High_{i,j}}^p|
\tag{11}
$$

$$
\Theta_{Low_i}^p \leq \Theta_i^p - \Theta_j^p \leq \Theta_{High_i}^p.
\tag{12}
$$

The variables in the equations above are defined in the Table 1.

Table 1. Nomenclature.

Variable	Definition
P	Active power
Q	Reactive power
V	Voltage
t	Transformer tap position
θ	Transformer phase shift angle
s	shunt reactances or capacitances
I	Branch current magnitudes
Θ	Voltage phase angle

4.1.2. Optimal Placement of Flexibilities

It is essential to optimally place the flexibilities in the grid to have the maximum impact on voltage control. Various methods are used to determine the location where flexibility is connected.

Most predominantly, they can be broadly classified into two types. Firstly, the voltage sensitivity method, like the quasi-dynamic simulation, is used similarly to those in [4]. This method is limited since it only provides information about the buses where most voltage violations occur for a given period. This method had several limitations since power grids are nonlinear and non-convex.

Secondly, an optimal heuristic technique uses flexibility models and OPF to determine the best location using a non-convex solver. Variations of this method are detailed in [34–36]. In this paper, the authors present a method that is based on the heuristic technique but does not need any flexibility models, which need to be included in the HELM-OPF formulation. They are determined based on only active and reactive power injections at the buses. This method applies to any flexibility or DER unit without including any information about it. Mixed-integer programming, along with the HELM method from the previous Section, is used, and the associated objective function is presented in Equation (13). This is a modification of Equation (2), where an additional integer term is added to determine the best location.

$$
\begin{aligned}
\text{minimize } J = \sum_{k \in \Omega} (DC_k + E \sum_{p \in P} (real(V^p_{k,balanced}) - real(V^p_k))^2 \\
+ (imag(V^p_{k,balanced}) - imag(V^p_k))^2),
\end{aligned}
\tag{13}
$$

where C_k represents the binary variable associated with each bus in the network leading to a set of optimal controllable buses. D and E are weights associated with the objectives.

4.1.3. Voltage Controllability

During the research, the voltage unbalances minimization at the buses, directly depending on the optimal schedule.

In other words, voltages at all the buses are controlled by PQ powers at flexibilities and at only certain controllable buses (Case 01). Therefore, using Equation (2), the following three scenarios are chosen:

$$
Y = \begin{cases} \Omega & \text{all buses (Case 01)} \\ V & \text{voltage violation buses (Case 02)} \\ C & \text{optimal controllable buses (Case 03),} \end{cases}
\tag{14}
$$

where V represents all the buses where voltage violation was observed. C represents optimal controllable buses from Section 4.1.2. The results of the three scenarios are discussed in Section 7.

5. Flexibility Controller Formulation

Flexibilities in this paper are mostly hosted in smart building energy management systems with the addition of a large community battery.

5.1. Smart Building Thermal Model

Smart building models are derived from [32]. Various smart building models with varying degrees of complexity are used in this paper. Figure 4 represents a three-phase unbalanced smart building energy management system with various single and three-phase loads.
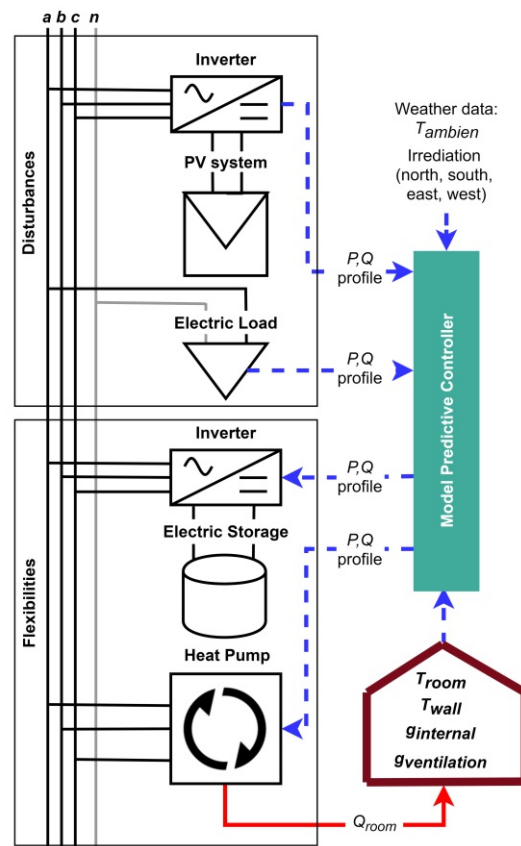
Figure 4. Schematic of three-phase HEMS with various electrical and thermal components. It can be observed that the electric appliances can have single, two or three-phase connection configurations.

Thermal models of smart buildings are based on typical buildings in Austria and are derived from [32] and are represented as a discrete state-space system with a sampling time of 15 min.

$$x_{room}(t+1) = A_{room} \quad x_{room}(t) + B_{room} \quad u_{room}(t). \tag{15}$$

Room and structure temperatures are the state variables in x_{room} (see Equation (16)). $T_{structure}$ is the temperature of the floor, walls and ceiling. A_{room} and B_{room} are the system matrices of the building.

$$x_{room} = \begin{bmatrix} T_{structure} \\ T_{room}. \end{bmatrix} \tag{16}$$

Equations (17) and (18) are the lower and upper limits of the temperatures in Equation (16).

$$T_{structure}^{min} \leq T_{structure}(t) \leq T_{structure}^{max} \tag{17}$$

$$T_{room}^{min} \leq T_{room}(t) \leq T_{room}^{max}. \tag{18}$$

u_{room} describes the input vector of the state–space system. The only controllable variable is q_{room}, which is the heat flowing into the room.

$$u_{room} = \begin{bmatrix} q_{room} \\ T_{ambient\ temperature} \\ i_{north} \\ i_{east} \\ i_{south} \\ i_{west} \\ g_{internal\ gain} \\ g_{ventilation\ losses}, \end{bmatrix} \tag{19}$$

where $T_{ambient\ temperature}$ is the outdoor temperature, solar irradiation from all directions is $i_{north,\ east,\ south,\ west}$ and $g_{internal\ gain,\ ventilation\ losses}$ are the internal gains and ventilation losses, respectively.

Equation (20) represents the limits on q_{room}. In this paper, only heating is assumed and therefore, q_{room} is greater than zero.

$$0 \leq q_{room}(t) \leq q_{room}^{max}. \tag{20}$$

5.2. Constraints on Heat-Pump

Equations (21) and (22) are the single and three-phase powers of the heart pump, respectively. Coefficient of performance ($cop_{heat\ pump}$) is assumed to be time-invariant and constant.

$$P_{heat\ pump}(t) = \frac{q_{room}(t)}{cop_{heat\ pump}} \tag{21}$$

$$P_{heat\ pump}^{p}(t) = \frac{q_{room}(t)}{3\ cop_{heat\ pump}}, \tag{22}$$

where $P_{heat\ pump}$ is the active power and $cop_{heat\ pump}$ is the coefficient of performance. $p \in phases(a, b, c)$. In order to model the on-off heat-pump model of certain house models, a binary variable $B_{heat\ pump}$ is used. This can be observed in Equation (23).

$$P_{heat\ pump}(t) = B_{heat\ pump}\ P_{heat\ pump}^{rated}. \tag{23}$$

The pump in the heat pump consists of an induction motor and is assumed to be lossless. Additionally, it is assumed to be operating at constant power factor ($pf_{heat\ pump}$) as described in Equation (24), using which, the reactive power ($Q_{heat\ pump}$) is calculated.

$$Q_{heat\ pump}(t) = tan(cos^{-1}(pf_{heat\ pump}))$$
$$P_{heat\ pump}(t). \tag{24}$$

$P_{heat\ pump}$ and $Q_{heat\ pump} \geq 0$, since the heating period is considered, are described in Equations (25) and (26)

$$0 \leq P_{heat\ pump}(t) \leq P_{heat\ pump}^{max} \tag{25}$$

Constraints on heat pump reactive power limits,

$$0 \leq Q_{heat\ pump}(t) \leq Q_{heat\ pump}^{max}, \tag{26}$$

where $P_{heat\ pump}^{max}$ and $Q_{heat\ pump}^{max}$ are rated active and reactive powers, respectively.

5.3. Constraints on Electric Storage

Distributed energy resources are inherently intermittent and it is essential to use their productions to the fullest extent. Therefore, electric storage is gaining importance in recent years. In this paper, the authors have used linear models for electric storage and inverters.

This model is also used to represent the community battery along with the inverter model in Section 5.4. The state of charge (SOC) is described in Equation (27), represents the energy balance in electric storage.

$$
\begin{aligned}
soc(t+1)\, C_{battery} = soc(t)\, C_{battery} \\
+ \Delta t\, \eta_{battery}\, P_{battery}(t).
\end{aligned}
\tag{27}
$$

SOC, battery charging and discharging power limits are as follows,

$$
soc^{min} \leq soc(t) \leq soc^{max}
\tag{28}
$$

$$
P_{battery}^{min} \leq P_{battery}(t) \leq P_{battery}^{max}.
\tag{29}
$$

5.4. Constraints on Inverter

The electric storage described in Section 5.3 is connected to a three-phase inverter. Due to the non-linearity and non-convexity of the three-phase inverter with both active and reactive control along with binary control variable from Section 5.2. In order to maintain the linearity, only active power control is chosen, described in Equations (30) and (31).

$$
(P_{battery}(t))^2 = (P_{inverter}(t))^2.
\tag{30}
$$

Per phase inverter is modeled as follows,

$$
P_{inverter}(t) = \sum_{p} P_{inverter}^{p}(t).
\tag{31}
$$

5.5. Constraints on Controllable Loads

Controllable loads are defined as simple dump loads, which are both single and three-phased. This is done due to the lack of data related to the presence of controllable loads in the field. In the future, this is to be replaced with realistic controllable load models. The constraints on limits of active and reactive powers are defined in Equations (32) and (33). They work with constant power factor ($pf_{controllable\ load}$), described in Equation (34).

$$
0 \leq P_{controllable\ load}^{p}(t) \leq P_{controllable\ load}^{max}
\tag{32}
$$

$$
0 \leq Q_{controllable\ load}^{p}(t) \leq Q_{controllable\ load}^{max}
\tag{33}
$$

$$
\begin{aligned}
Q_{controllable\ load}^{p}(t) = tan(cos^{-1}(pf_{controllable\ load})) \\
P_{controllable\ load}^{p}(t).
\end{aligned}
\tag{34}
$$

Real smart meter profiles from the Blockchain are used for uncontrollable loads and PV systems for each sample.

5.6. Constraints at Grid Connection Point

The bus at which a smart building is connected is referred to as a grid connection point. P_{grid}^{p} and Q_{grid}^{p} takes both positive and negative values. Constraints on active and reactive powers are constrained in Equations (35) and (36).

$$
\begin{aligned}
P_{grid}^{p}(t) = P_{inverter}^{p}(t) + P_{heat\ pump}^{p}(t) \\
+ P_{controllable\ load}^{p}(t) + P_{uncontrollable\ load}^{p}
\end{aligned}
\tag{35}
$$

$$
\begin{aligned}
Q_{grid}^{p}(t) = Q_{heat\ pump}^{p}(t) + Q_{controllable\ load}^{p}(t) \\
+ Q_{uncontrollable\ load}^{p}.
\end{aligned}
\tag{36}
$$

Forecasting of disturbances is carried out using neural networks [37,38]. This method is not described in the paper since it is not the focus. Weather data, such as temperature, are sourced from weather stations in Austria. Irradiation, ventilation losses and internal gains are collected from local sensors and sourced from the iWPP-Flex project. Forecasting uncertainties lead to an issue with the optimal set-points. However, for the sake of simplicity, these conditions are ignored in this paper.

5.7. Objective Function

The objective function used in the smart building is to provide grid support. The three-phase optimal power flow formulation from Section 4 produces optimal active and reactive power schedules, based on an objective function, for various controllable buses. Each smart building can support the grid by tracking the optimal schedules and by controlling various flexibilities, as described in Equation (37).

$$
\begin{aligned}
J_{grid\ support} = \sum_t \sum_p & (P^p_{grid\ optimal\ schedule}(t) - P^p_{grid}(t))^2 \\
& + (Q^p_{grid\ optimal\ schedule}(t) - Q^p_{grid}(t))^2 + .
\end{aligned}
\tag{37}
$$

Equation (38) represents the objective function of a smart building, $J_{grid\ support}$, the individual flexibility objective function, $\mathcal{G}$ and $\mathcal{F}$ are the respective weight. For the sake of simplicity, $J_{grid\ support}$ is to maximize comfort for all smart buildings (Keeping T_{room} at 22 °C).

$$
\text{minimize } J = \mathcal{G}\, J_{grid\ support} + \mathcal{F}\, J_{flexibility\ objective}.
\tag{38}
$$

Variables $P_{heat\ pump}$, $P_{battery}$ and $P_{controllable\ load}$ are controllable. Grid support is maximized while maintaining comfort with respect to temperature and load demands are being completely met.

6. Control Strategy

The smart buildings that are described in Section 5.1 are controlled hierarchically [32]. Inputs to the stratified controller are the smart meter active and reactive power forecasts (P^{sm}_i, Q^{sm}_i). The forecasting method is based on convolutional neural networks, and details about it are not presented in this paper. Three-phase unbalanced optimal power flow from Section 4.1.1 generates optimal active and reactive power set-points to controllable buses. The locations of these buses are chosen based on Section 4.1.2 and Equation (13). Since DERs are intermittent in nature, follow daily, weekly and seasonal cycles, these changes are reflected in the optimal set-points. The flexibility controller must be robust enough to accommodate these changes. The authors have chosen a model predictive control to schedule them optimally. MiQ-MPC receives set-points and is used as reference input signals.

Chronological control functions at grid and house level are presented below.

6.1. Grid Control

Grid control performs HELM-OPF described in Section 4 and broadcasts the optimal set-points to various smart buildings in the network. The chronological control events are presented in Algorithm 1.

6.2. Flexibility Control

Quadratic programming with mixed-integer is used with continuous and on/off heat-pumps, respectively (see Section 5.2). The chronological control events are presented in Algorithm 2.

Algorithm 1: Control actions performed at grid level controller

---

Result: Generate optimal schedules and transmit to flexibility controllers

while *time t = end time* **do**

> At time *t*, various smart meters in the grid write active and reactive power values into the Blockchain. Communication channels are assumed to be functioning ideally with no losses and is validated with a state estimator;
>
> PQ are forecasted are generated for an appropriate prediction horizon using the updated data from the flockchain for $(t/t + t_{grid\ prediction\ horizon})$;
>
> Setup constraints based on Equations (3) to (12) (see Section 4.1.1).
>
> Setup objective function using Equation (2) (see Section 4.1.1).
>
> OPF is run and optimal PQ set-points are generated at certain critical buses where smart buildings are connected;
>
> These optimal set-points are written into the blockchain;

end

Algorithm 2: Control actions performed at flexibility level controller

---

Result: Generate optimal schedules by tracking references from grid level controller.

while *time t = end time* **do**

> At time *t*, smart meter data written into the Blockchain ;
>
> Acquire ambient temperature, irradiation and ventilation data from various sensors in smart buildings along with PQ data from smart meter;
>
> Update the database with these new data points;
>
> Perform forecasts for various disturbances for a given prediction horizon and using an appropriate algorithm such as convolutional neural networks forecasts $(t/t + t_{flexibility\ prediction\ horizon})$;
>
> Apply user defined weights and reference temperature profiles;
>
> Setup constraints and objectives described in Section 5.1;
>
> Get optimal PQ set-points at that particular bus from the blockchain.
>
> MPC generates various set-points for controllable variables;
>
> The process is repeated for the next sample period, $(t + 1)$;

end

---

7. Simulation and Results

The grid selected for the analysis is a 264 bus three-unbalanced low voltage distribution network (three-phase four-wire) in Austria, represented in Figure 5. It contains single and three-phased loads along with DER units. The network is simplified by summing all the loads and generations at each bus to obtain one load per bus. Loads are active and reactive power profiles from real smart meters in the grid. For the sake of privacy, the data are not visualized or presented in this paper.

A simulation is performed to determine the optimal buses at which flexibilities are to be placed as mentioned in Section 4.1.2 and by using the objective function in Equation (13). The optimal buses are presented in Table 2 and are represented in Figure 5. At these buses, simple single-phase uncontrollable loads are replaced with three-phase flexibilities, smart building or a community battery. Having determined the optimal buses where flexibilities are to be placed, the simulation is performed based on the three cases mentioned in Section 4.1.2. These simulations are benchmarked against real smart meter active and reactive power profiles at the controllable buses where flexibilities are to be placed, and their forecasts and optimal schedules are to be produced by the grid level controller. The simulation is performed for two days between 2019-04-01 00:00:00 and 2019-04-02 23:45:00 with 29 smart buildings and one large community storage (Bus 077). Smart buildings are comprised of single and three-phased flexibilities as described in Section 5 and in Figure 4. Table 2 presents various limits on certain controllable variables for optimal buses.
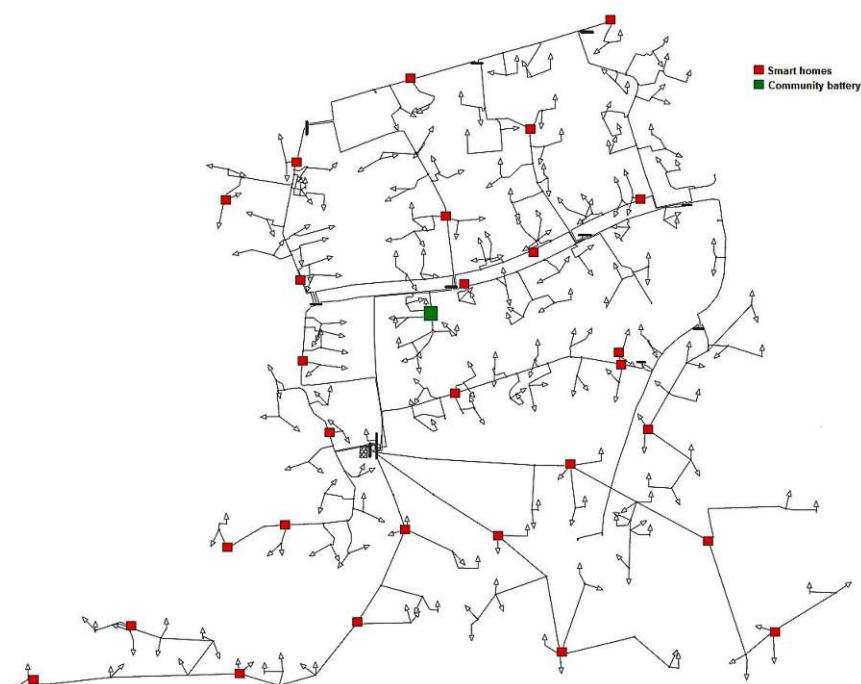
Figure 5. Topology of a real network in Austria with various smart buildings and a community battery.

Figure 6 presents the voltage magnitude results for three scenarios and benchmarks. It can be observed that under and over-voltages (0.95 pu. < voltage < 1.05 pu.) are observed for real and forecasted profiles. The optimal profiles from the grid-level controller have resulted in no voltage violation. The same can be observed for case 01 and 03, as flexibilities are tracking the optimal profiles. The reason for Case 02 to observe over-voltage is because voltage controllability is limited to only controllable buses, as described in Section 4.1.3. In case 01, since all the buses are included, the optimizer is able to mitigate violations. In case 03, since the voltage controllability is the optimal controllable buses, under voltage violation was observed. This is due to the fact that not all the buses are included in the voltage controllability. This enforces that the voltage is a local effect due to power flows in multiple directions. To mitigate voltage violations in all buses, voltage controllability should extend to all buses.
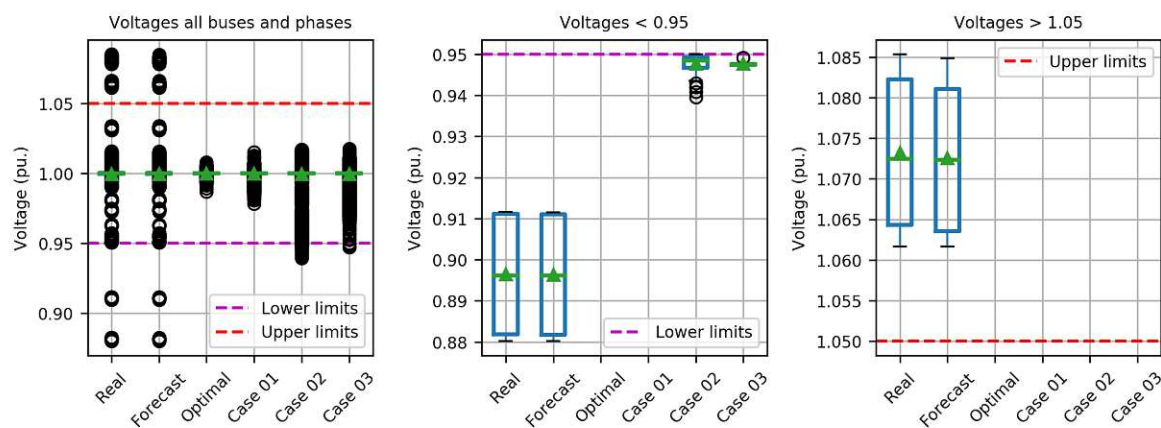

Figure 6. Voltage magnitude distributions for benchmarks, optimal and three cases with under and over voltages for each of the cases.

**Table 2.** Simulation parameter limits for optimal buses.

Optimal Buses	Bus 020	Bus 031	Bus 038	Bus 042	Bus 045	Bus 055	Bus 058	Bus 067	Bus 069	Bus 077
$P^{max}_{heat-pump}$ (kW)	5	9	8	9	5	9	5	6	9	-
$P_{heat-pump\ phase}$ (kW)	1P	1P	3P	1P	3P	1P	1P	1P	1P	-
$P^{max}_{battery}$ (kW)	20	20	27	24	26	27	21	20	22	30
$C_{battery}$ (kWh)	42	31	32	29	36	49	39	34	41	120
$P^{max}_{controllable\ load}$ (kW)	19	16	10	6	15	10	9	16	13	-
$P_{controllable\ load\ phase}$ (kW)	1P	3P	3P	1P	3P	1P	3P	3P	1P	-
Optimal Buses	**Bus 081**	**Bus 091**	**Bus 092**	**Bus 094**	**Bus 099**	**Bus 112**	**Bus 117**	**Bus 118**	**Bus 140**	**Bus 148**
$P^{max}_{heat-pump}$ (kW)	6	6	5	5	8	8	7	8	7	8
$P_{heat-pump\ phase}$ (kW)	3P	1P	1P	1P	1P	1P	3P	1P	3P	1P
$P^{max}_{battery}$ (kW)	24	22	27	26	26	23	20	27	26	21
$C_{battery}$ (kWh)	28	32	26	29	41	30	43	44	31	31
$P^{max}_{controllable\ load}$ (kW)	13	8	9	9	16	5	11	5	15	9
$P_{controllable\ load\ phase}$ (kW)	3P	3P	3P	1P	3P	3P	1P	1P	1P	1P
Optimal Buses	**Bus 168**	**Bus 169**	**Bus 171**	**Bus 184**	**Bus 207**	**Bus 217**	**Bus 225**	**Bus 234**	**Bus 238**	**Bus 241**
$P^{max}_{heat-pump}$ (kW)	8	9	5	7	5	5	7	8	8	6
$P_{heat-pump\ phase}$ (kW)	3P	3P	3P	1P	3P	3P	1P	3P	1P	1P
$P^{max}_{battery}$ (kW)	22	28	23	27	21	29	27	23	20	24
$C_{battery}$ (kWh)	35	31	26	26	33	38	42	40	27	28
$P^{max}_{controllable\ load}$ (kW)	16	16	6	11	14	13	12	7	5	11
$P_{controllable\ load\ phase}$ (kW)	1P	1P	3P	3P	1P	3P	1P	3P	1P	3P

The performance of the flexibilities directly depends on how well they can track the optimal grid schedules. In Figure 7 P_{grid}, $P_{grid\ optimal}$ and their absolute difference is presented for a smart building connected at Bus 020. Similarly, Q_{grid}, $Q_{grid\ optimal}$ and their absolute difference is presented in Figure 8. It can be observed that the smart building can track the optimal grid schedule. This depends on the flexibility composition available in the smart building. Therefore, due to this reason, the global optimum cannot be guaranteed. However, from Figure 9, it can be observed that the results are close to the global optimum.

Figure 9 presents the function values for all the scenarios based on the objective in Equation (2). As discussed earlier, it can be observed that the unbalance is minimized for each case when compared to the benchmarks. There is an 85.92%, 64.27%, and 77.02% reduction in three-phase unbalance for Cases 01, 02, and 03, respectively (the imbalances are in Voltage (p.u.) values). Stratified controllers are written in Python, including three-phase unbalanced optimal power flow and model predictive control.
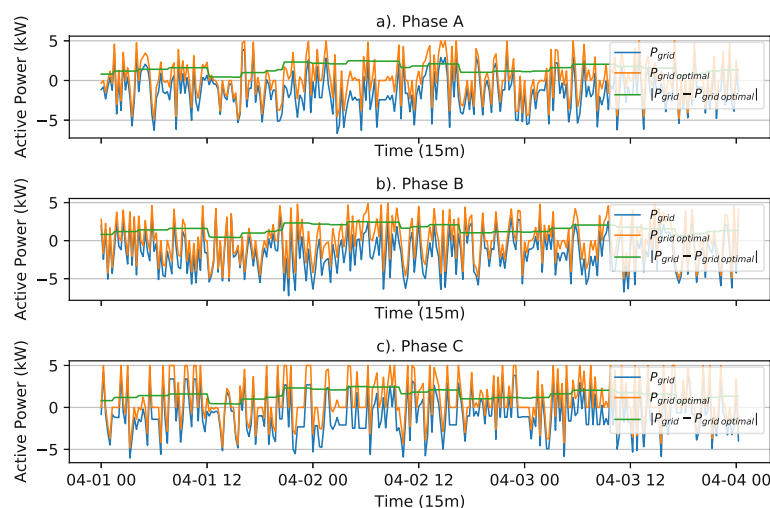
Figure 7. Per phase active powers at point of common coupling, grid optimal schedule and absolute difference between them at Bus 020.
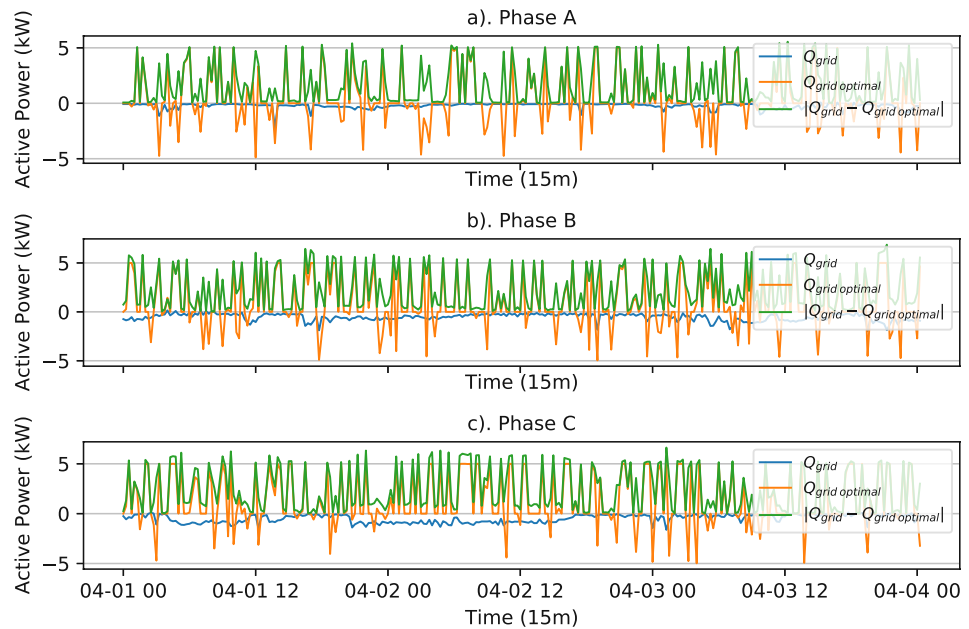
Figure 8. Per phase reactive powers at the point of common coupling, optimal grid schedule and the absolute difference between them at Bus 020. Due to the lack of reactive power control in flexibility models and devices working at a fixed power factor, reference profiles are not being followed when compared to active power tracking in Figure 7. This is done for the sake of simplicity, to maintain the linearity of flexibility models and their controllers.
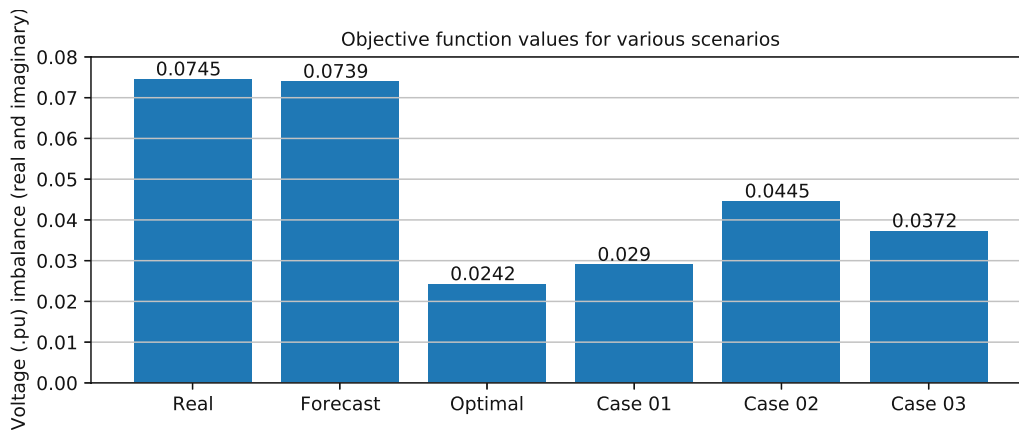
Figure 9. Objective function values for the three scenarios (see Section 4.1.3). Objective function values from Equation (2) are reduced to voltage (p.u.) for better understanding of results.

8. Conclusions and Outlook

In this paper, the authors present a stratified control scheme in a peer-to-peer local energy community (see Section 3). It uses a three-phase unbalanced optimal power flow based on holomorphic embedding load flow method and receding horizon control as described in Section 4. Blockchain acts as an enabler by making the data available at all the buses in the grid. Three-phase optimal active and reactive power set-points are generated for controllable buses, which are found using the objective function in Equation (13) in Section 4.1.2. Mixed integer quadratic model predictive control is hosted in flexibility controllers with various electrical connection configurations and thermal models (see Section 5).

An objective function to minimize three-phase voltage unbalance with three use cases is presented in Section 6. Voltage magnitudes for the simulation duration for all the scenarios are presented. It is observed that cases 01 and 03 have completely mitigated the voltage violations. Is observed that there is an 85.92%, 64.27%, and 77.02% reduction of phase unbalance for the three cases. In the context of local energy communities, such a system can provide services to the distribution system operator. Additionally, the objectives defined by the community operator can be included in the grid level control. One other advantage is the ability of individual flexibilities to have their own objectives and simultaneously support the grid. One of the limitations is the intense communication needs as all the measurement devices and the controllers are to be connected to the blockchain to send and receive data.

In future work, the stratified control structure needs to be integrated with the peer-to-peer energy market and modified accordingly to perform the market settlement process. Additionally, a control scheme should be tested with various other real networks for stability and replication analysis. The smart building models used in this paper are linear. More realistic, nonlinear models are to be used to obtain a better optimal profile tracking along with appropriate sizing of various flexibilities. Additionally, reactive power control is limited in flexibility models. By implementing them, better tracking of set-points is possible, leading to a solution being closer to a global optimum.

Author Contributions: Conceptualization, B.V.R., M.S., F.K. and M.K.; methodology, B.V.R., M.S. and R.K.; validation, R.S., B.V.R. and R.K.; formal analysis, B.V.R., M.S., F.K. and M.K.; investigation, B.V.R.; resources, R.S.; data curation, R.S.; writing—B.V.R., M.S.; writing—review and editing, B.V.R., R.S., R.K., F.K. and M.K.; project administration, M.S.; funding acquisition, M.S. All authors have read and agreed to the published version of the manuscript.

Institutional Review Board Statement: Not applicable.

Informed Consent Statement: Not applicable.

Data Availability Statement: Not applicable.

Conflicts of Interest: The authors declare no conflict of interest.

References

1. Babaiahgari, B.; Ullah, M.H.; Park, J.D. Coordinated Control and Dynamic Optimization in DC Microgrid Systems. *Int. J. Electr. Power Energy Syst.* **2019**, *113*, 832–841. [CrossRef]
2. Bazmohammadi, N.; Tahsiri, A.; Anvari-Moghaddam, A.; Guerrero, J.M. A Hierarchical Energy Management Strategy for Interconnected Microgrids Considering Uncertainty. *Int. J. Electr. Power Energy Syst.* **2019**, *109*, 597–608. [CrossRef]
3. Dou, C.X.; Liu, B. Hierarchical Hybrid Control for Improving Comprehensive Performance in Smart Power System. *Int. J. Electr. Power Energy Syst.* **2012**, *43*, 595–606. [CrossRef]
4. Brandstetter, M.; Schirrer, A.; Miletić, M.; Henein, S.; Kozek, M.; Kupzog, F. Hierarchical Predictive Load Control in Smart Grids. *IEEE Trans. Smart Grid* **2017**, *8*, 190–199. [CrossRef]
5. Glavitsch, H.; Bacher, R. Optimal Power Flow Algorithms. In *Control and Dynamic Systems*; Elsevier: Amsterdam, The Netherlands, 1991; Volume 41, pp. 135–205. [CrossRef]
6. Dommel, H.W.; Tinney, W.F. Optimal Power Flow Solutions. *IEEE Trans. Power Appar. Syst.* **1968**, *PAS-87*, 1866–1876. [CrossRef]
7. Stott, B.; Hobson, E. Power System Security Control Calculations Using Linear Programming, Part I. *IEEE Trans. Power Appar. Syst.* **1978**, *PAS-97*, 1713–1720. [CrossRef]
8. Stott, B.; Hobson, E. Power System Security Control Calculations Using Linear Programming, Part II. *IEEE Trans. Power Appar. Syst.* **1978**, *PAS-97*, 1721–1731. [CrossRef]
9. Rao, B.V.; Kupzog, F.; Kozek, M. Three-Phase Unbalanced Optimal Power Flow Using Holomorphic Embedding Load Flow Method. *Sustainability* **2019**, *11*, 1774. [CrossRef]

10. Sun, Y.; Li, P.; Li, S.; Zhang, L.; Sun, Y.; Li, P.; Li, S.; Zhang, L. Contribution Determination for Multiple Unbalanced Sources at the Point of Common Coupling. *Energies* **2017**, *10*, 171. [CrossRef]

11. Yong, J.Y.; Ramachandaramurthy, V.K.; Tan, K.M.; Mithulananthan, N. A Review on the State-of-the-Art Technologies of Electric Vehicle, Its Impacts and Prospects. *Renew. Sustain. Energy Rev.* **2015**, *49*, 365–385. [CrossRef]

12. Karimi, M.; Mokhlis, H.; Naidu, K.; Uddin, S.; Bakar, A. Photovoltaic Penetration Issues and Impacts in Distribution Network—A Review. *Renew. Sustain. Energy Rev.* **2016**, *53*, 594–605. [CrossRef]

13. Al-badi, A.H.; Ieee, S.M.; Elmoudi, A.; Metwally, I.; Ieee, S.M.; Al-wahaibi, A.; Al-ajmi, H.; Bulushi, M.A. Losses Reduction in Distribution Transformers. In Proceedings of the International Multi Conference of Engineers and Computer Scientists 2011 (IMECS 2011), Hong Kong, China, 16–18 March 2011; Volume II.

14. Gnacinski, P. Windings Temperature and Loss of Life of an Induction Machine Under Voltage Unbalance Combined With Over- or Undervoltages. *IEEE Trans. Energy Convers.* **2008**, *23*, 363–371. [CrossRef]

15. Lee, S.Y.; Wu, C.J. On-Line Reactive Power Compensation Schemes for Unbalanced Three Phase Four Wire Distribution Feeders. *IEEE Trans. Power Deliv.* **1993**, *8*, 1958–1965. [CrossRef]

16. Soltani, S.; Rashidinejad, M.; Abdollahi, A. Dynamic Phase Balancing in the Smart Distribution Networks. *Int. J. Electr. Power Energy Syst.* **2017**, *93*, 374–383. [CrossRef]

17. Zeng, X.; Zhai, H.; Wang, M.; Yang, M.; Wang, M. A System Optimization Method for Mitigating Three-Phase Imbalance in Distribution Network. *Int. J. Electr. Power Energy Syst.* **2019**, *113*, 618–633. [CrossRef]

18. Kaveh, M.R.; Hooshmand, R.A.; Madani, S.M. Simultaneous Optimization of Re-Phasing, Reconfiguration and DG Placement in Distribution Networks Using BF-SD Algorithm. *Appl. Soft Comput.* **2018**, *62*, 1044–1055. [CrossRef]

19. Soltani, S.; Rashidinejad, M.; Abdollahi, A. Stochastic Multiobjective Distribution Systems Phase Balancing Considering Distributed Energy Resources. *IEEE Syst. J.* **2018**, *12*, 2866–2877. [CrossRef]

20. Mostafa, H.A.; El-Shatshat, R.; Salama, M.M.A. Multi-Objective Optimization for the Operation of an Electric Distribution System With a Large Number of Single Phase Solar Generators. *IEEE Trans. Smart Grid* **2013**, *4*, 1038–1047. [CrossRef]

21. Schweickardt, G.; Alvarez, J.M.G.; Casanova, C. Metaheuristics Approaches to Solve Combinatorial Optimization Problems in Distribution Power Systems. An Application to Phase Balancing in Low Voltage Three-Phase Networks. *Int. J. Electr. Power Energy Syst.* **2016**, *76*, 1–10. [CrossRef]

22. Wang, K.; Skiena, S.; Robertazzi, T.G. Phase Balancing Algorithms. *Electr. Power Syst. Res.* **2013**, *96*, 218–224. [CrossRef]

23. Sun, S.; Liang, B.; Dong, M.; Taylor, J.A. Phase Balancing Using Energy Storage in Power Grids Under Uncertainty. *IEEE Trans. Power Syst.* **2016**, *31*, 3891–3903. [CrossRef]

24. Watson, J.D.; Watson, N.R.; Lestas, I. Optimized Dispatch of Energy Storage Systems in Unbalanced Distribution Networks. *IEEE Trans. Sustain. Energy* **2018**, *9*, 639–650. [CrossRef]

25. Mateo, V.; Gole, A.M.; Ho, C.N.M. Design and Implementation of Laboratory Scale Static Var Compensator to Demonstrate Dynamic Load Balancing and Power Factor Correction. In Proceedings of the 2017 IEEE Electrical Power and Energy Conference (EPEC), Saskatoon, SK, Canada, 22–25 October 2017; pp. 1–6. [CrossRef]

26. Nejabatkhah, F.; Li, Y.W. Flexible Unbalanced Compensation of Three-Phase Distribution System Using Single-Phase Distributed Generation Inverters. *IEEE Trans. Smart Grid* **2019**, *10*, 1845–1857. [CrossRef]

27. Jia, L.; Yu, Z.; Murphy-Hoye, M.C.; Pratt, A.; Piccioli, E.G.; Tong, L. Multi-Scale Stochastic Optimization for Home Energy Management. In Proceedings of the 2011 4th IEEE International Workshop on Computational Advances in Multi-Sensor Adaptive Processing (CAMSAP), San Juan, Puerto Rico, 12–15 December 2011; pp. 113–116. [CrossRef]

28. Giorgio, A.D.; Pimpinella, L.; Liberati, F. A Model Predictive Control Approach to the Load Shifting Problem in a Household Equipped with an Energy Storage Unit. In Proceedings of the 2012 20th Mediterranean Conference on Control Automation (MED), Barcelona, Spain, 3–6 July 2012; pp. 1491–1498. [CrossRef]

29. Chen, C.; Wang, J.; Heo, Y.; Kishore, S. MPC-Based Appliance Scheduling for Residential Building Energy Management Controller. *IEEE Trans. Smart Grid* **2013**, *4*, 1401–1410. [CrossRef]

30. Hidalgo Rodríguez, D.I.; Myrzik, J.M. Economic Model Predictive Control for Optimal Operation of Home Microgrid with Photovoltaic-Combined Heat and Power Storage Systems. *IFAC-PapersOnLine* **2017**, *50*, 10027–10032. [CrossRef]

31. Godina, R.; Rodrigues, E.; Pouresmaeil, E.; Matias, J.; Catalão, J. Model Predictive Control Home Energy Management and Optimization Strategy with Demand Response. *Appl. Sci.* **2018**, *8*, 408. [CrossRef]

32. Rao, B.; Kupzog, F.; Kozek, M. Phase Balancing Home Energy Management System Using Model Predictive Control. *Energies* **2018**, *11*, 3323. [CrossRef]

33. Bazrafshan, M.; Gatsis, N. Comprehensive Modeling of Three-Phase Distribution Systems via the Bus Admittance Matrix. *IEEE Trans. Power Syst.* **2018**, *33*, 2015–2029. [CrossRef]

34. Prakash, K.; Islam, F.R.; Mamun, K.A.; Ali, S. Optimal Generators Placement Techniques in Distribution Networks: A Review. In Proceedings of the 2017 Australasian Universities Power Engineering Conference (AUPEC), Melbourne, VIC, Australia, 19–22 November 2017; pp. 1–6. [CrossRef]

35. Tang, Y.; Low, S.H. Optimal Placement of Energy Storage in Distribution Networks. *IEEE Trans. Smart Grid* **2017**, *8*, 3094–3103. [CrossRef]

36. Suresh, M.C.V.; Belwin, E.J. Optimal DG Placement for Benefit Maximization in Distribution Networks by Using Dragonfly Algorithm. *Renew. Wind Water Sol.* **2018**, *5*, 4. [CrossRef]

37. Kobylinski, P.; Wierzbowski, M.; Piotrowski, K. High-Resolution Net Load Forecasting for Micro-Neighbourhoods with High Penetration of Renewable Energy Sources. *Int. J. Electr. Power Energy Syst.* **2020**, *117*, 105635. [CrossRef]
38. Chaturvedi, D.; Sinha, A.; Malik, O. Short Term Load Forecast Using Fuzzy Logic and Wavelet Transform Integrated Generalized Neural Network. *Int. J. Electr. Power Energy Syst.* **2015**, *67*, 230–237. [CrossRef]

2.4 Publication D

Rao, B.V.; Stefan, M.; Brunnhofer, T.; Schwalbe, R.; Karl, R.; Kupzog, F.; Taljan, G; Zeilinger, F.; Stern, P.; Kozek, M.

Optimal capacity management applied to a low voltage distribution grid in a local peer-to-peer energy community

Own contribution

Conceptualization and methodology was developed by the candidate along with second, sixth and tenth author. Formal analysis, methodology, implementation of algorithms and coding was performed by the candidate. Modelling was performed by the candidate and the fourth author. Interfaces were developed by third, fourth, fifth, eighth and ninth author. Validation and investigation was performed by the candidate. Structuring and writing of the manuscript was done by the candidate under the supervision of sixth and tenth author.

Optimal capacity management applied to a low voltage distribution grid in a local peer-to-peer energy community☆

Bharath Varsh Rao [a,*], Mark Stefan [a], Thomas Brunnhofer [a], Roman Schwalbe [a], Roman Karl [a], Friederich Kupzog [a], Gregor Taljan [b], Franz Zeilinger [c], Peter Stern [c], Martin Kozek [d]

[a] Austrian Institute of Technology, Giefinggasse 4, 1210 Vienna, Austria
[b] Energienetze Steiermark GmbH, Leonhardgürtel 10, 8010 Graz, Austria
[c] Siemens Aktiengesellschaft Oesterreich, Siemensstraße 90, 1210 Vienna, Austria
[d] Institute of Mechanics and Mechatronics, Vienna University of Technology, Getreidemarkt 9, 1060 Vienna, Austria

ARTICLE INFO

ABSTRACT

This paper presents a methodology to optimally share the available grid capacity among customer assets connected within a low voltage distribution grid. Distributed energy resources (DERs) and a new generation of loads such as heat pumps, thermal, hydrogen, electric storages, and vehicles are increasingly being connected to distribution grids. These DERs and loads are intermittent and it is essential to optimally control them for the safe operation of the grid. Additionally, there is increased interest in the local generation, production, trading, and consumption of energy. New regulations to establish local energy communities (LEC) have come to fruition among member nations across Europe. This is to provide a control, market, and legal framework for managing such distributed generators and flexibilities in low and medium-voltage distribution grids and conclusively empower end-users to democratize the energy system. Within a LEC, a local energy market (LEM) is to be implemented. A significant constraint of a LEM or energy accounting system is the grid settlement process. The grid should remain in a steady state when the bids in the market are executed. The methodology discussed in this paper will preemptively stabilize the grid and generate limiting profiles at various locations for individual flexibilities that are part of the local energy market. This is achieved by using an Optimal Capacity Management system which generates limiting profiles at the points of common couplings of various controllable devices in the grid. The controllable devices are required to maintain their active power injection and consumption within the generated limiting profiles to ensure optimum grid level. This will ensure that grid limits are maintained, which are simulated on a test feeder and also applied to a real network model from the Heimschuh pilot site in Styria, Austria.

1. Introduction

Clean energy for all Europeans, as part of the Clean Energy Package from the European Commission, for the first time, recognizes the formation of energy communities [1]. Energy communities can induce both challenges and opportunities in the energy ecosystem. They can encourage the community members to increase renewable energy production and provide flexibility services to the network operators. Load aggregation can lead to communities offering flexibility services such as grid congestion management, peak load shaving, and improve power quality. However, although energy management within the community may decrease costs locally, overall system costs may increase due to individual loads and renewable energy generators' coordination.

Blockchain Grid project funded by the Austrian Research Promotion Agency [2], demonstrates a blockchain-based peer-to-peer local energy community (LEC). The project does not consider how to deal with excess renewable energy production but rather how to use remaining free grid resources (time-varying power and voltage bands) in the community's merit. Such a system is possible due to the utilization of a high level of trusted automation provided by Blockchain technology. The method is to implement a Blockchain-based application that allows prosumers to share free grid resources for their surplus generation and load. The

distribution system operator (DSO) acts as a facilitator. Technical and organizational requirements are analyzed for a distributed solution in which grid customers can share excess grid capacities for their flexible loads. One of the focuses is on potential regulatory designs and the challenge to design equity among grid participants, given that users are physically different depending on their localization within the grid.

In Austria, LEC will facilitate the creation of a local energy market (LEM), located in a low or medium voltage distribution grid. Community members can trade the energy, locally. With the roll-out of a large number of smart meters and measurement devices, distribution grids are becoming more observable. Simultaneously, with a large number of smart devices connected with the distributed renewable energy sources and a new generation of loads like heat-pumps, thermal, electric, hydrogen storage, and vehicles, increasing the controllability. However, LEMs have a significant limitation. The bids in the market need to be managed and therefore, a settlement mechanism is needs to be implemented to ensure grid security, when the bids agreed in the market are executed. This is discussed further in Section 2.1.

In the literature, various methods related to capacity management are presented. Most of the methods are based on either numerical iteration or optimization. Optimal hosting capacity, grid capacity, and optimal placement problems are fundamental variations of optimal power flow (OPF) described in [3]. Hosting capacity is commonly used in the context of distributed renewable energy (DER) generators (photo-voltaic (PV), micro-wind, micro-hydro…) connected to distribution grids [4–6]. However, this term can be extended to loads such as heat pumps, thermal, hydrogen, electric storage, and electric vehicles (EV), or any other kind of controllable and uncontrollable loads. Nevertheless, the term grid capacity is used mostly for loads.

Authors in [7] have developed a methodology to provide power regulation services to the DSO using aggregated EV. This method can be used to calculate the regulation of power in the upward and downward direction of the EV fleet, providing voltage services to the grid. Futhermore, the research work does not present the impact on the grid when these services are active, and since they are aggregated, insufficient control is provided to a single customer or a charging station. Additionally, more intensive control mechanisms are required within a local energy market (LEM) for concluding settlement procedures. In [8], authors present a probabilistic hosting capacity method with the inclusion of uncertainties related to RES and loads. The method is mostly used for planning purposes and is bench-marked using a network model. However, the method cannot provide schedules or control set-points to individual generators or loads and cannot be included in a LEC without major modifications. In [9], a stochastic optimization method is presented. Similar to [8], it cannot be used for set-point generation meant for individual flexibility or RES units connected at a particular bus in the grid. A methodology to optimally control EVs within a region (region-based) is provided in [10]. This is used to generate an EV chargeable region and an EV charging upper limit for active power for each bus. This method can be compatible with the local peer-to-peer energy market but is limited only to electric vehicles and does not consider other types of loads or RES generation. In the research work presented in [11], an electric storage system is used to provide voltage regulation services to the grid and to increase PV hosting capacity. However, the method is designed for instantaneous control and does not focus on scheduling flexibilities. Authors in [12] postulate a deterministic and probabilistic control scheme for EV control to improve power quality in a distribution grid. This paper, similar to [8], does not focus on control of individual EVs. Authors in [13], have presented a scalable optimization problem to optimally configure the RES placement to maximize the hosting capacity. The optimization approach looks promising as it can deliver global optimum, the method is not suitable for real time operation but rather for planning purpose. Research work described in [14], presents a novel energy management system to manage interconnected micro-grid. It involves the creation of a step-wise demand response strategy to manage various assets in the micro-grids with two

levels of control. A major limitation of this approach is the not being able to reach a global optimum due to multi-level control. Very detailed information about the assets are needed. In [15], a bi-level power and energy management system for a micro-grid is presented. It consists of a upper level which is responsible for power management and lower level for energy, using evolutionary algorithms. This approach has similar disadvantages as [14]. A global optimum is difficult to achieve. Moreover, the set-points are directly transmitted to the flexibilities, where as, in this paper, a band of limiting profiles are generated. Authors in [16] presented a stochastic energy management system to manage RES units like solar, wind and tidal sources in the presence of the demand response program and storage devices, in a micro-grid. It uses a linear multi-objective programming method. It does not however, include a method to segregate the load types and provide a method to include multiple variety of flexibilities without the need for comprehensive data. In [17], the authors describe an optimal control problem using two approaches, direct method and Bellman's Dynamic Programming Principle, respectively and the method looks promising. However, it does not include the power flow. This method cannot be extended to a low voltage distribution grid consisting of power lines, where power flows need to be taken into consideration. An energy management strategies is presented in [18], which uses deep reinforcement learning, within an energy internet. The approach is similar to OPF type C, as presented in [19], where a load flow solver is used in congention with an OPF solver for power flow related information and OCM is based on OPF Type C (see Section 2, for more information).

From the literature, it can be established that currently a methodology does not exist that can generate active power set-points (operation band or limits) by calculating the hosting or grid capacity at each node in the low voltage distribution grid, including multiple RES and load types. Additionally, methods cited above are not readily compatible with a LEM to provide settlement services for grid stability. A holistic methodology that can accommodate all flexibility types coupled with DERs is missing or needs improvement. Moreover, such a system should be able to run online with a short reaction or sampling time to counter stochastic RES and loads.

Therefore, this paper presents the following contributions which are beyond the state-of-the-art,

1. A holistic methodology, which includes multiple flexibilities and load types, entitled Optimal Capacity Management (OCM) control scheme to manage available grid capacity in low voltage distribution grid (see Section 2.2).
2. A real-time local peer-to-peer energy market settlement process alongside its relation to OCM (see Section 2.1).
3. OCM methodology which is based on holomorphic embedding load flow method (HELM) and genetic algorithm (GA) with various objectives and constraints for test and real grid scenarios (see Sections 2, 2.2.2 and 2.2.3) to generate the limiting profiles for market settlement process, in a peer-to-peer LEC.
4. Validation of the methodology using test (see Section 3) and a real feeder (see Section 4) located in Austria with real measurements.

This paper is structured as follows; the OCM methodology is presented in Section 2, the introduction to the relationship between OCM and a local peer-to-peer energy market is presented in Section 2.1. OCM formulation, objectives, inequality and HELM used as equality constraints are presented in Sections 2.2, 2.2.2 and 2.2.3, respectively. Results based on a test feeder and Heimschuh pilot site is presented in Sections 3 and 4, respectively. Finally, conclusions and outlooks are presented in Section 5. Table 1 is a list of abbreviations used in the paper.

2. Methodology

Local energy communities are generally located in a low or medium

B.V. Rao et al.

Table 1
Abbreviations.

OCM	Optimal Capacity Management
DER	Distributed Energy Resources
DSO	Distribution System Operator
TSO	Transmission System Operator
RES	Renewable Energy Sources
OPF	Optimal Power Flow
LEC	Local Energy Community
LEM	Local Energy Market
EV	Electric Vehicles
PV	Photo Voltaic
HELM	Holomorphic Embedding Load flow Method
GA	Genetic Algorithm
CS	Charging Station
CB	Community Battery
UL	Uncontrollable Load

Fig. 2. Limiting active power profiles (P_t^{min} and P_t^{max}) generated at Buses 05 and 07, respectively, where the community battery and charging station are connected.

voltage distribution grid, as represented by a general schematic shown in Fig. 1, comprising a low voltage distribution feeder connected to a certain number of uncontrollable loads (UL01, UL02, …) and flexibilities like a community battery (CB), connected at Bus05 and electric vehicle charging stations (CS01 and CS02) at Buses 07 and 09, respectively. Customers connected to the distribution grid have the opportunity to either opt-in (agree) or opt-out (decline) when participating as part of the LEC. Flexibilities either on the customer premises or at the grid level can be part of the community [20]. They can support the grid and the community, either directly or through a local ancillary services market. In the Heimschuh pilot site, a large community battery and two charging stations were provided as available flexibilities and are part of the community (see Section 4).

The DSO is required to maintain the grid security at the distribution level and this role is to be continued after the formulation of a LEC [20]. Since LEMs are located at the distribution grid level they should contain a settlement mechanism that ensures high power quality and supply continuity. This is to make sure that the bids agreed upon in the market, when executed, will not cause grid instability. OCM is presented in this paper to enable the DSOs to enforce power quality. OCM will be deployed at the DSO control center or the LEC authority premises. At the Heimschuh pilot site, the OCM is deployed at the location of the community battery.

OCM involves the generation of limiting active power profiles (P_t^{min} and P_t^{max}) at the buses where flexibilities are connected (see Fig. 2). This is pertaining to Fig. 1. Similar limits are generated at all the flexibilities in the grid. This is based on the method presented in [21], where limiting profiles are generated at the bus where controllable loads are located. However, in this paper, the limiting profiles are generated directly for the flexibility itself. This enables multiple flexibilities at the
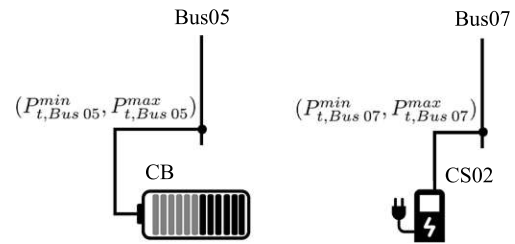
same bus to participate in the LEM. Additionally, in [21], poor reactive power control is observed due to the lack of reactive power controllable devices in the grid. Therefore, reactive power limits (Q_t^{min} and Q_t^{max}) are omitted. Moreover, reactive power is irrelevant in a LEM. Compared to [21], this paper presents additional explanation and validation of the OCM and relation to LEM, along with a detailed explanation based on two experimental setups.

Limiting profiles can be observed in Fig. 10 (adapted from the figure presented in [21]). Subsequently, this can also be observed in Fig. 3 which represents the P_t^{min} and P_t^{max} profiles for a particular flexibility. Such profiles are generated for all the flexibilities participating in the LEM. The active power consumed by the flexibility during market operation is required to be in-between the P_t^{min} and P_t^{max} limits to maintain the grid within its prescribed limits. The limiting profiles can take both positive (power consumption) and negative (power injection) values. This is applicable to the community battery, which can either charge and discharge. The load flow analysis of a power grid suggests that, for a particular grid loading condition, the grid capacity is constant i.e. the power that can be fed-into or consumed for a particular feeder is fixed. This is due to the non-causal nature of the load flow solution. This is also affected by the distance from the transformer and voltage drop along the lines. These specific limiting profiles are sharing the available grid capacity among the flexibilities depending on the objective function and constraints. This is observed in a simple example presented in Section 3 and Fig. 6.

The flexibilities are required to remain within the operation range provided by the OCM while participating in the LEM. Doing so will ensure that no limits are violated at any of the buses in the distribution grid.

2.1. Relevance to local peer-to-peer energy markets

Traditionally, in national or European level energy markets, the physical settlement process is done by the transmission system operator (TSO) who is responsible for maintaining transmission grid security. This is possible due to the fact that transmission grids are over observed and controllable. However, such a market structure, cannot be readily transposed to a distribution grid, which is neither controllable nor observable.
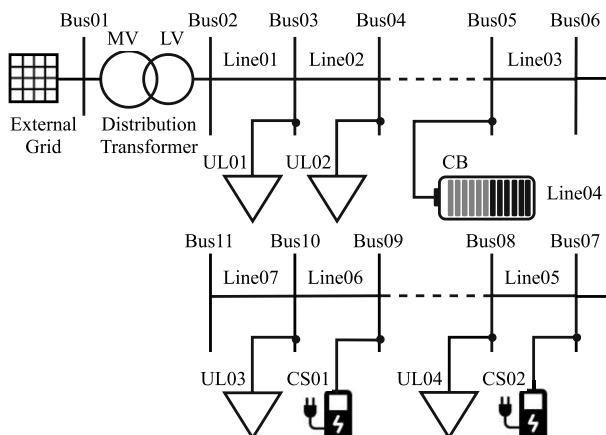
Fig. 1. General schematic of a LEC.
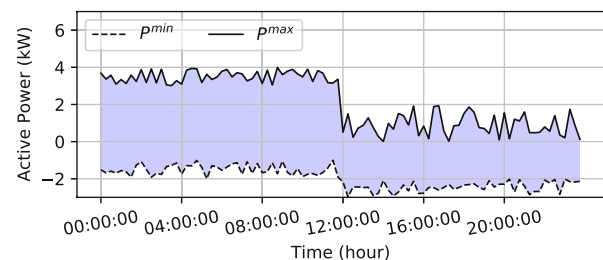
Fig. 3. Representation of limiting profiles of a flexibility in a LEC.

In recent years, distribution grids are moving towards increased controllability and observability, with the help of smart meters and a new generation of loads and distributed generators. Contrary to TSO, a DSO cannot be responsible for managing the settlement process due to the large number of distributed loads and generators. Therefore, a control mechanism is needed to preemptively controlled the flexibilities even before the market bidding begins. OCM generates the limiting profiles and if the flexibilities operate within the limits, the physical settlement has occured. This will ensure that the bids in the LEM, when enacted, will not lead to grid violations or power quality issues. The Blockchain Grid project addresses this issue by coupling the LEM with the OCM system.

In this publication, the LEM structure is not presented, as it is out of the scope of this study. Rather, the linkage between the OCM and the market is provided. There are multiple blockchain based energy markets approached available in the literature [22–24]. The system architecture of the Blockchain Grid project is presented in Fig. 4. A permissioned public Blockchain, based on Parity Ethereum is used in the project. The consensus algorithm used is "proof of authority" procedure. Each authorized participants (so-called "sealers"), can generate blocks with transactions into the Blockchain. The platform can dynamically add or remove participants. This feature is essential as sealers in the "proof of authority" mechanism generate blocks in a well defined sequence and the block is only generated by the next sealer, if one sealer fails.

There are two smart contracts considered, the first focusing on enabling peer-to-peer trading in the energy market and, second, the managing of the grid capacities. Customers in the pilot can own a certain amount of battery capacity in the community battery and be part of the market. Additionally, charging stations are connected to the blockchain to provide flexibility services. Measurement devices in the field record the active and reactive powers, voltage and phase angle (P, Q, V, Θ) at all the customers in the low voltage grid. This data is directly written into the blockchain and is available at all other nodes in the system in the next sample. The sampling rate of the system is 1 min.

Active powers are used in the market smart contract for market action, which will lead the generation of battery power (P_{CB}) values (charging or discharging). This is dependent on the market mechanism.

OCM will receive the P, Q, V, Θ to generate P^{min} and P^{max} values and is acquired by the capacity smart-contract. Flexibilities are required to operate within the provided limits and community battery limits are considered in the market mechanism, which calculates the battery power.

2.2. Optimal capacity management

As discussed in Section 1, OCM is based on OPF. OPF problems are non-linear and non-convex in nature [3]. In [3], OPF methods are classified into two classes. Class A set of algorithms is based on an intermediate load flow solution. As the optimal solution is close to those generated by a complete load flow, it is assumed to be operable, and the optimum is determined iteratively using Jacobian and sensitivity relationships. Class B involves using the entire search space by using a solver that can handle non-linearity and non-convexity or by convex relaxation methods. In [19], authors present Class C type of algorithms which combines class A and B. OCM is based on the OPF Class C presented in [19]. However, in [19], the objective is to minimize the three phase voltage unbalance in contrast to OCM, which has the objective to generate limiting profiles and integrating it into a LEM. It uses a non-linear non-convex solver wrapped around a reliable load flow method like HELM to generate a global optimum.

OCM is defined as an optimization problem as,

$$
\begin{aligned}
&\underset{u}{\text{minimize}} && F(x, u) \\
&\text{subject to} && H(x, u) = 0, \\
& && G(x, u) \leqslant 0
\end{aligned}
\tag{1}
$$

where, $F(x, u)$ is the objective function of OCM. $H(x, u)$ and $G(x, u)$ are the equality and inequality constraints respectively.

x, u are the state and input variables. For a low voltage distribution grid containing only load buses, in the context of load flow, input variables are active and reactive power injection or consumption at loads, while the state variables are voltages, phase angles and reactive powers at all the buses.

Active power limiting profiles are to be generated at all the controllable buses in grid, as discussed in Section 2.

2.2.1. Objective function

As presented in Figs. 2 and 3, limiting profiles are generated by defining the objective function as,

$$
F(x, u) = \sum_{t \in T} \sum_{c \in C} P_{c,t}
\tag{2}
$$

Limiting profiles (P_t^{min}, P_t^{max}) are generated as follows,

$$
\begin{aligned}
P_t^{min} &= \underset{u}{\text{minimize}} && F(x, u) \\
P_t^{max} &= -\underset{u}{\text{minimize}} && F(x, u)
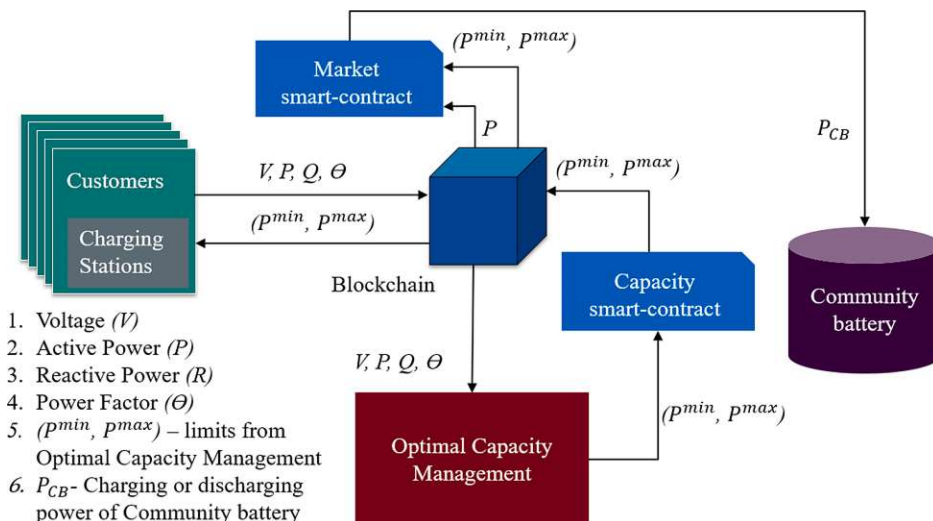\end{aligned}
\tag{3}
$$

Fig. 4. System architecture of the Blockchain Grid project at the Heimschuh pilot site.

where $P_{c,t}$ are the active powers at the controllable devices and at the time step t. C, represents the set of controllable devices/flexibilities. T is the optimization time horizon. Eq. 2 is minimized and maximized (-minimized) to generate P^{min} and P^{max} values as represented in Eq. 3.

2.2.2. Inequality constraints

Set of inequality constraints $G(x,u)$ in Eq. 1, are described as follows,

Limits on active power of controllable devices, $c \in C$, set of controllable devices and $t \in T$, time horizon,

$$P_{c,t}^{low} \leqslant P_{c,t} \leqslant P_{c,t}^{high} \tag{4}$$

Limits on voltage, $\omega \in \Omega$ represents all the buses in the grid,

$$|V_{\omega,t}^{low}| \leqslant |V_{\omega,t}| \leqslant |V_{\omega,t}^{high}| \tag{5}$$

Phase shift angles limits,

$$\theta_{\omega}^{low} \leqslant \theta_{\omega} \leqslant \theta_{\omega}^{high} \tag{6}$$

Limits on shunt reactances or capacitances,

$$s_{\omega}^{low} \leqslant s_{\omega} \leqslant s_{\omega}^{high} \tag{7}$$

Upper limits on active power flow in distribution transformer or lines, between ω'th and l'th nodes,

$$P_{\omega,l,t} \leqslant P_{\omega,l,t}^{high} \tag{8}$$

Limits on voltage angles between ω'th and l'th nodes,

$$\Theta_{\omega,t}^{low} \leqslant \Theta_{\omega,t} - \Theta_{l,t} \leqslant \Theta_{\omega,t}^{high} \tag{9}$$

P, Q, V and θ are active power, reactive power, voltage and phase shift angle respectively. s is the shunt reactances or capacitances. Θ is the voltage phase angle. (See Fig. 5)

2.2.3. Equality constraints

Load flow results are used as equality constraints $H(x,u)$, as described in the type C class of OPF algorithms. Load flow methods based on numerical techniques are capable of solving a system of nonlinear equations [25]. Convergence of such methods cannot be ensured as the operable solution is directly dependent on the assumed initial seed (starting point or initial condition). If the system has multiple solutions, it becomes difficult to determine whether the converged solution is operable. Therefore, to overcome the limitations of iterative numerical solutions, HELM is used in this research work. The distribution grid is modeled based on the methodology developed in [26].

HELM, described in [25], involves a non-iterative load flow approach which guarantees an operable solution if it exists. Eq. 10 refers to the power balance in the load bus. Inherently, it is non-holomorphic (non-analytical) in nature. A function is said to be holomorphic if it satisfies the Cauchy-Riemann condition.

$$\sum_l Y_{\omega l} V_l(\alpha) = \frac{\alpha S_{\omega}^*}{V_{\omega}^*(\alpha^*)} - \alpha Y_{\omega,shunt} V_{\omega}(\alpha), \ \omega \in \Omega_{PQ} \tag{10}$$

where $Y_{\omega,l}$ is the ω'th and l'th element of the series bus admittance matrix. V_l is the voltage at bus ω. Similarly, $Y_{\omega,shunt}$ refers to the shunt admittance matrix. Ω_{PQ} is the set of PQ buses. S represents the apparent power.

By the process of embedding a complex variable α, V becomes a function of this new complex variable. This new function is holomorphic
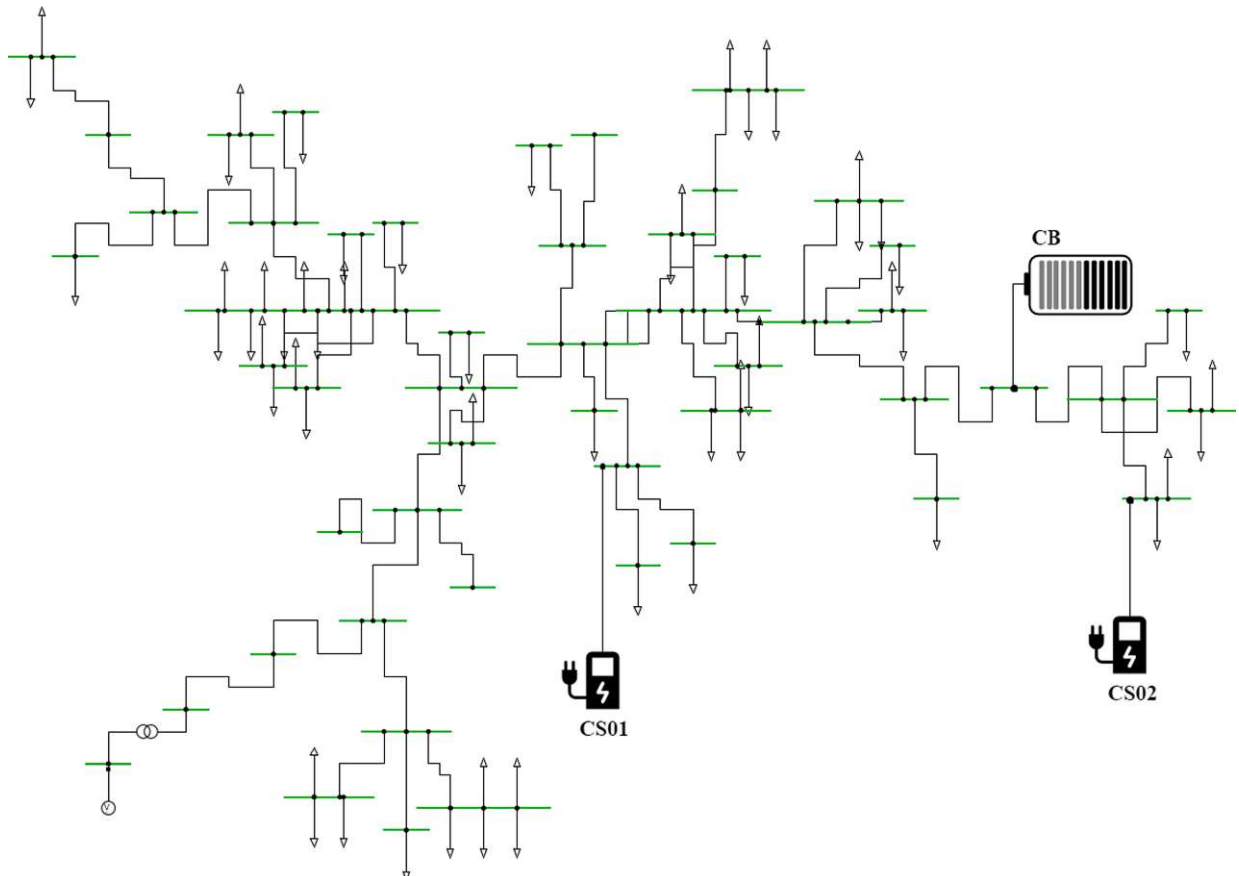
Fig. 5. Topology of the Heimschuh low voltage test feeder.

in nature. If $\alpha = 0$, there is an exact mathematical solution to the problem, but it is not the desired solution. $\alpha = 1$ provides the desired solution. It can be expressed as a power series, specifically as a Taylor or Maclaurin series represented in Eqs. 11 and 12 and which, in-turn, is a function of bus active and reactive power injections. By calculating the coefficients of series, bus voltages can be approximated. This eliminates the use of the computationally expensive Jacobian matrix. For $\alpha = 0$, $S = 0$, Eq. 10 becomes linear and the solution is mathematically exact. In order to use the linear solution, the admittance matrix is split into series and shunt elements.

The term αS is varied to determine the voltage function from $\alpha = 0$ to $\alpha = 1$ and thus, embedding is essential.

$$V_\omega(\alpha) = \sum_{n=0}^{\infty} V_\omega[n]\alpha^n, \quad \omega \in \Omega \tag{11}$$

$$V_\omega^*(\alpha) = \sum_{n=0}^{\infty} V_\omega^*[n]\alpha^n, \quad \omega \in \Omega \tag{12}$$

The coefficients of Maclauren series are determined using Pade approximation. The Pade approximation gives the rational approximation of a function. It accelerates the convergence with more accurate results with less coefficients. The approximation is valid for over a small domain. In this case, the domain $\alpha = [0, 1]$.

$$H(x, u) = V_\omega = f_{HELM}(P_\omega), \quad \omega \in \Omega \tag{13}$$

Generalized equality constraint is presented in Eq. 13. P_ω is the active power injections at all the PQ (Load) buses.

3. Experimental setup I: Low voltage test feeder

OCM is applied to a low voltage test feeder to demonstrate its effectiveness. The test network consists of five buses. Two uncontrollable loads and two charging stations are connected to it. The topology of the test feeder is presented in Fig. 6. The test feeder consists of only one branch to produce logical and understandable results. Moreover, only loads are included in the feeder to eliminate multi-directional power flows, also leading to an understandable solution.

To validate the generated limiting profiles as described in Section 2.2, the results from the OCM are fed back into the load flow from Section 2.2.3 and Eq. 13, to get the voltage values along with other state and unknown variables. For the sake of simplicity and with a focus on voltage management, the right-hand side of the Eq. 14 (for a low voltage distribution grid with PQ buses) only contains bus voltage magnitudes while voltage angles are not considered.

$$V_\omega = f_{HELM}(P_{UL01}, P_{CS01}, P_{CS02}, P_{UL02}) \tag{14}$$

where $\omega \in \Omega$ represents all the buses in the grid.

Fig. 7.a. represents the limiting profiles ($P_{CS01}^{min}, P_{CS01}^{max}$) and ($P_{CS02}^{min}, P_{CS02}^{max}$), for the two charging stations, respectively. The limits on the two charging stations are, $0kW \leqslant P_{CS01} \leqslant 22kW$ and $0kW \leqslant P_{CS02} \leqslant 22kW$. It also
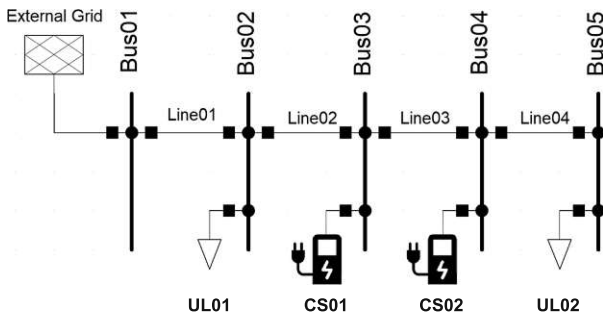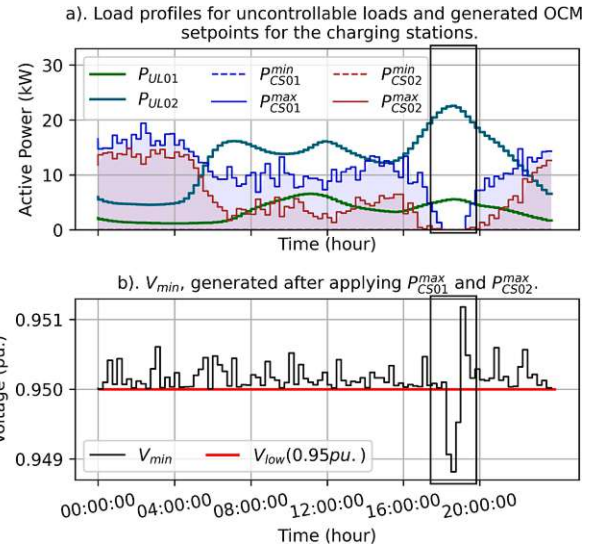

Fig. 7. Limiting profiles generated for the charging stations.

shows the active power profiles for the two uncontrollable loads (P_{UL01}, P_{UL02}). It can be observed that the total maximum available capacity is $P_{CS01}^{max} + P_{CS02}^{max}$ as the voltages are very close to 0.95 pu in Fig. 7.b. This shows that the OCM shares the available capacity between the two charging stations. Since CS01 is closer to the transformer, more capacity is assigned to it. It is also influenced by the two uncontrollable loads and voltage drops across the lines. The flexibility closest to the transformer is naturally able to accommodate more loads and generation and therefore leads to an unfair scenario for the flexibilities at the end of the feeder. The objective function can be modified to make the problem more fair. This is however not included in this paper as the authors are interested in presenting a pure power system solution, without the social factors.

Fig. 7.b is generated using Eq. 14, where $P_{CS01} = P_{CS01}^{max}$ and $P_{CS02} = P_{CS02}^{max}$, and V_{min} is obtained. This represents the worst case scenario with maximum loading. It can be observed that all the voltage values are above V_{low} (0.95pu), as described in Section 2.2.2.

However, in the highlighted region, V_{min} goes below V_{low}, indicating an under-voltage violation. Only V_{min} (under-voltage violation) is provided since there is no in-feed considered in this test scenario, which could lead to a over voltage violation.

This is caused due to high loading on P_{UL01} (an uncontrollable load). OCM reduces the P_{CS01}^{max} and P_{CS02}^{max} values to 0 to counter the increased loading. Since the charging station values cannot go below 0 (start injecting), voltage violations will sustain. This can be rectified with electric storage, which can take both positive and negative values.

Recalling from Section 2, as long as $P_{CS01}^{min} \leqslant P_{CS01} \leqslant P_{CS01}^{max}$ and $P_{CS02}^{min} \leqslant P_{CS02} \leqslant P_{CS02}^{max}$ holds, no voltage violations can occur.

In Fig. 8.d, V_ω values are obtained by considering random values for P_{CS01} (see Fig. 8.a) and P_{CS02}(see Fig. 8.b) while maintaining $P_{CS01}^{min} \leqslant P_{CS01} \leqslant P_{CS01}^{max}$ and $P_{CS02}^{min} \leqslant P_{CS02} \leqslant P_{CS02}^{max}$, respectively.

It can be observed that as long as the limiting profiles are considered by the flexibility, no voltage violations occur. Similarly, as previously explained, in the highlighted region, under-voltage violations are observed.

4. Experimental setup II: Heimschuh pilot site feeder

Heimschuh is a town in the federal state of Styria, Austria, with the largest concentration of PV installations (200 kWp installed generation capacity) in the grid owned by the Energienetze Steiermark GmbH, a DSO responsible for management of the Styrian distribution grid. The power generation is mostly concentrated on one low voltage feeder. The

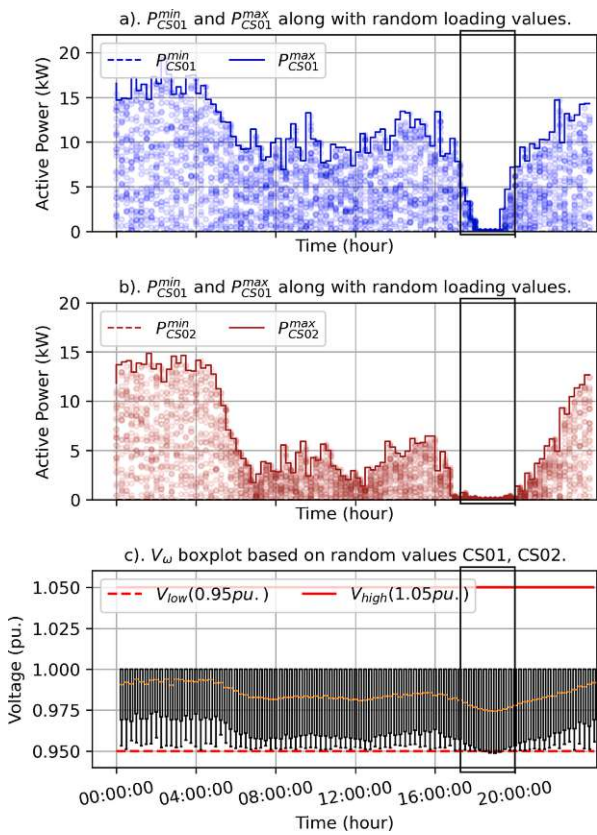**Fig. 6.** Topology of the low voltage test feeder.

B.V. Rao et al.

Fig. 8. Random values for P_{CS01} and P_{CS02} while observing the limiting profiles and the corresponding V_ω boxplots for each time step based on Eq. 14.

generated PV power is straining the grid and it is at its capacity limit. Therefore, the additional 50 kWp of PV installations and a micro-CHP cannot be connected to the grid without grid reinforcement or a smart grid solution with active generation load management.

There is a large utility sized battery on site with 100 kWh of community electric storage (see Fig. 9). A number of buildings/households are involved in the project demonstration. Twenty-one single or multi-family home customers are participating, all of which are fitted with controllers and measurement devices. Other customers are involved passively with measurements collected from smart meters for modeling and validation. OCM algorithm is running on an industrial computer installed inside the container where community electric storage is located (see Fig. 9).

For the Heimschuh pilot site, the OCM objective presented in Section

Fig. 9. Community battery located at the Heimschuh pilot site in Styria, Austria.

2.2 is modified into a two step optimization problem. As the community battery is part of the LEC and community members own a share of the battery capacity as part of LEM, priority is first given to the community battery above any other flexibility participating in the community. OCM is connected to the blockchain network and receives measurements from customers who part of the pilot and transformer located at the secondary substation.

The modified two step OCM is presented in Eqs. 15 and 16.

$$F_{CB}(x,u) = \sum_{t \in T} (P_{CB,t}) \tag{15}$$

where $F_{CB}(x,u)$ is the community battery objective function. $P_{CB,t}$ is the active power of the community battery. $(P_{CB,t}^{min}, P_{CB,t}^{max})$ is generated using the Eq. 3.

$$F_{CS}(x,u) = \sum_{t \in T} \sum_{CS \in C} (P_{CS,t}) \tag{16}$$

where $F_{CS}(x,u)$ is the charging station objective function. $_{CS,t}$ is the active power of the two charging stations. $CS \in C$ represents the set of flexibilities (two charging stations). $(P_{CS,t}^{min}, P_{CS,t}^{max})$ is generated using the Eq. 3.

Similarly to the low voltage test feeder in Section 3, limiting profiles are generated for the three flexibilities in the pilot site for each sample time of 1 min. This can be observed in Fig. 11.a. and.b. V_{min} is generated when $P_{CS01} = P_{CS01}^{max}$ and $P_{CS02} = P_{CS02}^{max}$ and $P_{CB} = P_{CB}^{max}$ and can be observed in Fig. 11.d. As expected, V_{min} are located around V_{low} (0.95pu.). V_{max} is generated when $P_{CS01} = P_{CS01}^{min}$ and $P_{CS02} = P_{CS02}^{min}$ and $P_{CB} = P_{CB}^{min}$. This is the least loading or power injection condition. It can be observed that there is capacity left over to accommodate more power
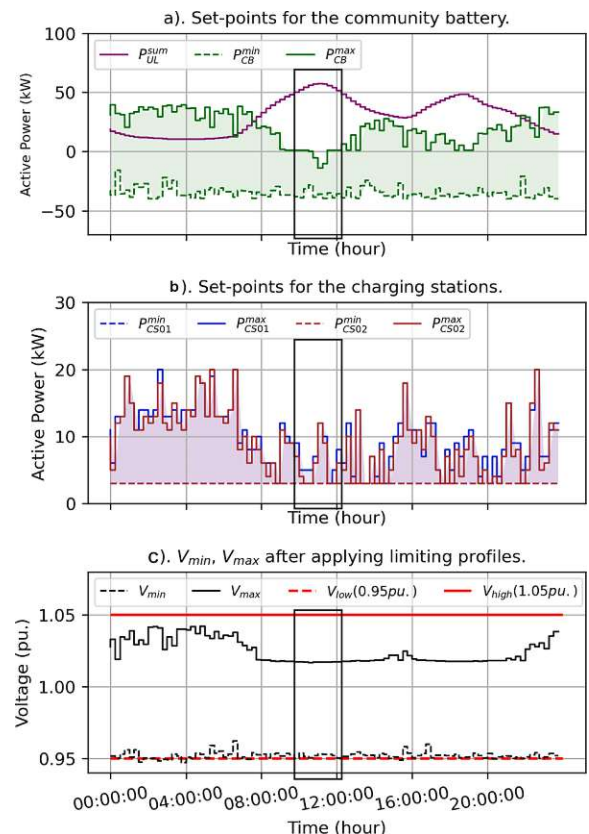

Fig. 10. Limiting profiles for the community battery and the two charging stations, similar to Fig. 7.
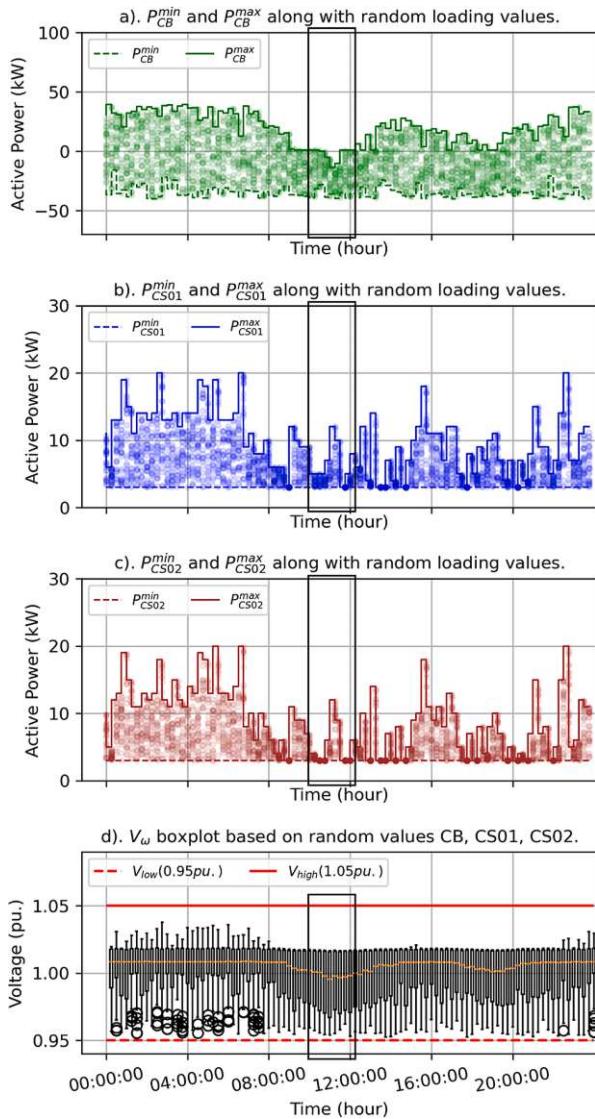
B.V. Rao et al.

Fig. 11. Random values for P_{CB}, P_{CS01} and P_{CS02} while observing the limiting profiles and the corresponding V_{min} boxplots for each time step based on Eq. 14. Voltage reference at the transformer is at 1.01 pu.

injection into the grid. However, to accomplish this, in the highlighted region in Fig. 11.a, the community battery had to momentarily discharge. This is attributed to high loading conditions observed in the feeder P_{UL}^{sum}, which is the sum of all uncontrollable loads. With the necessary discharge, and having both P_{CS01} and P_{CS02}, close to zero kW, the voltages in Fig. 11.c are clustered around the 0.95 pu. limit. Therefore, by actively managing the low voltage distribution grid with a community battery, more PV or generators can be hosted.

Similar to Fig. 8, V_ω values are calculated by considering random values for P_{CB} (see Fig. 11.a), P_{CS01} (see Fig. 11.b) and P_{CS02} (see Fig. 11.c). V_ω values are in-between the prescribed limits as mentioned in Section 2.2.2. $V_\omega \leqslant 1pu$ because, there are no power injections in the feeder.

5. Conclusion

In order to facilitate the market settlement process, OCM was presented. OCM is used to generate limiting profiles (P_t^{min} and P_t^{max}) values at all the flexibilities in a LEC, participating in the LEM. The flexibilities are required to operate within these limits to avoid voltage violations.

By doing so, the bids in the market are preemptively grid secure and, when executed, will not lead to power quality issues. OCM and its relation to blockchain LEM was presented along with the system architecture. OCM is based on OPF type C using a non-linear non-convex solver, GA, wrapped around a reliable load flow, HELM. This method was tested using a low voltage test feeder, and a detailed explanation of the results was provided. It was proved in both experimental setups that when the the limiting profiles are applied and the flexibilities are operated within its limits, voltages at all the buses will remain within the prescribed (+5, −5%) pu. voltage. This is observed in Figs. 8 and 11. However, if the flexibilities are not able to respect the limits, the voltage constraints cannot be fulfilled and is observed in Fig. 7. Based on the test feeder's learning, the method was applied to a real pilot feeder from Heimschuh, Austria. It was proven in Fig. 11, that no voltage violations will be observed as long as the limits were observed.

5.1. Future research

In this paper, only voltage violations are mitigated. In the future, the algorithm will be adapted to include line loading constraints. Since the OCM uses a non-linear, non-convex optimization solver, it is numerically expensive to calculate the global optimum. Therefore, for field deployment, machine learning models will be trained to behave like the OCM based on real and simulated data from the field and simulations, respectively. The machine learning model will be deployed in the field to cope with the low sampling time.

CRediT authorship contribution statement

Declaration of Competing Interest

The authors declare that they have no known competing financial interests or personal relationships that could have appeared to influence the work reported in this paper.

Acknowledgment

B.V. Rao et al.

References

[1] P.O. o. t. E. Union. Clean energy for all Europeans; July 2019. http://op.europa.eu/en/publication-detail/-/publication/b4e46873-7528-11e9-9f05-01aa75ed71a1/language-en.

[2] Blockchain Grid. https://projekte.ffg.at/projekt/3089755.

[3] Glavitsch H, Bacher R. Optimal Power Flow Algorithms. Contr Dyn Syst 1991;41:135–205.

[4] Niederhuemer W, Schwalbe R. Increasing PV hosting capacity in LV grids with a probabilistic planning approach. In: 2015 International Symposium on Smart Electric Distribution Systems and Technologies (EDST); 2015. p. 537–40.

[5] Navarro BB, Navarro MM. A comprehensive solar PV hosting capacity in MV and LV radial distribution networks. In: 2017 IEEE PES Innovative Smart Grid Technologies Conference Europe (ISGT-Europe); 2017. p. 1–6.

[6] Wardana FT, Riady T. Hosting Capacity Analysis for Rooftop PV in Indonesia: A Case Study in Gayo Lues District, Aceh. In: 2020 International Conference on Technology and Policy in Energy and Electric Power (ICT-PEP); 2020. p. 12–5.

[7] Lam AYS, Leung Ka-Cheong, Li VOK. Capacity management of vehicle-to-grid system for power regulation services. In: 2012 IEEE Third International Conference on Smart Grid Communications (SmartGridComm); 2012. p. 442–7.

[8] Al-Saadi H, Zivanovic R, Al-Sarawi SF. Probabilistic Hosting Capacity for Active Distribution Networks. IEEE Trans Industr Inf 2017;13(5):2519–32.

[9] Jothibasu S, Santoso S, Dubey A. Optimization Methods for Evaluating PV Hosting Capacity of Distribution Circuits. In: 2019 IEEE 46th Photovoltaic Specialists Conference (PVSC); 2019. p. 0887–91.

[10] Zhao J, Wang J, Xu Z, Wang C, Wan C, Chen C. Distribution Network Electric Vehicle Hosting Capacity Maximization: A Chargeable Region Optimization Model. IEEE Trans Power Syst 2017;32(5):4119–30.

[11] Hashemi S, Østergaard J. Efficient Control of Energy Storage for Increasing the PV Hosting Capacity of LV Grids. IEEE Trans Smart Grid 2018;9(3):2295–303.

[12] Lamedica R, Geri A, Gatta FM, Sangiovanni S, Maccioni M, Ruvio A. Integrating Electric Vehicles in Microgrids: Overview on Hosting Capacity and New Controls. IEEE Trans Ind Appl 2019;55(6):7338–46.

[13] Takenobu Y, Yasuda N, Minato S-I, Hayashi Y. Scalable enumeration approach for maximizing hosting capacity of distributed generation, vol. 105. p. 867–76. [Online]. Available: https://linkinghub.elsevier.com/retrieve/pii/S01420615318309347.

[14] Ahmadi SE, Rezaei N. A new isolated renewable based multi microgrid optimal energy management system considering uncertainty and demand response, vol. 118. p. 105760. [Online]. Available: https://linkinghub.elsevier.com/retrieve/pii/S0142061519331497.

[15] Parol M, Wjtowicz T, Ksi-yk K, Wenge C, Balischewski S, Arendarski B. Optimum management of power and energy in low voltage microgrids using evolutionary algorithms and energy storage, vol. 119. p. 105886. [Online]. Available: https://linkinghub.elsevier.com/retrieve/pii/S0142061519314449.

[16] Hajiamoosha P, Rastgou A, Bahramara S, Bagher Sadati SM. Stochastic energy management in a renewable energy-based microgrid considering demand response program, vol. 129. p. 106791. [Online]. Available: https://linkinghub.elsevier.com/retrieve/pii/S0142061521000314.

[17] Heymann B, Bonnans JF, Martinon P, Silva FJ, Lanas F, Jimnez-Estvez G. Continuous optimal control approaches to microgrid energy management, vol. 9, no. 1. p. 59–77. [Online]. Available: http://link.springer.com/10.1007/s12667-016-0228-2.

[18] Hua H, Qin Y, Hao C, Cao J. Optimal energy management strategies for energy Internet via deep reinforcement learning approach, vol. 239. p. 598–609. [Online]. Available: https://linkinghub.elsevier.com/retrieve/pii/S0306261919301746.

[19] Rao BV, Kupzog F, Kozek M. Three-Phase Unbalanced Optimal Power Flow Using Holomorphic Embedding Load Flow Method. Sustainability 2019;11(6):1774.

[20] Lowitzsch J, Hoicka CE, van Tulder FJ. Renewable energy communities under the 2019 European Clean Energy Package – Governance model for the energy clusters of the future? Renew Sustain Energy Rev 2020:13.

[21] Rao BV, Stefan M, Schwalbe R, Zeilinger F, Schenk A, Frischenschlager A, et al. Grid Capacity Management for peer-to-peer Local Energy Communities. In: 2020 IEEE Power & Energy Society General Meeting (PESGM). Montreal, QC: IEEE; 2020. p. 1–5.

[22] Thomas L, Zhou Y, Long C, Wu J, Jenkins N. A general form of smart contract for decentralized energy systems management, vol. 4, no. 2. pp. 140–9. [Online]. Available: https://www.nature.com/articles/s41560-018-0317-7.

[23] Kavousi-Fard A, Almutairi A, Al-Sumaiti A, Farughian A, Alyami S. An effective secured peer-to-peer energy market based on blockchain architecture for the interconnected microgrid and smart grid, vol. 132. p. 107171. [Online]. Available: https://linkinghub.elsevier.com/retrieve/pii/S0142061521004105.

[24] Al-Obaidi A, Khani H, Farag HE, Mohamed M. Bidirectional smart charging of electric vehicles considering user preferences, peer to peer energy trade, and provision of grid ancillary services, vol. 124. p. 106353. [Online]. Available: https://linkinghub.elsevier.com/retrieve/pii/S0142061520307468.

[25] Trias A. The Holomorphic Embedding Load Flow method, in: 2012 IEEE Power and Energy Society General Meeting; 2012. p. 1–8.

[26] Bazrafshan M, Gatsis N. Comprehensive Modeling of Three-Phase Distribution Systems via the Bus Admittance Matrix. IEEE Trans Power Syst 2018;33(2):2015–29.

Bibliography

[1] Publications Office of the European Union. Clean energy for all Europeans.

[2] Bernadette Fina and Hubert Fechner. Transposition of European Guidelines for Energy Communities into Austrian Law: A Comparison and Discussion of Issues and Positive Aspects. 14(13):3922.

[3] Hans Glavitsch and Rainer Bacher. Optimal Power Flow Algorithms. In *Control and Dynamic Systems*, volume 41, pages 135–205. Elsevier, 1991.

[4] A. Trias. The Holomorphic Embedding Load Flow method. In *2012 IEEE Power and Energy Society General Meeting*, pages 1–8.

[5] L. Jia, Z. Yu, M. C. Murphy-Hoye, A. Pratt, E. G. Piccioli, and L. Tong. Multi-scale stochastic optimization for Home Energy Management. In *2011 4th IEEE International Workshop on Computational Advances in Multi-Sensor Adaptive Processing (CAMSAP)*, pages 113–116.

[6] C. Chen, J. Wang, Y. Heo, and S. Kishore. MPC-Based Appliance Scheduling for Residential Building Energy Management Controller. 4(3):1401–1410.

[7] C. R. Touretzky and M. Baldea. Model reduction and nonlinear MPC for energy management in buildings. In *2013 American Control Conference*, pages 461–466.

[8] Z. Yu, L. Jia, M. C. Murphy-Hoye, A. Pratt, and L. Tong. Modeling and Stochastic Control for Home Energy Management. 4(4):2244–2255.

[9] J. A. Momoh, F. Zhang, and W. Gao. Optimizing renewable energy control for building using model predictive control. In *2014 North American Power Symposium (NAPS)*, pages 1–6.

[10] K. X. Perez, M. Baldea, and T. F. Edgar. Integrated smart appliance scheduling and HVAC control for peak residential load management. In *2016 American Control Conference (ACC)*, pages 1458–1463.

[11] M. Rahmani-andebili and H. Shen. Energy Scheduling for a Smart Home Applying Stochastic Model Predictive Control. In *2016 25th International Conference on Computer Communication and Networks (ICCCN)*, pages 1–6.

[12] C. Sundström, D. Jung, and A. Blom. Analysis of optimal energy management in smart homes using MPC. In *2016 European Control Conference (ECC)*, pages 2066–2071.

[13] O. Alrumayh and K. Bhattacharya. Model predictive control based home energy management system in smart grid. In *2015 IEEE Electrical Power and Energy Conference (EPEC)*, pages 152–157.

[14] Chun-Xia Dou and Bin Liu. Multi-Agent Based Hierarchical Hybrid Control for Smart Microgrid. 4(2):8.

[15] Adam Milczarek, Mariusz Malinowski, and Josep M. Guerrero. Reactive Power Management in Islanded Microgrid—Proportional Power Sharing in Hierarchical Droop Control. 6(4):1631–1638.

[16] Liang Che, Mohammad Shahidehpour, Ahmed Alabdulwahab, and Yusuf Al-Turki. Hierarchical Coordination of a Community Microgrid With AC and DC Microgrids. 6(6):3042–3051.

[17] Dhananjay M. Anand, Rupert Tull de Salis., Yijie Cheng, James Moyne, and Dawn M. Tilbury. A Hierarchical Incentive Arbitration Scheme for Coordinated PEV Charging Stations. 6(4):1775–1784.

[18] Chengcheng Shao and Chao Du. Hierarchical Charge Control of Large Populations of EVs. 7(2):9.

[19] Zhiwei Xu, Yonghua Song, and Hongcai Zhang. A Hierarchical Framework for Coordinated Charging of Plug-In Electric Vehicles in China. 7(1):11.

[20] Markus Brandstetter, Alexander Schirrer, Maja Miletic, Sawsan Henein, Martin Kozek, and Friederich Kupzog. Hierarchical Predictive Load Control in Smart Grids. 8(1):10.

[21] Meysam Razmara, Guna R Bharati, Mahdi Shahbakhti, Sumit Paudyal, and Rush D Robinett. Bilevel Optimization Framework for Smart Building-to-Grid Systems. 9(2):12.

[22] A. Y. Saber, T. Khandelwal, and A. K. Srivastava. Fast Feeder PV Hosting Capacity using Swarm Based Intelligent Distribution Node Selection. In *2019 IEEE Power Energy Society General Meeting (PESGM)*, pages 1–5.

[23] Haochen Hua, Yuchao Qin, Chuantong Hao, and Junwei Cao. Optimal energy management strategies for energy Internet via deep reinforcement learning approach. 239:598–609.

[24] F. T. Wardana and T. Riady. Hosting Capacity Analysis for Rooftop PV in Indonesia: A Case Study in Gayo Lues District, Aceh. In *2020 International Conference on Technology and Policy in Energy and Electric Power (ICT-PEP)*, pages 12–15.

[25] Mirosław Parol, Tomasz Wójtowicz, Krzysztof Księżyk, Christoph Wenge, Stephan Balischewski, and Bartlomiej Arendarski. Optimum management of power and energy in low voltage microgrids using evolutionary algorithms and energy storage. 119:105886.

[26] Pouria Hajiamoosha, Abdollah Rastgou, Salah Bahramara, and S. Muhammad Bagher Sadati. Stochastic energy management in a renewable energy-based microgrid considering demand response program. 129:106791.

[27] Benjamin Heymann, J. Frédéric Bonnans, Pierre Martinon, Francisco J. Silva, Fernando Lanas, and Guillermo Jiménez-Estévez. Continuous optimal control approaches to microgrid energy management. 9(1):59–77.

[28] M. Bazrafshan and N. Gatsis. Comprehensive Modeling of Three-Phase Distribution Systems via the Bus Admittance Matrix. 33(2):2015–2029.

[29] I. Wallace, D. Roberts, A. Grothey, and K. I. M. McKinnon. Alternative PV Bus Modelling with the Holomorphic Embedding Load Flow Method. *arXiv:1607.00163 [math]*, July 2016.

[30] A. Trias. The Holomorphic Embedding Load Flow method. In *2012 IEEE Power and Energy Society General Meeting*, pages 1–8, July 2012.

[31] M. K. Subramanian, Y. Feng, and D. Tylavsky. PV bus modeling in a holomorphically embedded power-flow formulation. In *2013 North American Power Symposium (NAPS)*, pages 1–6, September 2013.

[32] Tara Esterl. *iWPP-Flex Projekt Endbericht. Österreichisches Forschungsprojekt (FFG-Nummer 848894)*. (Siehe S. 3, 9, 12–14, 27–32, 65).

[33] Bharath Varsh Rao, Mark Stefan, Thomas Brunnhofer, Roman Schwalbe, Roman Karl, Friederich Kupzog, Gregor Taljan, Franz Zeilinger, Peter Stern, and Martin Kozek. Optimal capacity management applied to a low voltage distribution grid in a local peer-to-peer energy community. 134:107355.

Curriculum vitae

BHARATH VARSH RAO

Scientist, AIT Austrian Institute of Technology

@ bharath-varsh.rao@ait.ac.at ♦ Vienna, Austria in linkedin.com/in/bharathvarshrao

EXPERIENCE

Scientist and Project Manager

AIT - Austrian Institute of Technology

🗓 May 2019 – Ongoing ♦ Vienna, Austria

- Numerous Austrian and European level projects on smart grids, local energy communities, control aspects in distribution grids, machine learning and data analysis in integrated energy systems and peer-to-peer energy markets. Blockchain Grid (FFG), PoSyCo (FFG), Integrid (H2020), REACT (H2020), LocalRES (H2020) and many more.
- Manager of ERA-Net funded project, CLUE.

Doctoral Fellow

AIT - Austrian Institute of Technology

🗓 Jan 2017 – Apr 2019 ♦ Vienna, Austria

- Doctoral dissertation on advanced concepts in stratified smart grid and building control strategies in local energy communities, as part of Blockchain Grid project.
- Novel three phase unbalanced load and optimal power flow method development coupled with three phase unbalanced home and building energy management system with active and reactive power control.
- Nonlinear non-convex optimization methods applied to grids and mixed integer nonlinear model predictive control applied to various building models. Online stratified control with system level optimization.

Research Fellow

AIT - Austrian Institute of Technology

🗓 Feb 2016 – Dec 2016 ♦ Vienna, Austria

- Project - iNIS - Integrated Network Information System Data-based load modeling by incorporating voltage, frequency and power dependencies by including consumer loads, distributed generation, identification and analysis of load characteristics based on the meter and sensor data.
- Forecasting models aggregated from LV networks to MV nodes, up to HV interconnection points.

Engineering Intern

Grenoble Génie Electrique Lab

🗓 Jun 2015 - Sep 2015 ♦ Grenoble, France

- Development of methodologies and tools for new and evolving DSO roles for efficient Distributed Renewable Energy Sources integration in distribution networks. Production of trial decisions for evolvDSO-WP4 with survey for the DSO partners and report deliverable.

STRENGTHS

Hard-working   Eye for detail

Motivator & Leader

Flexibility and Adaptability

Creating a positive work environment

Python   Matlab

DIgSILENT PowerFactory

Power System Engineering and Design

Control System for Distribution Networks

LANGUAGES

English ●●●●●

German ●●○○○

EDUCATION

Doctor of Technical Science (Dr. techn.)

Technische Universität Wien

🗓 January 2017 – Ongoing

Thesis title: Model-based Control Strategies applied to Distribution Grids in Local Energy Communities.

Master of Science in Engineering (M.Sc.Eng)

École nationale supérieure de l'énergie, l'eau et l'environnement

🗓 September 2014 – August 2016

Bachelor of Engineering (B.Eng.)

Visvesvaraya Technological University

🗓 Sept 2010 – August 2014

PUBLICATIONS

1. B. V. Rao et al., "Optimal capacity management applied to a low voltage distribution grid in a local peer-to-peer energy community," International Journal of Electrical Power Energy Systems, vol. 134, p. 107355, Jan. 2022, doi: 10.1016/j.ijepes.2021.107355.

2. S. Potenciano Menci et al., "Functional Scalability and Replicability Analysis for Smart Grid Functions: The InteGrid Project Approach," Energies, vol. 14, no. 18, Art. no. 18, Jan. 2021, doi: 10.3390/en14185685.

3. Rao, B.V.; Stefan, M.; Schwalbe, R.; Karl, R.; Kupzog, F.; Kozek, M. Stratified Control Applied to a Three-Phase Unbalanced Low Voltage Distribution Grid in a Local Peer-to-Peer Energy Community. Energies 2021, 14, 3290. https://doi.org/10.3390/en14113290

4. B. V. Rao et al., "Grid Capacity Management for peer-to-peer Local Energy Communities," 2020 IEEE Power Energy Society General Meeting (PESGM), 2020, pp. 1-5, doi: 10.1109/PESGM41954.2020.9281969.

5. Rao, B.V.; Kupzog, F.; Kozek, M. Three-Phase Unbalanced Optimal Power Flow Using Holomorphic Embedding Load Flow Method. Sustainability 2019, 11, 1774. https://doi.org/10.3390/su11061774

6. Rao, B.V.; Kupzog, F.; Kozek, M. Phase Balancing Home Energy Management System Using Model Predictive Control. Energies 2018, 11, 3323. https://doi.org/10.3390/en11123323

7. Zehetbauer, P., Stifter, M. Rao, B.V. Phase preserving profile generation from measurement data by clustering and performance analysis: a tool for network planning and operation. Comput Sci Res Dev 33, 145–155 (2018). https://doi.org/10.1007/s00450-017-0381-4

8. S Kloibhofer, M Stifter, F Leimgruber, BV Rao. Comparing and improving residential demand forecast by disaggregation of load and PV generation. CIRED-Open Access Proceedings Journal 2017 (1), 1638-1641

9. P. Zehetbauer, S. Kloibhofer, M. Stifter, B. V. M. Vasudevarao, F. Leimgruber. Identification and reconstruction of photovoltaic measurement gaps based on temporal correlation and spatial distance. 6th International Workshop in Integration of Solar Power into Power Systems (SIW 2016), 276-282

10. B. V. M. Vasudevarao, M. Stifter and P. Zehetbauer, "Methodology for creating composite standard load profiles based on real load profile analysis," 2016 IEEE PES Innovative Smart Grid Technologies Conference Europe (ISGT-Europe), 2016, pp. 1-6, doi: 10.1109/ISGTEurope.2016.7856300.

11. M. Stefan, B.-V. Rao, P. Zehetbauer, G. Taljan, P. Stern, and A. Schenk, "Blockchain-enabled flexibility activation for distribution grid management (Blockchain Grid)," p. 11, 2021.

12. Rao, B.V.; Kupzog, F.; Kozek. Three-phase Active and Reactive Power Control in Home Energy Management System. Hybrid Power Systems Workshop 2019.

13. P. Zehetbauer, M. Stifter, and B. V. Rao, "Phase preserving profile generation from measurement data by clustering and performance analysis: a tool for network planning and operation," Comput Sci Res Dev, vol. 33, no. 1–2, pp. 145–155, Feb. 2018, doi: 10.1007/s00450-017-0381-4.

REFEREES

Dipl.-Ing. Dr.Techn. Friederich Kupzog

@ Head of Competence Unit Electric Energy Systems, AIT Austrian Institute of Technology

✉ friederich.kupzog@ait.ac.at

Giefinggasse 4, 1210 Vienna, Austria

- -

Ao.Univ.Prof. Dipl.-Ing. Dr.techn. Martin Kozek

@ Head of Research Group for Regelungsmethoden-Energiesysteme, Faculty of Mechanical and Industrial Engineering, Vienna University of Technology

✉ martin.kozek@tuwien.ac.at

Getreidemarkt 9, 1060 Vienna, Austria

- -